이학박사 학위논문

Cell-non-autonomous neurogenesis by exosome-mediated transfer of neurogenic miRNA in microfluidic system

미세유체소자를 이용한 신경성 마이크로RNA의
엑소좀 매개 이동에 의한 신경분화 유도

2016 년 2 월

서울대학교 융합과학기술대학원
분자의학 및 바이오제약학과
오 현 정

Cell-non-autonomous neurogenesis by exosome-mediated transfer of neurogenic miRNA in microfluidic system

지도교수 이 동 수

이 논문을 이학박사 학위논문으로 제출함
2016 년 2 월

서울대학교 융합과학기술대학원
분자의학 및 바이오제약학과
오 현 정

오현정의 이학박사 학위논문을 인준함
2016 년 2 월

위 원 장 _____ (인)

부위원장 _____ (인)

위 원 _____ (인)

위 원 _____ (인)

위 원 _____ (인)

Contents

Contents…….……3

Abstract……...…….…….4

List of Figures and Tables……....7

List of Abbreviations……..…….....10

Introduction…….....11

Materials and Methods…….....22

Results…….…….33

Discussion…….…...82

References…….....90

Abstract in Korean…….……...……...102

Abstract

Cell-non-autonomous neurogenesis by exosome-mediated transfer of neurogenic miRNA in microfluidic system

Hyun Jeong Oh

Department of Molecular Medicine and Biopharmaceutical Science,

The Graduate School of Convergence Science and Technology,

Seoul National University

Neuronal cells release small vesicles known as secretory exosomes containing mRNAs, miRNAs and proteins to exchange signals as a form of intercommunication between cells. MicroRNAs (miRNAs) such as miR-124 or miR-9 play an important role in regulation of neuronal differentiation. Intercellular transfer of neurogenic microRNA (miRNA) induces neurogenesis and exosomes can mediate miRNA delivery from the leading differentiated cells to neighboring

undifferentiated cells. The aim of this study is to confirm cell-non-autonomous miRNA/exosome-mediated differentiation of neural progenitor cells and to visualize exosomes carrying this neurogenic miRNA from leading to neighboring cells. F11 cells, neural progenitor cells, were stably transfected with reporter vector of pRV-effLuc/3xPT_miR-193a which luciferase signal could be turned off by binding of the identified miRNA to the triplicates of miRNA binding site in the 3' UTR of effLuc. Exosomes were isolated from the conditioned media and characterized by western blot. Transwell chambers system and microfluidic device were used to examine exosome-mediated miRNA transfer. The CMV-driven GFP-tagged CD63 vector was used to visualize endogenous exosomes. Target genes of MiR-193a considered as neurogenic miRNAs were related to cell proliferation, differentiation and axon guidance. Neurite outgrowth and neuronal marker expression such as βIII-tubulin, NeuroD and MAP2 were observed 3 days after identified MiR-193a treatment. Isolated exosomes were characterized for protein markers such as CD63, TSG101. qRT-PCR results showed that exosomes isolated from conditioned media in differentiated F11 cells highly increased miR-193a level. In addition to 2D co-culture and transwell culture setting, fluorescence signals of incorporated GFP-exosomes were detected within 2 days after co-culture with GFP-exosomes producing cells. Time-lapse live-cell confocal imaging using microfluidic device visualized the transport of single exosomes from differentiated to undifferentiated F11 cells. MiR-193a within the exosomes from differentiated donor F11 cells reached the recipient cells and was taken up to lead them to neuronal differentiation, showing increased neuronal marker expression. And these

phenomenon were also reproduced in NE-4C, neural stem cells. Inhibition of the exosomal production by manumycin-A and treatment of anti-miR-193a in the differentiated donor cells failed to induce neurogenesis in undifferentiated recipient cells. These findings indicate that exosomes of neural progenitors and neurogenic miRNA within these exosomes propagate cell-non-autonomous differentiation to neighboring progenitors, which was captured visually on microfluidic device to delineate the roles of extracellular vesicles mediating neurogenesis of population of homologous progenitor cells.

Key Words: Neuronal differentiation, Cell-non-autonomous, Single exosome imaging, miR-193a, Microfluidic platform

Student number: 2013-30835

LIST OF FIGURES AND TABLES

FIGURE 1. MiRNA expression profiling of F11-Mock and F11-Ngn1 using a miRNA microarray.

FIGURE 2. A scatter plot analysis for the normalized signal intensities of miRNAs expressed in F11-Mock and F11-Ngn1 cells.

FIGURE 3. Top 17 of the up-regulated miRNAs.

FIGURE 4. Pie charts for summary of candidate miRNAs.

FIGURE 5. Gene ontology (GO) analysis for target genes of miR-193a.

FIGURE 6. The expression of miR-193a was assessed by qRT-PCR in F11 cells treated with Mock or Ngn1.

FIGURE 7. Novel neurogenic function of miR-193a.

FIGURE 8. Immunofluorescence staining to examine miR-193a-induced neuronal differentiation in F11-miR-scr and F11-miR-193a cells.

FIGURE 9. Luciferase assay for the expression of miR-193a.

FIGURE 10. Signal pathway classification for target genes of miR-193a.

FIGURE 11. Validation for target genes of miR-193a.

FIGURE 12. Enhanced levels of miR-193a in D-F11 cell-derived exosomes.

FIGURE 13. Size distribution of UD-Exo and D-Exo.

FIGURE 14. Quantitative analysis for total number and exosomal miRNA of UD- and D-Exo.

FIGURE 15. Immunofluorescence staining for Tuj-1 of GFP-exosome UD-F11

and GFP-exosome D-F11 cells.

FIGURE 16. GFP-exosome producing donor F11 cells co-cultured with DiI-labeled recipient F11 cells.

FIGURE 17. Diagram of co-culture system of GFP-exosome producing donor F11 cells and recipient UD-F11 cells in the transwell system.

FIGURE 18. Schematic representation of the transwell co-culture system for donor D-F11 cells and recipient UD-F11/effLuc-miR-193a_3XPT cells.

FIGURE 19. The induction of exosome-mediated neurogenesis in recipient cells cultured with D-donor cells**.**

FIGURE 20. qRT-PCR analysis for target genes of miR-193a.

FIGURE 21. qRT-PCR results for miR-193a and miR-124a levels in recipient UD-F11 cells 3 and 5 days after co-culture with donor UD- or D-F11 cells.

FIGURE 22. Luciferase assay for the expression of miR-193a in differentiating donor cells after anti-miR-193a treatment and in recipient cells 3 days after co-cultured with donor cells.

FIGURE 23. Immunofluorescence staining for neural marker, Tuj-1 in recipient cells 3 days after co-culture with undifferentiated or differentiated donor cells in the presence of anti-miR-193a.

FIGURE 24. Schematic depiction of the microfluidic cell culture system.

FIGURE 25. Procedure for preparation of hydrogel-incorporating microfluidic cell culture system.

FIGURE 26. Live imaging to track for exosomes from GFP-exosome donor F11 cells cultured with recipient F11 cells.

FIGURE 27. Representative fluorescence images show moving exosomes from donor cells to recipient cells in gel region.

FIGURE 28. Time-lapse images for uptake of exosomes by recipient cells incorporated with hydrogel.

FIGURE 29. 3D fluorescence images for exosomes in recipient cells of neural stem and progenitor cells in the microfluidic assay.

FIGURE 30. Microfluidic cell culture assay for exosome-mediated transfer of miR-193a.

FIGURE 31. Phase contrast images for morphology of recipient cells incorporated with hydrogel 4 days after co-culture.

FIGURE 32. Immunofluorescence staining for the expression of Tuj-1 and MAP2 in donor and recipient cells 4 days and 7 days after co-culture.

FIGURE 33. Inhibition of exosome biogenesis impairs transfer of exosome and the induction of neurogenesis in recipient F11 cells.

FIGURE 34. Exosome-mediated neurogenesis in neural stem cells.

FIGURE 35. Inhibition exosome-mediated neurogenesis by blocking exosome secretion in neural stem cells.

FIGURE 36. Representative scheme for elevated neuronal differentiation by exosome-mediated miR-193a transfer.

Table 1. Top 17 upregulated miRNAs in F11 cells following the expression of Ngn 1

Table 2. List of qRT-PCR primers sequences for neuron-specific genes and target genes of miR-193a used in the study

LIST OF ABBREVIATIONS

NSCs, Neural Stem Cells

NPs, Neural Progenitor Cells

EVs, Extracellular Vesicles

ECM, ExtraCellular Matrix

Effluc, Enhanced FireFly Luciferase

db-cAMP, dibutyryl-cAMP

CMV, CytoMegalo Virus

qRT-PCR, quantitative Reverse Transcription-Polymerase Chain Reaction

NTA, Nanoparticle Tracking Analysis

PDMS, poly-dimethylsiloxane

FBS, Fetal Bovine Serum

BCA, BicinChoninic acid Assay

Ngn1, Neurogenin1

DAVID, Database for Annotation, Visualization, and Integrated Discovery

GO, Gene Ontology

UD cells, Undifferentiated cells

D cells, Differentiated cells

UD-Exo, exosomes isolated from undifferentiated F11 cells

D-Exo, exosomes isolated from differentiated F11 cells

INTRODUCTION

Reciprocal information exchange between cells is crucial *in vivo* for cellular proliferation and differentiation in cell-non-autonomous way (Harandi and Ambros, 2015; Zhang and Wrana, 2014). Also known as spatiotemporal regulation of development, the leading cells deliver the information to the neighboring cells using small molecules, peptide or lipid mediators (Lo Cicero et al., 2015). This phenomenon warrants *in vitro* simulation such as neuronal differentiation. During neuronal differentiation, different intra- and extracellular signals stimulate neural stem cells (NSCs) to become neural progenitor cells (NPs), which ultimately irreversibly exit from the cell cycle to begin the first step of neurogenesis (Gage, 2000; Li and Jin, 2010). NSCs and NPs can differentiate into all the cell types that constitute the central nervous system (CNS; Gage, 2000; Li et al., 2008; Li and Jin, 2010; Liu et al., 2009; Markakis et al., 2004; Roese-Koerner et al., 2013). NPs divide asymmetrically and one of the two daughter cells obtains a reduced self-renewal potential and finally differentiates into a neuron (Gage, 2000; Markakis et al., 2004). During the induction of neurogenesis, gene expression or networks responsible for regulation of cell proliferation must be tightly controlled (Markakis et al., 2004). Even in immortalized lines of NSCs or NPs, extra-chemicals treatment (cAMP, retinoid acid; Cho et al., 2001; Kim et al., 2004) or transgenes (neurogenin1, neuroD; Cho et al., 2001; Kim et al., 2002; Kim et al., 2004; Oh et al., 2013a) were sufficient to induce cell differentiation into the neuronal lineage by regulating relevant signal transduction pathway. However, it is unclear how

undifferentiated cells generate a large number of differentiated neurons and whether inter-cellular signals regulate the neuronal differentiation process. I thought that extracellular vesicles (EVs) including exosomes are related to generate a large number of differenentiated neuron in cell-non-autonomous manner.

1) Extracellular vesicles (EVs)

Cells communicates using soluble factors, such as adhesion molecules related to cell-to-cell interaction including cytonemes that enable ligand–receptor-mediated transfer of surface-associated molecules by connecting adjacent cells, or nanotubules that facilitate the transfer of surface and cytoplasmic molecules by tunneling between cells (Majka et al., 2001; Rustom et al., 2004; Sherer and Mothes, 2008). Recent studies have suggested that extracellular vesicles (EVs), circular membrane fragments, were discovered in communication between many cells (Ratajczak et al., 2006b). Extracellular vesicles (EVs) were also proposed as vehicles of the information transfer between cells, heterogeneous or autologous (Camussi et al., 2013; Yuan et al., 2009). These vesicles are secreted from various cell types including reticulocytes (Pan and Johnstone, 1983), dendritic cells (Thery et al., 1999), B cells (Raposo et al., 1996), T cells (Blanchard et al., 2002), neuronal cells (Cossetti et al., 2012) and tumour cells (Mears et al., 2004). In the CNS, extracellular vesicles (EVs) are secreted from all type of cells, such as microglia, oligodendrocytes and neurons, and have been suggested to contribute to the physiology of the nervous system (Cossetti et al., 2012; Fruhbeis et al., 2012).

EVs were discovered as vesicles-shaped in the interstitial space of tissues or in blood using electron microscopy. They were considered as the fragment of plasma membrane turnover or the debris from damaged cells for a long time (Siekevitz, 1972). EVs were made from endosomal membrane compartment after fusion of plasma membrane, released from cell surface of activated cells as exosomes (Heijnen et al., 1999; Rozmyslowicz et al., 2003). And EVs may also derived from direct budding with plasma membrane of cells as shedding vesicles (Cocucci et al., 2009). Secreted EVs may stay in the interstitial or extracellular space of adjacent region from the place of origin or may move in the biological fluids spreading distant region. This can support the existence of EVs in the urine, mild, cerebrospinal fluid (CSF) and plasma. EVs observed in the circulation were derived from platelets (George et al., 1982). The secretion of EVs may be following cell activation by soluble factors, by shear stress, by chemical stress including hypoxia and oxidative stress (Camussi et al., 2010).

Exosomes are endosome-originated a size raging 50-150 nm small vesicles (Heijnen et al., 1999). They are stored in multivesicular bodies (MVB) as intraluminal vesicles and secreted after fusion of multivesicular bodies and cell membrane (Camussi et al., 2010). They are also released by exocytosis using a mechanism of the regulation for p53 protein and cytoskeleton activation (Yu et al., 2006). It is considered that EVs are important part of the intercellular microenvironment and play a role of regulators for cell-to-cell communication (Camussi et al., 2010). EVs secreted from various cells may connect through specific receptor ligands with other cells, stimulating target cells or by delivering

surface receptor (Janowska-Wieczorek et al., 2001; Morel et al., 2004). This communication may lead to cell signaling or be restricted to a receptor-mediated binding to the surface of recipient cells by forming multimolecular complexes. And it was followed by internalization throughout uptake by recipient cells or direct fusion (Cocucci et al., 2009). After internalization, EVs were fused with their membranes to those of endosomes, leading to the delivery of their components in the cytosol of recipient cells (Camussi et al., 2010). Recent studies represent that EVs may transfer mRNAs and miRNAs to target cells (Yuan et al., 2009). Of the EVs, exosomes are known to mediate intercellular communications via delivery of their components, including proteins, mRNAs or miRNAs (Valadi et al., 2007). In particular, extracelluar vesicles harbor a variety of miRNAs (Deregibus et al., 2007; Skog et al., 2008; Valadi et al., 2007), which can deliver genetic information to recipient cells and regulate their function (Deregibus et al., 2007; Pegtel et al., 2010; Ratajczak et al., 2006a; Skog et al., 2008; Zernecke et al., 2009). They show that miRNAs are contained in EVs derived from ESCs and that they can delivery to mouse embryonic fibroblasts *in vitro* (Yuan et al., 2009). MiRNAs play an important role of regulators form protein translation and it can provide clues that stem cells can control the expression of genes in target cells by EVs-mediated transfer of miRNAs (Camussi et al., 2010).

2) MicroRNA (miRNA)

MiRNAs are small non-coding regulatory RNAs of approximately 22 nucleotides in length that are derived from hairpin precursors (pre-miRNA) and devide several defined features (Zeng and Cullen, 2006). These structural features were made by the nuclear ribonuclease III (RNaseIII) enzyme Drosha, which cleaves the primary miRNA transcript (pri-miRNA) to produce an approximately 70–100 nucleotide premiRNA. Drosha cleaves the structure of RNA hairpins that have a large terminal loop (usually ~10 nucleotides), at a part of approximately two helical RNA turns into the stem to yield the pre-miRNA (Zeng et al., 2005). After then, This precursor is translocated to the cytoplasm by exportin (Kim et al., 2004a), a nuclear export molecule that binds to pre-miRNAs and in a Ran guanosine triphosphate-dependent manner (Lund et al., 2004; Yi et al., 2003). A second cleavage has taken placed in the cytoplasm and another RNAase III enzyme named Dicer and another double-stranded RNA-binding domain protein named loquacious were related to the action of a complex (Forstemann et al., 2005; Saito et al., 2005). After cleavage, the RNA duplex was unwound. An RNA-induced silencing complex (RISC), a complex of proteins that is responsible for silencing the target RNA was involved in asymmetries in the duplex, one strand of duplex, named the guide strand that is usually avoid for delivery to RISC. Several mechanisms for RNA silencing such as RNA interference (RNAi) and the miRNA pathway have been proposed. The Dicer substrate related to RNAi is entirely double stranded and then, a short interfering RNA (siRNA) was made from the cleavage. Finally, the targeted complementary RNA was destructed. In the RNAi pathway, target RNAs of miRNA can be suppressed at the post-transcriptional level or undergo degradation. It may depend

on the degree of complementarity of the duplex between the guide strand and its target RNAs (Bartel, 2004; He and Hannon, 2004; Sempere et al., 2004). MicroRNAs bind to complete or partial complementary pairing in the 3′-untranslated region (3′UTR) of target mRNAs, leading to the degradation of target mRNAs or translational inhibition of the target mRNAs (Bartel, 2004). For good complementarity, the 5′ end of the miRNA seed region need to be crucial for the recognition of target mRNAs (Kosik, 2006). MicroRNAs are participated in diverse biological processes, including developmental stages, cellular proliferation, differentiation, and cell death (Brennecke et al., 2003; Dostie et al., 2003; Reinhart et al., 2000; Xu et al., 2003). MiRNAs have been shown to regulate differentiation of various types of cells such as neurons, adipocytes, myoblasts and osteoblasts (Eskildsen et al., 2011; Gagan et al., 2011; Jing et al., 2011; Karbiener et al., 2011). Representative miRNAs playing essential roles in neurogenesis are let-7, miR-124 and miR-9, which are highly conserved during evolution and have been shown to promote differentiation of NSCs and NPs into neuronal cells (Akerblom and Jakobsson, 2013; Delaloy et al., 2010; Makeyev et al., 2007; Meza-Sosa et al., 2014; Zhao et al., 2013). These miRNAs are delivered within exosomes to recipient cells and regulate neurogenesis (Delaloy et al., 2010; Zernecke et al., 2009). MiR-124a and miR-9 have been associated in the decision of a mouse neural precursor to differentiate into a neuronal or glial lineage (Krichevsky et al., 2006). These miRNAs were identified after neurogenesis in mouse embryonic stem cell *in vitro* by expression profiling of miRNAs, which represented the simultaneous induction of several miRNAs during neurogenesis from neural progenitor cells to neurons

and astrocytes. The expression of these miRNAs was correlated to the onset of that during embryonic neurogenesis *in vivo* (Kosik, 2006).

3) Neurogenesis

Neurogenesis is controlled by a variety of miRNAs; thus, novel types of miRNAs are possibly responsible for governing neurogenesis. Neurogenesis (birth of neurons) is the process that new neurons are generated from neural stem and progenitor cells. It plays a crucial role in neural development. Neurogenesis is most important process during pre-natal development and is responsible form growing brain with new neurons (Ming and Song, 2011). The neural stem cells are undifferentiated cells and have a capability for self-renewal and differentiation (Bryder et al., 2006; Mimeault and Batra, 2006; Mimeault et al., 2007). When some of stem cells differentiated into a defined cell fate, they became progenitor cells. Recent studies suggested that niche of stem cells, interacted with the microenvironment, play a crucial role in defining the stem cell phenotypes (Quesenberry and Aliotta, 2008). EVs have a regulatory task by delivering genetic information between cells. They proposed that a continuous genetic modulation by EVs-mediated transfer of genetic information between cells is important factor of stem cell fate variation. Indeed, stem cells are an abundant source of EVs. EVs are related to paracrine effect of signaling between stem cells and differentiated cells by transferring several selected molecules of proteins, mRNAs and microRNAs (Camussi et al., 2010).

In this study, I focused on the miRNAs with neurogenic function of the exosome carrying molecules. Therefore, I firstly performed miRNA microarray to identify miRNA, functions to induce neurogenesis during neurogenesis in neural progenitor cells.

4) MiRNA microarray

MiRNAs microarray analysis is a powerful high-throughput tool to study the miRNAs expression profiling. Microarray technology has been generally used for the identification of new miRNAs that were for comparison of miRNA expression profiles from different tissue or cells and a genome-wide analysis of miRNA expression. MiRNAs microarray analysis is also useful to investigate the expression profiles of miRNAs during differentiation, development, oncogenesis, and processes of other disease (Liu et al., 2008). Moreover, miRNA microarrays need a small amounts total RNA to evaluate the miRNAs expression profiles in the sample at once.

Therefore, to further understand the involvement of miRNAs in neurogenesis, I performed the miRNA microarray expression profiling method. I identified an exemplary miRNA that mediates neurogenesis to find miR-193a as a model in F11 cells and investigated whether this neurogenic miR-193a within exosomes from the NPs of precedent differentiation migrates to neighboring cells to facilitate neurogenesis in 2D and transwell co-culture system.

5) Co-culture system

Transwell co-culture systems are widely used to study for migration, invasion and chemoattractant responses of the cells and exosome transfer between cells cultured on filters of upper chamber. However, they can't visualize in real time at high-resolution or regulate various condition of extracellular microenvironments (Shin et al., 2012). In contrast, microfluidic co-culture system has the ability to observe cell-to-cell communication, cell-matrix interaction and spatial-temporal single-cell behavior at high-resolution in real-time imaging. Moreover, they are able to detect the various complex behaviors of *in vivo* microenvironment, compared with 2D or transwell co-culture systems *in vitro* assays (Shin et al., 2012). Therefore, in this study, I used microfluidic co-culture systems to acquire time-lapse real-time imaging for exosome transfer during neurogenesis. In addition to co-culture and transwell culture experiments, real-time singleton imaging of the migration of miR-193a-containing exosomes was realized using a customized microfluidic device. This microfluidic system was to simulate *in vivo* cell-non-autonomous mechanism of cellular interaction under *in vitro* setting using tissue-mimetic architectures under controllable fluidic microenvironment (Shin et al., 2012). They could be used to reconstitute *in vitro* tissue-mimetic architectures under controllable fluidic microenvironments. Using the well-organized microfluidic technique, I established a device to monitor the dynamics flow of GFP-tagged exosomes through the gel barrier mimicking extracellular matrix (ECM) from donor to recipient cells. And I also used miRNA imaging reporter system to detect the expression and exosome-mediated transfer of miR-193a during neurogenesis.

6) MiRNA optical reporter gene

An optical reporter system has been widely used to evaluate the expression and biogenesis of target miRNA *in vitro* and *in vivo* (Ko et al., 2009b; Ko et al., 2008; Lee et al., 2008). MiRNA reporter gene used a seed sequence of target genes, fused with their 3' UTR. Reporter gene construct are designed to contain multiple copies of seed sequence of miRNA target between reporter exon and their poly (A) tail. If miRNA is bound to target sequences, the activity of reporter gene is down-regulated, called as a "signal-off system" (Oh et al., 2013b). In this study, I used miRNA optical imaging reporter gene using a bioluminescence reporter to detect the expression of miR-193a. Because the bioluminescence signals can be detected only in case of an enzymatic reaction between a luciferase and its substrate, bioluminescence reporter gene is advantageous over fluorescence-based reporter in terms of high signal to background ratio. I designed microRNA bioluminescence reporter system using firefly luciferase (Fluc), bioluminescent proteins, to monitor miR-193a expression levels during neurogenesis and to validate the delivery of miR-193a from donor to recipient cells during neurogenesis. As exosomes are known to participate in regulating physiological function, I hypothesized that differentiated neurons could communicate with adjacent undifferentiated cells to accelerate their neurogenesis by transferring neurogenic miRNAs via exosomes and that this phenomenon could be a key modulatory process for neuronal differentiation in cell-non-autonomous fashion. Therefore, in this study, I (1)

discovered a novel miR-193a responsible for governing neuronal differentiation by down-regulating target genes, and (2) established a microfluidic system to acquire time-lapse live images of exosome secretion, migration, and uptake from differentiated cells state to undifferentiated cells, and (3) elucidated the new phenomenon that miRNA-containing exosomes secreted from differentiated neurons, once delivered to the undifferentiated NP cells, facilitate the progression toward a neuronal fate.

MATERIALS AND METHODS

Microarray Analysis

Total RNA was isolated during neuronal differentiation induced by Ngn1 in F11 cells by using Trizol (Invitrogen). For control and test RNAs, the synthesis of target miRNA probes and hybridization were performed using the GenoExplorer™ miRNA Labeling Kit (GenoSensor) according to the manufacturer's instructions. Briefly, for biotin labeling the 5′-end of uncapped RNA, 5 ~ 10 μg of total RNA were labeled with Enzyme L, followed by incubation for 3 h at 37 °C. The biotin-labeled RNA was combined with the same volume of Hyb buffer (GenoSensor), boiled for 5 min, and pipetted onto GenoExplorer™ miRNA Biochip (GenoSensor). Hybridization was performed for 16 h at 42 °C using LifterSlip™ (GenoSensor) according to the manufacturer's instruction. After incubation for hybridization, first wash was performed and microarrays were spin-dried. For fluorescent dye staining, SA-S (streptavidin-stain) dye was added onto the chips on which the biotin-labeled RNAs were hybridized, followed by incubation for 30 min at 25 °C. Finally, hybridized microarrays were washed to remove non-specific binding, dried, and scanned with a GenePix 4000B scanner (Axon Instruments). The hybridized

images were quantified with GenePix Software (Axon Instruments). All data normalization and selection of fold-changed genes were performed using GeneSpringGX 7.3 (Agilent Technology). The averages of normalized ratios were calculated by dividing the average of normalized signal channel intensity by the average of normalized control channel intensity.

Gene Annotation Analysis.

Functional annotation for target genes of candidate miRNAs was carried out by searching the Database for Annotation, Visualization, and Integrated Discovery (DAVID 6.7) (National Institute of Allergy and Infectious Diseases, NIH) (david.abcc.ncifcrf.gov). Functional annotation categories included Gene ontology (GO) terms, protein–protein interactions, molecular function, cellular component, protein functional domains, and biological pathways. This program provides the functional annotation chart that lists annotation terms and their associated genes. To avoid excessive counting of duplicated genes, the Fisher's exact test was used for calculations based on corresponding DAVID gene IDs.

Cell culture and transfection

F11 cells, rat dorsal root ganglion and mouse neuroblastoma hybrid cells, and HeLa cells (human cervical cancer cells) were cultured in Dulbecco's modified Eagle's medium (DMEM, Gibco) containing with 10% fetal bovine serum (FBS; Gibco), 10 U/ml penicillin, and 10 μg/ml streptomycin. The NE-4C, neural stem cell line, established from cerebral vesicles of $p53^{-/-}$ 9-day-old mouse embryos was obtained from the American Type Culture Collection (ATCC). The NE-4C cells

were routinely cultured in Dulbecco's modified Eagle's medium (DMEM, Gibco) containing with 10% fetal bovine serum (FBS; Gibco), 10 U/ml penicillin, and 10 μg/ml streptomycin. The cells were maintained at 37 °C in a humidified 5% CO_2 atmosphere. HeLa cells were plated on 24-well plates and co-transfected with the pRV-effluc-miR-193a_3XPT reporter gene, chemically modified miRNA-193a and miRNA-scr (Ambion®) using Lipofectamine2000 (Invitrogen) and diluted in OPTI-MEM medium (Gibco). The transfected cells were incubated in DMEM supplemented with 10% FBS for 2 days. F11 cells expressing an enhanced firefly luciferase (effLuc) reporter gene containing three copies of complementary binding sequence for miR-193a (designated as pRV/effLuc/3xPT_miR-193a) were established through retroviral infection. F11 cell/effLuc/3xPT_miR-193a cells were transfected with pcDNA/His-Ngn1 and pcDNA3.1/His (B) using Lipofectamine2000 (Invitrogen) and resuspended in OPTI-MEM medium (Gibco). The transfected cells were cultured in DMEM supplemented with 0.5 % FBS for 24 h. For induction of neuronal differentiation, F11 cells were treated with DMEM containing 0.5% FBS and 1 mM db-cAMP (Sigma) for 3 days or transfected (Lipofectamine2000; Invitrogen) with miR-193a (Ambion®). The NE-4C cells were treated with DMEM containing 2% FBS and 1 μM retinoic acid (RA, Sigma-Aldrich) for 2 days. The medium was replaced with DMEM containing 2% FBS 2 days after RA treatment. F11/effLuc-miR-193a_3×PT cells were treated with anti-miR miRNA-specific inhibitors of miR-193a (Ambion®) using Lipofectamine2000 (Invitrogen) for 2 days. F11 and NE-4C cells were preincubated with manumycin-A (5 μM; Enzo Life Science) before co-culture with recipient cells.

Quantitative reverse transcription-PCR

Total RNA was isolated during the neuronal differentiation of F11 cells using Trizol reagent (Invitrogen) and mirVana™ miRNA Isolation Kit (Ambion®), and was screened for purity and concentration in a Nanodrop-1000 Spectrophotometer (Thermo Scientific). Total RNA (1 μg/ml) was reverse transcribed using reverse transcriptase (Invitrogen) for qRT-PCR analysis. qRT-PCR was performed using neuron-specific primers and primers specific for target genes of miR-193a listed in Table 2. The PCR reactions were performed in triplicate using an ABI® 7500 (Applied Biosystems™) with TaKaRa SYBR Green Master mix (Clontech Laboratories). To normalize the experimental samples, β-actin was used as a control. miRNA was reverse transcribed (RT) with the miRNA 1st-strand cDNA synthesis kit (Agilent Technologies) and RT-PCR amplification was performed with the TaKaRa SYBR Green Master mix (Clontech Laboratories), which is specific for mature miRNA sequences. U6 snRNA was used as an internal control. Exosomal miRNA was isolated using ExoMir™ PLUS Kit (Bioo Scientific). miRNA was reverse transcribed (RT) with the miRNA 1st-strand cDNA synthesis kit (Agilent Technologies) and real-time PCR amplification was performed with the TaKaRa SYBR Green Master mix (Clontech Laboratories), which is specific for mature miRNA sequences. U6 snRNA was used as an internal control. All experiments were conducted in triplicate.

Immunofluorescence staining

F11 cells were fixed with 4% paraformaldehyde (PFA) in PBS for 15 min at room temperature. The cells were then washed 3 times with PBS and treated with 0.5% Triton X-100 in PBS for 5 min at 4 °C to permeabilize cells. The samples were rinsed 3 times with PBS and non-specific binding sites were blocked with 1% normal goat serum in PBS for 1 h at room temperature. Anti- rabbit Tuj-1 (1:1300 dilution; Sigma), anti-rabbit NeuroD (1:500 dilution; Abcam), anti-rabbit MAP2 (1:1000 dilution; Sigma), anti- rabbit GAP43 (1:2000 dilution; Sigma), and anti-rabbit PSD-95 (1:100 dilution; MILLIPORE) antibodies were diluted in PBS and incubated with the samples at 4 °C overnight. The samples were then incubated with Alexa Fluor 488-conjugated anti-rabbit secondary antibodies (Invitrogen) for 1 h at room temperature to visualize the antibody reactions. Nuclei were counterstained with 4'-6-diamidino-2-phenylindole (DAPI, Vector Laboratories) and observed at 461 nm. F11 cells co-cultured in 3D microfluidic device were fixed in 4% PFA-PBS for 15 min at room temperature and washed three times with PBS. After fixation, cells were permeabilized with 0.5% Triton X-100 for 5 min and washed three times with PBS, and then blocked with 1% normal goat serum in PBS for 1 h. Thereafter, diluted primary solutions of Anti- rabbit Tuj-1 (1:1300 dilution; Sigma), anti- rabbit MAP2 (1:1000 dilution; Sigma) were added into the microchannels and incubated at 4 °C overnight. After washing with PBS, Alexa Fluor 488-conjugated anti-rabbit secondary antibodies (Invitrogen) were added and incubated at 4 °C overnight. Cell nuclei were stained with DAPI (Vector Laboratories). Fluorescent images were acquired using a confocal laser scanning microscope (Carl Zeiss LSM 510; Carl Zeiss).

In vitro luciferase assay

Cells were washed with PBS and lysed using a lysis buffer (Promega). The cell lysates were collected with a cell scraper and redistributed into a 96-well plate. The luciferase assay was carried out using a luciferase assay kit (Promega). The bioluminescence intensity of each cell lysate was measured using a microplate luminometer (TR717; Applied Biosystems^{TM}). Each luciferase assay was performed three times, with three replicates per group. Luciferase activity was normalized using total protein content.

Preparation and characterization of exosomes

Exosome-depleted FBS was collected by ultracentrifugation at 150000 × g for 16 h at 4 °C. F11 cells were incubated in DMEM containing 10% exosome-depleted FBS for 2 days or in DMEM containing 0.5% exosome-depleted FBS with 1 mM db-cAMP for 3 days. Cells and debris were removed by serial centrifugation at 500 × g for 10 min and 3000 × g for 20 min at 4 °C. Exosomes were isolated by ultracentrifugation at 150000 × g for 2 h at 4 °C and resuspended in PBS. Protein was estimated using the bicinchoninic acid assay (BCA; Thermo Scientific). Nanoparticle tracking analysis (NTA) system (LM10; Nanosight) was used for measurement of exosome size distribution and particle number.

Fluorescent labeling of exosomes and cells

F11 cells (0.8×10^5 cells per well) were plated in 24-well plates. The CMV-

driven copepod GFP-tagged CD63 vector (System Biosciences) was transfected into F11 cells using Lipofectamine2000 (Invitrogen) and diluted in OPTI-MEM medium (Gibco). The transfected cells were incubated in DMEM supplemented with 10% FBS or 0.5% FBS and 1 mM db-cAMP for 2 days. F11 cells were resuspended in 1 ml PBS and a CM-DiI cell labeling solution (Life Technologies) was mixed directly with PBS (1 μl of CM-DiI labeling solution (1mg/ml) per ml of solution). The F11 cells were then incubated with CM-DiI/PBS for 5 min at 37 °C, and then for an additional 15 min at 4 °C. After labeling, cells were washed with PBS and resuspended in fresh medium. DiI-labeled F11 cells (recipient cells) were seeded into GFP-exosome producing F11 cells (donor cells) 2 days after transfection of the CD63-GFP vector, and then co-cultured for 2 days. Fluorescent images were acquired using a confocal laser scanning microscope (LSM 510; Carl Zeiss).

Transwell assay

In order to monitor the transfer of exosomes, transwell chambers with a PET membrane of 0.4-μm pore size (BD Bioscience) were used. GFP-exosome-producing F11 cells (0.8×10^5 cells per well) were plated on the lower wells and the top chamber (24-well insert; BD Bioscience) were seeded with F11 cells (1×10^4 cells) and then co-cultured for 3 days. For confirmation of exosome-mediated transfer of miR-193a, F11 cells were plated on lower wells and then cultured in DMEM containing 10% FBS or in DMEM supplemented with 0.5% FBS and 1 mM db-cAMP for 2 days. After 2 days, F11 cells treated with 1 mM db-cAMP

were washed with PBS and were maintained in DMEM supplemented with 0.5% FBS. F11/effLuc-miR-193a_3XPT cells into the top chambers (24-well insert; BD Bioscience) and then co-cultured with cells seeded in lower wells for 3 days. For observation of neuronal differentiation by exosomes secreted from differentiated cells, F11 cells were plated on lower wells and then cultured in DMEM containing 10% FBS or in DMEM supplemented with 0.5% FBS and 1 mM db-cAMP for 2 days. F11 cells were cultured in DMEM containing 0.5% FBS 2 days without db-cAMP. F11 cells were added in the top chamber (6-well insert; BD Bioscience) and then cultured with cells seeded in lower wells for 3 and 5 days. F11/effLuc-miR-193a_3×PT cells of lower wells were transfected with anti-miR miRNA-specific inhibitors of miR-193a (Ambion®) for 2 days. The medium was replaced with DMEM containing 2% FBS before co-culture with recipient F11/effLuc-miR-193a_3×PT cells of the top chambers (BD Bioscience). And then, F11 cells of lower cells and top chambers were co-cultured for 3 days. All experiments were performed in triplicate.

Western blotting

Cells were lysed in RIPA buffer, and then centrifuged for 30 min at 12,000 rpm to remove cell debris. Protein concentration was determined using the BCA assay (Thermo Scientific). Equal amounts of protein were resolved by SDS-PAGE and transferred onto PVDF membranes (Millipore). The membrane was probed with primary antibodies against anti-rabbit KRAS, PLAU, CCKAR, CYSLTR1 and GALR1 (1:1000 dilution; Abcam) and exosomal markers such as anti-mouse

TSG101 (1:1000 dilution; Abcam), anti-rabbit CD63 (1:1000 dilution; Santa Cruz biotechnology), and the ER membrane marker, anti-rabbit Calnexin (1:1000 dilution; Abcam) overnight at 4 °C. Membranes were incubated with HRP-conjugated anti- mouse or anti-rabbit secondary antibody for 2 h at room temperature, and proteins were visualized with a chemiluminescence detection system (Promega). The cropped versions of original scanned images are presented in the figures. Band intensities were quantified using AlphaView Software (ProteinSimple) and results are expressed relative to the control condition. Three independent experiments were performed and one set of representative results is shown.

Microfluidic cell culture device

Microfluidic Device Fabrication: A microfluidic device was fabricated by bonding microchannel-patterned PDMS (poly-dimethylsiloxane; Sylgard 184; Dow Corning) to a glass coverslip. The photoresist SU-8 (MicroChem) was used as a master mold, fabricated by a conventional soft-lithography process, to replicate the microchannel-patterned PDMS. PDMS elastomer thoroughly mixed with the curing agent at a 10:1 weight ratio was poured onto the wafer and cured by baking in an oven at 80 °C for 1 h 30 min. After curing, PDMS replica was removed from the wafer and all reservoir patterns on the PDMS replica were punched using dermal biopsy punches (a 6 mm punch for media reservoirs and a 1 mm punch for gel filling reservoirs). The sterilized PDMS replica and glass coverslip were

bonded together via oxygen plasma (Femto Science) and placed at 80 °C in an oven for at least 24 h to restore hydrophobicity of the microchannel surfaces.

Co-culture in the microfluidic system: Collagen type 1 hydrogel (2 mg/ml; BD Biosciences) was injected into two hydrogel channels and gelled for 30 minutes. Medium was then added into the microfluidic channel to prepare cell seeding. Donor cells were seeded in one reservoir of the cell culture channel (left channel) and conditioned medium was added into other reservoir of the cell culture channel (right channel). After cell attachment, only in donor cells of the differentiated group, the medium was replaced with differentiation medium (DMEM containing 0.5% FBS and 1 mM db-cAMP) and freshly refreshed daily. The type 1 collagen hydrogel containing recipient cells were injected into hydrogel channel between the pre-gelled hydrogels to culture recipient cells in 3D microenvironment and incubated at 37 °C in 5% CO_2 atmosphere for 30 min. Density of cells suspended in the type 1 collagen solution was 1×10^6 cells/mL. The hydrogel was diluted to 2 mg/mL in a mixture of 10 × phosphate-buffered saline (PBS; Gibco) and distilled deionized water. The pH of the hydrogel solution was adjusted to 7.4 with 0.5 N NaOH.

Time-lapse imaging of exosomes

Donor cells were seeded in one reservoir of the cell culture channel (left channel) and conditioned medium was added into other reservoir of the cell culture channel (right channel). After cell adhesion, donor cells were transfected with the CMV-driven copepod GFP-tagged CD63 vector (System Biosciences) using

Lipofectamine2000 (Invitrogen) and diluted in OPTI-MEM medium (Gibco). The transfected cells were incubated in DMEM supplemented with 10% for 2 days. Recipient cells suspended in the collagen solution at a density of 1×10^6 cells/mL were injected into hydrogel channel of microfluidic device 2 days after transfection and incubated at 37 °C in 5% CO_2 atmosphere for 30 min. Real-time fluorescence imaging was acquired right after injection of recipient cells. For live-cell imaging, cells were maintained at 37 °C in a 5% CO_2 atmosphere. Exosomes were monitored by time-lapse confocal microscopy (Nikon) at 30s intervals. Fluorescent images were processed and assembled using NIS-Elements Viewer (Nikon).

Bioluminescence imaging

Bioluminescence images for F11/effLuc-miR-193a_3×PT cells (recipient cells) were acquired 1 and 3 days after co-culture with UD or D F11 cells (donor cells). The media were aspirated from the cell channel and washed with PBS. The same volume of 150 μg/ml D-luciferin (Caliper) in PBS was added into both cell culture channels. The device was then placed in an IVIS-100 imager (Xenogen). Bioluminescence images for Fluc activity were obtained 5 min after treatment of D-luciferin (Caliper) in PBS. After imaging, D-luciferin was immediately removed from cells and fresh medium was added into the cell culture channel. The cells were cultured for additional 2 days. Quantitative ROI data for bioluminescence images are expressed as photons per second.

Statistical analysis

Data are displayed as means ± standard deviation (SD) and were assessed using Student's *t*-test. Statistical significance was accepted at *P*-values of < 0.05 or 0.005.

Results

Identification of miR-193a newly associated with neurogenesis in Ngn1-overexpressing F11 cells

In my earlier work (Oh et al., 2013a), neurogenin1 (Ngn1) transcription factor alone was sufficient to accelerate neurogenesis of neural progenitor cells *in vivo*. I identified the key miRNAs involved in Ngn1-induced neurogenesis. MiRNA expression profiles upon microarray analysis of F11 cells treated with Ngn1 for 24 h, and among the 1090 miRNAs present on the array chip, 240 miRNAs exhibited greater than 2-fold changes (Ngn1/Mock) and based on the absolute signal value (> 5) 17 were considered as neurogenic miRNAs (Figure 1). On the scatter plot analysis, 208 miRNAs were up-regulated and 32 were down-regulated that differed 2-fold or greater in F11-Ngn1 cells (Figure 2). Top 17 of up-regulated miRNAs were listed in Table 1. Among the top 17 up-regulated miRNAs, miR-193a satisfied both high fold change and absolute signal value in F11 cells (Figure 3) and its target genes are related to cell cycle and neuronal activity (Figure 4). MiR-193a

targets were predicted using three conventional methods: TargetScan, microRNA.org and microcosm. Gene ontology (GO) analysis revealed that miR-193a targets were closely related to the intracellular signaling cascade (29%), especially regulation of cell proliferation (15%), embryonic development (12%), cellular protein (10%) and macromolecule (9%) localization (Figure 5). The expression of miR-193a was validated by quantitative reverse transcription PCR (qRT-PCR), showing a 5-fold increase in Ngn1-induced F11 cells (Figure 6), which was consistent with the microarray results.

Enhanced neuronal differentiation in neural progenitor cells by overproduction of miR-193a

When F11 cells were treated with miR-scr or miR-193a for 3 days, miR-scr treated cells underwent proliferation and their morphology did not change, miR-193a transfected cells showed a significant neurite outgrowth (Figure 7A). Neuron-specific genes such as Tuj-1, NeuroD and MAP2 expressed significantly higher after miR-193a transfection than miR-scr transfection and synaptic markers PSD-95 and GAP43 showed a tendency to express higher on the qRT-PCR (Figure 7B). Immunofluorescence staining also showed that Tuj-1, NeuroD, MAP2, PSD-95, and GAP43 were highly expressed in the cytoplasm of F11 cells transfected with miR-193a, compared with those in F11 cells treated with miR-scr (Figure 8).

An enhanced firefly luciferase (effLuc) reporter gene vector was engineered to contain three copies of complementary binding sequence for miR-193a at their 3'-UTR (designated as pRV/effLuc/3xPT_miR-193a). The specificity of this reporter

gene was examined in HeLa cells transiently transfected with various concentrations (0, 5, 10, 20, 40 nM) of miR-scr or miR-193a oligomer. The effLuc activity of HeLa cells treated with miR-193a showed a decrease in a dose-dependent manner, unlike those treated with miR-scr (Figure 9A). When F11 cells expressing the above miR-193a reporter gene were treated with 1 mM dibutyryl cyclic AMP (db-cAMP), luciferase activity decreased and showed the shape of differentiated cells (D-F11 cells) different from undifferentiated cells (UD-F11 cells) (Figure 9B). I concluded that miR-193a was highly expressed in F11 cells after their neuronal differentiation by Ngn1 or db-cAMP, and thus miR-193a was the miRNA that promotes neurogenesis in F11 cells. The relevance of miR-193a for neuronal differentiation in neural progenitor cells was examined using the functional classification analysis based on KYOTO Encyclopedia of Genes and Genome Analysis (GeneSifter software). The most significantly affected pathways were those of neuroactive ligand-receptor interaction (five genes), cell cycle (four genes), calcium signaling (four genes), arginine and proline metabolism (three genes), nitrogen metabolism (two genes), SNARE interaction in vesicular transport (two genes), and RNA degradation (two genes) (Figure 10). As the predicted targets of miR-193a involved in neuroactive ligand-receptor interaction were assumed to influence neuronal differentiation, I performed a qRT-PCR to know whether the predicted targets were directly regulated by miR-193a. I also confirmed that the binding sites of miR-193a were in the 3′-UTR of the cholecystokinin A receptor (CCKAR), cysteinyl leukotriene receptor 1 (CYSLTR1), and galanin receptor 1 (GALR1) genes using computational algorithms. Finally,

when the effects of miR-193a overexpression were examined on the expression of its targets including PLAU and KRAS, well-known as target genes of miR-193a, F11 cells treated with miR-scr or miR-193a showed lower expression of these target genes (Figure 11A). Consistent with the decrease in mRNA level of miR-193a target genes on the qRT-PCR, the expression of all the genes, PLAU, KRAS, CCKAR, CYSLTR1 and GALR1 decreased on the western blot analysis 3 days after miR-193a treatment. In particular, the expression of GALR1 decreased most by miR-193a (Figure 11B). Neuronal differentiation in F11 cells by miR-193a is accompanied by the regulation of target genes of the neuroactive ligand-receptor pathway.

Elevated levels of miR-193a in differentiated F11 cell-derived exosomes

I postulated that miR-193a are secreted within the exosomes and transported from D-F11 cells to the adjacent UD-F11 cells to accelerate the neurogenesis of these cells. I isolated the exosomes from D-F11 cells after F11 cell were cultured in DMEM containing 0.5% depleted-FBS and 1 mM db-cAMP for 3 days when neurite elongation was observed as was reported (Figure 12A; Cho et al., 2001; Kim et al., 2002). I performed western blot analysis to examine whether isolated exosomes have exosomal protein markers including CD63, and TSG101 in the exosomes (D-Exo) isolated from D-F11 cells as well as in the exosomes (UD-Exo) from UD-F11 cells. Calnexin, an ER membrane marker, was not detected in either group (Figure 12B) indicating that exosomes were purified without contamination of cell debris. Nanoparticle-tracking analysis (NTA) of the isolated UD-Exo and D-

Exo showed a relatively uniform distribution of their size with a peak diameter of approximately 150-200 nm (Figure 13). When I purified exosomes (D-Exo and UD-Exo) and measured the total protein concentration, D-Exo showed an approximately 6-fold increase in total protein, compared to UD-Exo per the same number of D-F11 or UD-F11 cells (Figure 14A). On the qRT-PCR, exosomal miRNAs (D-Exo) were quantified and high amount of miR-193a was found in D-Exo, compared to miR-193a level in UD-Exo (Figure 14B).

Exosomes-mediated transfer of miR-193a from differentiated cells to undifferentiated cells

As I hypothesized that the initially differentiated single neurons (pioneers) induced by db-cAMP in a clonal population influence undifferentiated cells (followers) and promote their differentiation into neuronal cells by transferring neurogenic miRNAs-loaded exosomes, transwell system was used for the examination of transfer of exosomes and its functional outcome on the undifferentiated cells. The migration of exosomes between undifferentiated and differentiated F11 cells was tracked using a vector containing CD63 fused with GFP according to the previous report (Mittelbrunn et al., 2011). When GFP-tagged CD63 plasmid vector was transfected into F11 cells, fluorescence were clearly seen in the cytoplasm of D-F11 cells indicating the endogenous exosomes under production before excretion. When CD63-GFP-transfected F11 cells were cultured with normal or differentiation-inducing medium for 2 days, endogenous exosomes were produced in D-F11 cells stained with Tuj-1 marker as well as in UD-F11 cells without any markers (Figure 15). CD63-GFP-transfected F11 cells (donor cells)

were pretreated with db-cAMP (D-F11 CD63-GFP cells) or none (UD-F11 CD63-GFP cells) and then DiI-labeled F11 cells (recipient cells; UD-F11 DiI cells) were mixed (1:1), followed by co-cultured with donor cells for 2 days. In this co-culture system, CD63-GFP-exosomes were transferred from donor D-F11 cells into recipient UD-F11 DiI cells (Figure 16).

Transwell chambers with polyethylene terephthalate membranes of 0.4 μm pore size allowed passage of exosomes but prevented larger microvesicles (ranging 0.1 ~ 1 μm in diameter) and apoptotic bodies (> 1 μm in diameter) from passing through the pores. Recipient UD-F11 cells added to the upper insert chamber showed GFP-exosomes in the cytoplasm when co-cultures with donor D-F11 CD63-GFP cells plated in the bottom plate under the time course and procedural scheme depicted in Figure 17. Recipient UD-F11 infected with effLuc-miR-193a_3XPT in the upper insert chamber showed an increase of the luciferase activity along with cell proliferation. When co-cultured with donor D-F11 CD63-GFP cells after db-cAMP treatment, the luciferase activity of recipient UD-F11/effLuc-miR-193a_3XPT cells decreased (Figure 18), which recapitulated that miR-193a was shuttled within the exosomes. These co-culture and transwell experiments confirmed that both miR-193a and exosomes are delivered from differentiated to undifferentiated cells and along with these transfers, the recipient cells came to differentiate into neuronal lineage. Combined with the previous finding that D-F11 derived exosomes contained miR-193a, the modest speculation until now was that miR-193a will be the messenger in the exosomes which travels from differentiated neural progenitor cells to the undifferentiated cells.

I next tested morphological and functional outcomes upon the recipient UD-F11 cells induced by transfer of miR-193a via exosomes secreted from D-F11 cells. Neurite extension was shown in recipient cells cultured with D-F11 cells at 3 days and 5 days after co-culturing, but not in UD-F11 cells. Neuronal markers of Tuj-1 and MAP2 were found 3 and 5 days of co-culture in recipient cells using qRT-PCR (Figure 19A) and on immunofluorescence results (Figure 19B). The mRNAs of target genes (CCKAR, CYSLTR1) of miR-193a in the neuroactive-ligand receptor pathway decreased in the recipient cells (Figure 20) while neurogenic miRNAs such as miR-193a and miR-124a increased in recipient cells on qRT-PCR (Figure 21). These results indicated that miR-193a in the exosome delivered from the donor D-F11 cells to the recipient UD-F11 cells, was active and resulted in functionally significant outcome in the recipient cells such as down-regulation of the target genes of miR-193a.

To verify the contribution of miR-193a for inducing neurogenesis, the expression of miR-193a was inhibited in differentiating donor cells by treatment of chemically modified antisense miR-193a. Luciferase activity from donor F11/effLuc-miR-193a_3×PT cells was not decreased in differentiating donor cells treated with anti-miR-193a. The expression of miR-193a was also repressed in recipient cells cultured with differentiated donor cells in presence of anti-miR-193a 3 days after co-culture (Figure 22). The induction of neurogenesis was also inhibited in recipient cells cultured with differentiated donor cells after the inhibition of miR-193a expression (Figure 23). These results represented that miR-193a act as the one of key players to induce neurogenesis.

Visualization of transport of individual exosomes using a microfluidic device

To visualize intercellular delivery of exosomes for neuronal differentiation, I designed a microfluidic device for time-lapse live imaging of exosomal transport. Compared with transwell, microfluidic cell culture device provides high-resolution real-time imaging and controllability on micro-scale fluidic microenvironment to be feasible as molecule and exosome transport advective by interstitial flow and diffusive by diffusion, which might be distinct from macro-scale behavior. In this study, hydrogel-incorporating microfluidic device was used to visualize exosome transport from UD or D-F11 cells to UD-F11 cells (Figure 24). Basic protocol came from previous study (Shin et al., 2012), but was revised for the specific goal of visualizing exosome transport. Cells were seeded 3-dimensinoally in type 1 collagen extracellular matrix (ECM) hydrogel, sequentially filled during several days to form multi-compartment. Recipient F11 cells were injected into the middle channel with gel 2 days later than seeding and transfecting of donor F11 CD63-GFP cells in the left channel (Figure 25). Fluorescent images were obtained using live-cell confocal microscopy at 30-sec intervals. Exosomes from donor cells moved in the cell culture channel during the first 4 min 30 sec and moved into the interfiber space of type 1 collagen hydrogel (Figure 26). Following images showed that exosomes clearly transported to the recipient cells 3-dimensionally through type 1 collagen hydrogel for the next 8 min (Figure 27). Time-lapse imaging of CD63-GFP-tagged exosomes showed that exosomes were transported from donor to recipient and successfully attached and taken up by recipient cells in 1 to 3 min

(Figure 28). Z-stack images using confocal microscopy of recipient cells proves uptake of exosome by the recipient, by exosome color change to yellow due to co-localization. 3D reconstruction of Z-stack images showed exosomes accumulated in recipient cells co-cultured with D donor cells. This phenomenon was also observed in recipient cells co-cultured with UD-F11 cells and NE-4C neural stem cells (Figure 29).

Reporting the action of exosomally delivered miR-193a in recipient F11-UD cells on microfluidic chamber

F11 cells infected with effLuc/3xPT_miR-193a reporters were seeded to the right channel of the microfluidic device as recipients and donor F11 cells were seeded to the left channel (Figure 30A). Two days after the culture with normal or differentiation (db-cAMP) medium, the medium of donor cells was changed to DMEM containing 0.5% FBS without db-cAMP. Bioluminescence signals of recipient UD-F11 cells/effLuc/3xPT_miR-193a began to decrease after 1 day and significantly decreased after 3 days with donor D-F11 cells compared with the donor UD-F11 cells (Figure 30B). Quantitative analysis showed significant decrease after 5 days (Figure 30C). Mir-193a delivered within exosomes was functionally active by binding to the targets of the 3'-UTR of effLuc/3xPT_miR-193a reporters. Recipient UD-F11 cells responded to the donor D-F11 cells but not to donor UD-F11 cells after 4 days, in terms of morphological changes such as neurite outgrowth (Figure 31) and immunofluorescence study for neuron-specific markers, Tuj-1 and MAP2 (Figure 32). These results are consistent with the

immunofluorescence findings from the transwell culture studies.

To confirm whether neurogenesis of recipient cells is mediated by exosomes released from differentiated donor cells, I blocked exosome production in differentiated donor cells. Ceramide produced by neutral sphingomyelinase-2 (nSMase2) triggers the budding of exosomes into multivesicular bodies (MVBs). Therefore, inhibition of nSMase2 causes the reduction for the secretion of CD63-containing exosomes (Trajkovic et al., 2008). The secretion of exosomes from the differentiated donor cells and the transfer of CD63-GFP were impaired when nSMase2 activity was inhibited by treatment of manumycin-A. Interestingly, the induction of neurogenesis in recipient cells was also inhibited by addition of the inhibitor manumycin-A in the differentiated donor cells (Figure 33). These results indicate that exosomes from differentiated donor cells act as a key player to induce neurogenesis of undifferentiated recipient cells. Moreover, this phenomenon, neurogenesis induced by exosomes released from differentiated cells, was also observed in neural stem cells (Figure 34 and 35). Proliferative target genes of miR-193a were down-regulated during the above neuronal differentiation induced by exosomal transfer of miR-193a from D-F11 cells (Figure 36).

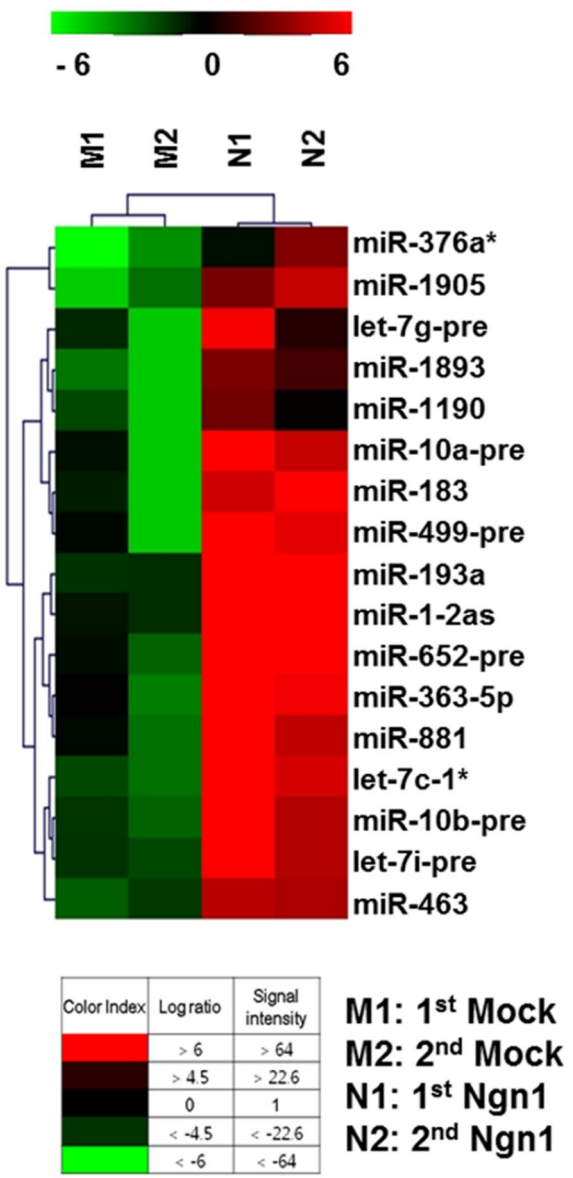

Figure 1. MiRNA expression profiling of F11-Mock and F11-Ngn1 using a miRNA microarray. Data are represented in duplicate. The heat map represents up-regulated genes (red) and down-regulated genes (green). Mock versus Ngn1 array-1 (M1, N1), Mock versus Ngn1 array-2 (M2, N2).

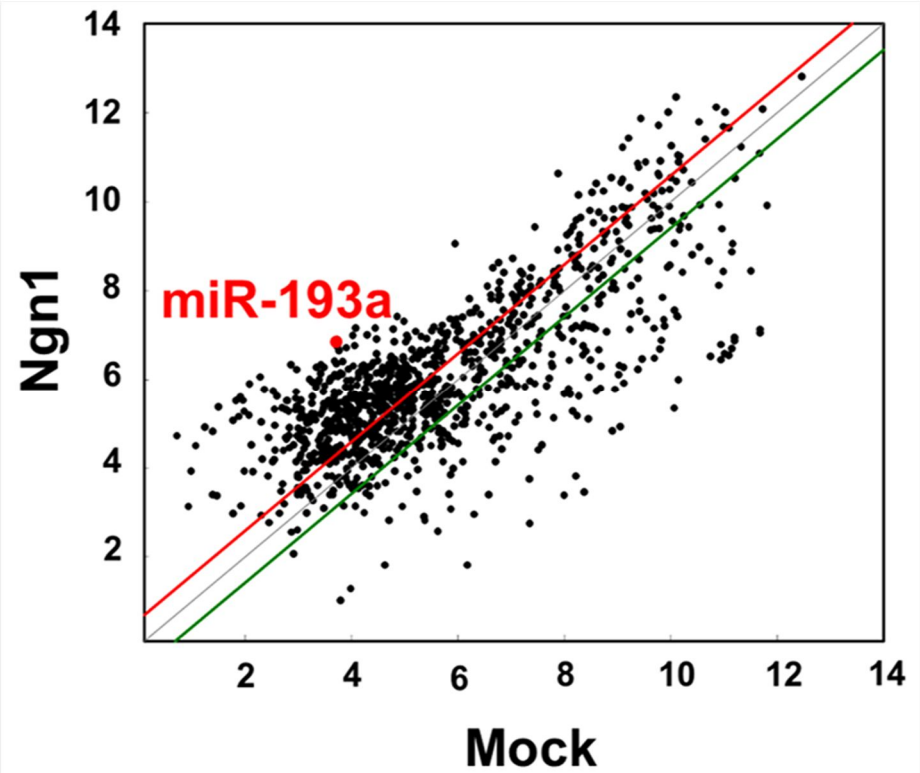

Figure 2. A scatter plot analysis for the normalized signal intensities of miRNAs expressed in F11-Mock and F11-Ngn1 cells.

The 208 up-regulated or 32 down-regulated microRNAs showing 1.5-fold or greater difference were analyzed (*P <0.05)*. MiRNA identified above the center line were up-regulated miRNAs and below the center line were down-regulated. The candidates of neurogenic miRNAs are selected on the scatter plot.

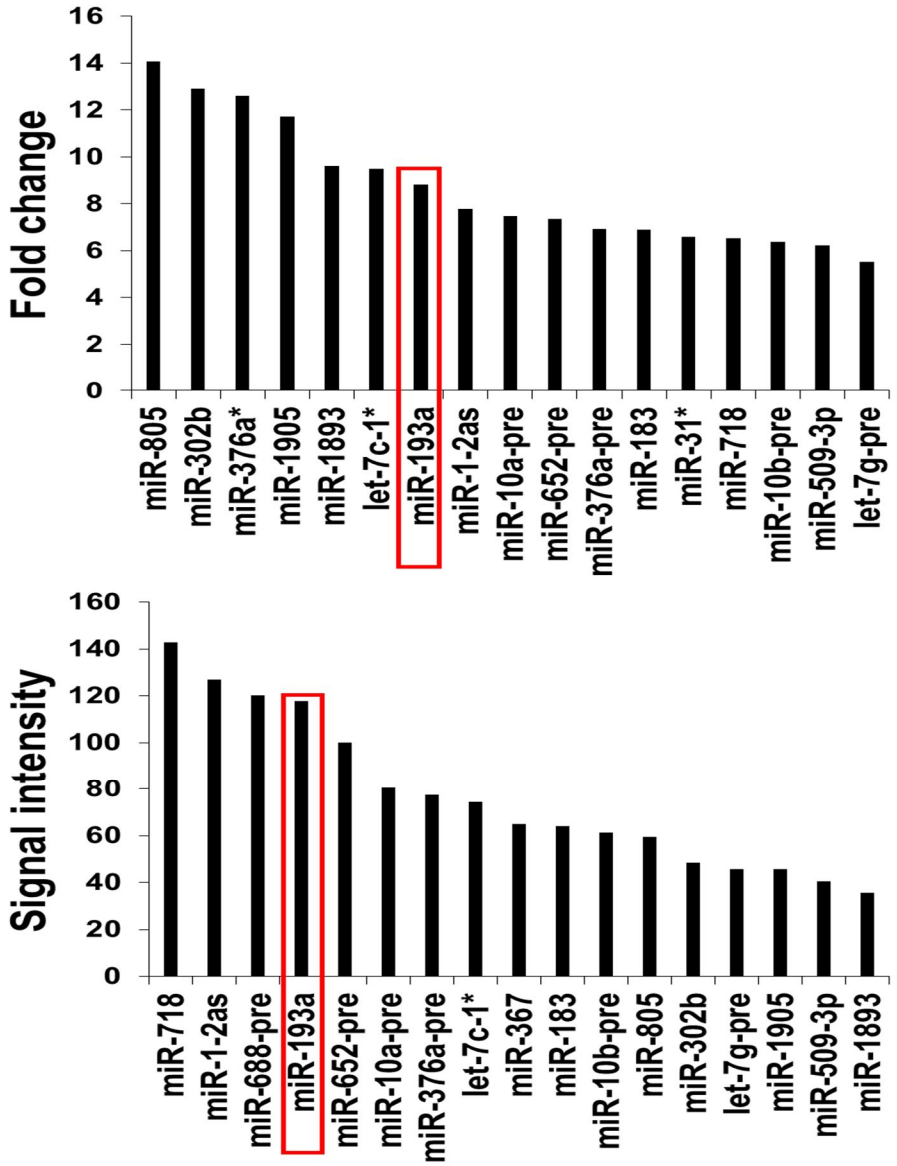

Figure 3. Top 17 of the up-regulated miRNAs.

It based on their significant changes (2-fold change and absolute fluorescence signal value > 5) in F11-Ngn1 cell.

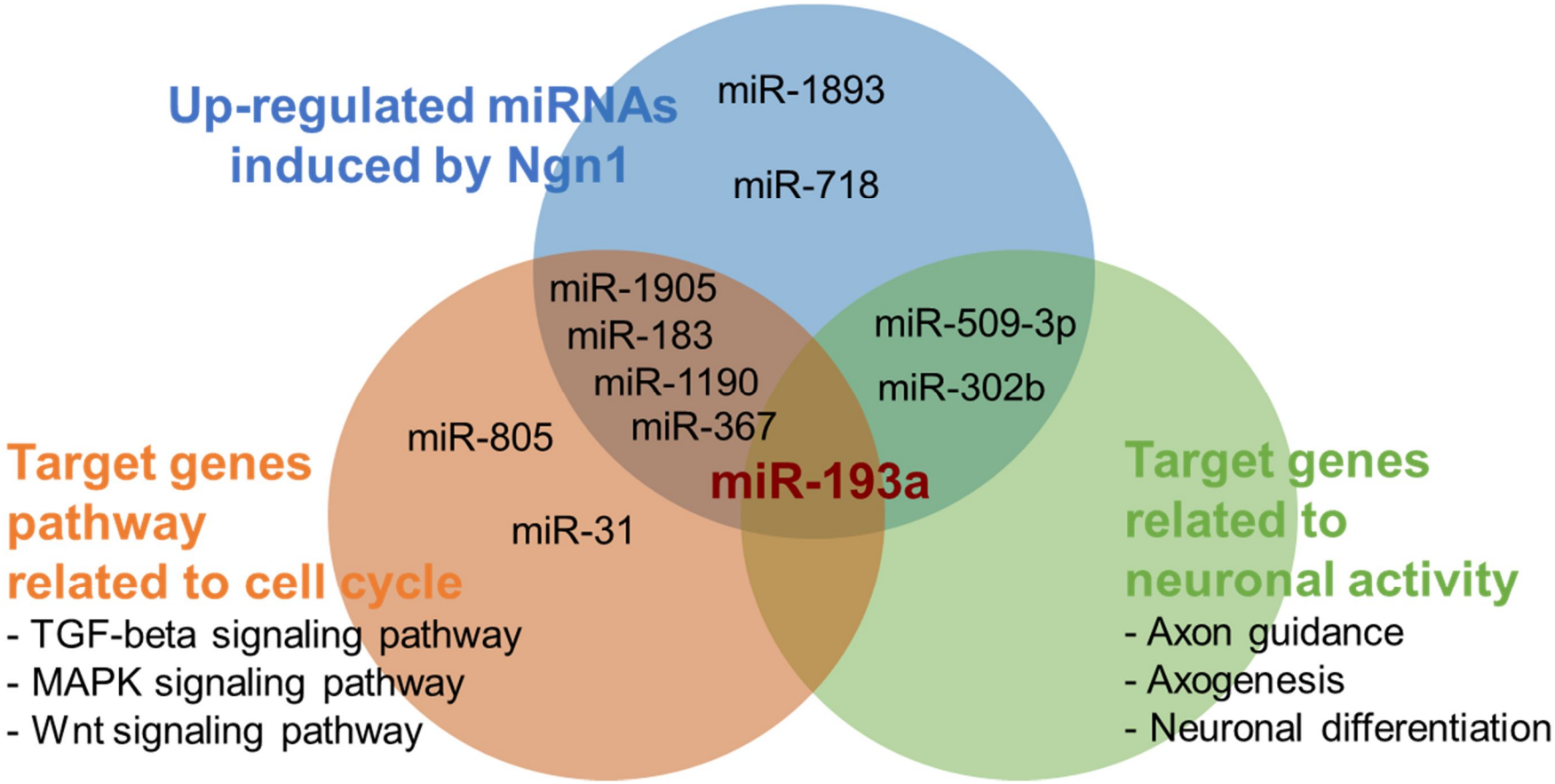

Figure 4. Pie charts for summary of candidate miRNAs.

MiR-193a was up-regulated by Ngn1 and modulated cell cycle and neural activity.

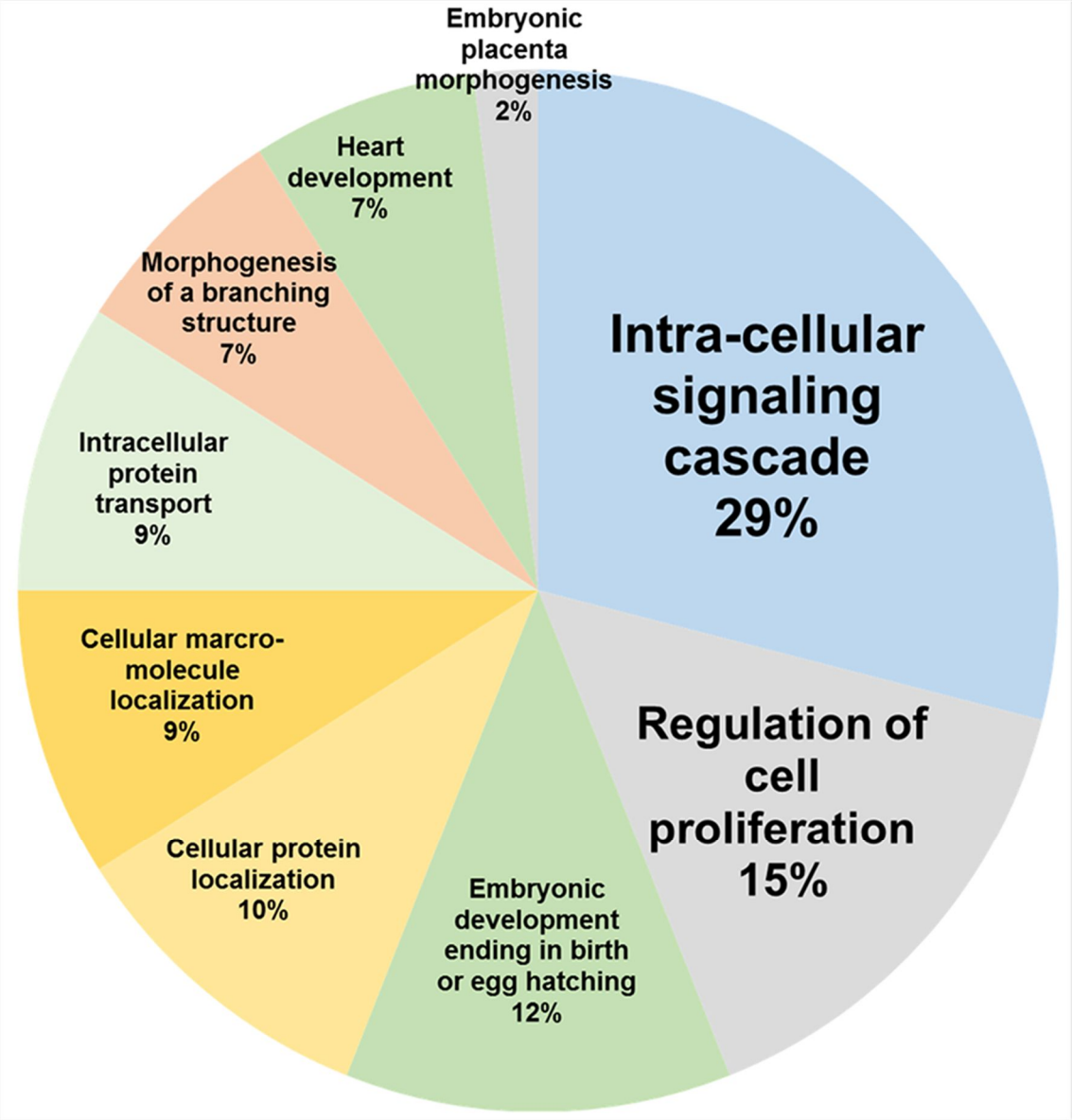

Figure 5. Gene ontology (GO) analysis for target genes of miR-193a.

A pie chart represents a variety of biological function for target genes of miR-193a analyzed by DAVID v6.7.

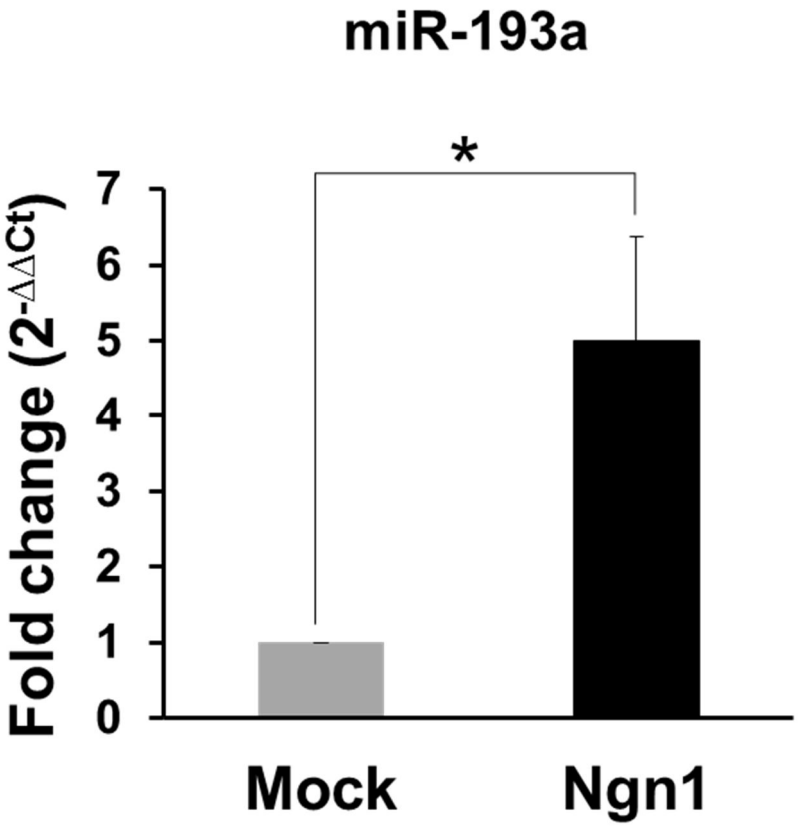

Figure 6. The expression of miR-193a was assessed by qRT-PCR in F11 cells treated with Mock or Ngn1.

Data are representative of three experiments. Each bar was plotted as mean ± s.d. *$P<0.05$.

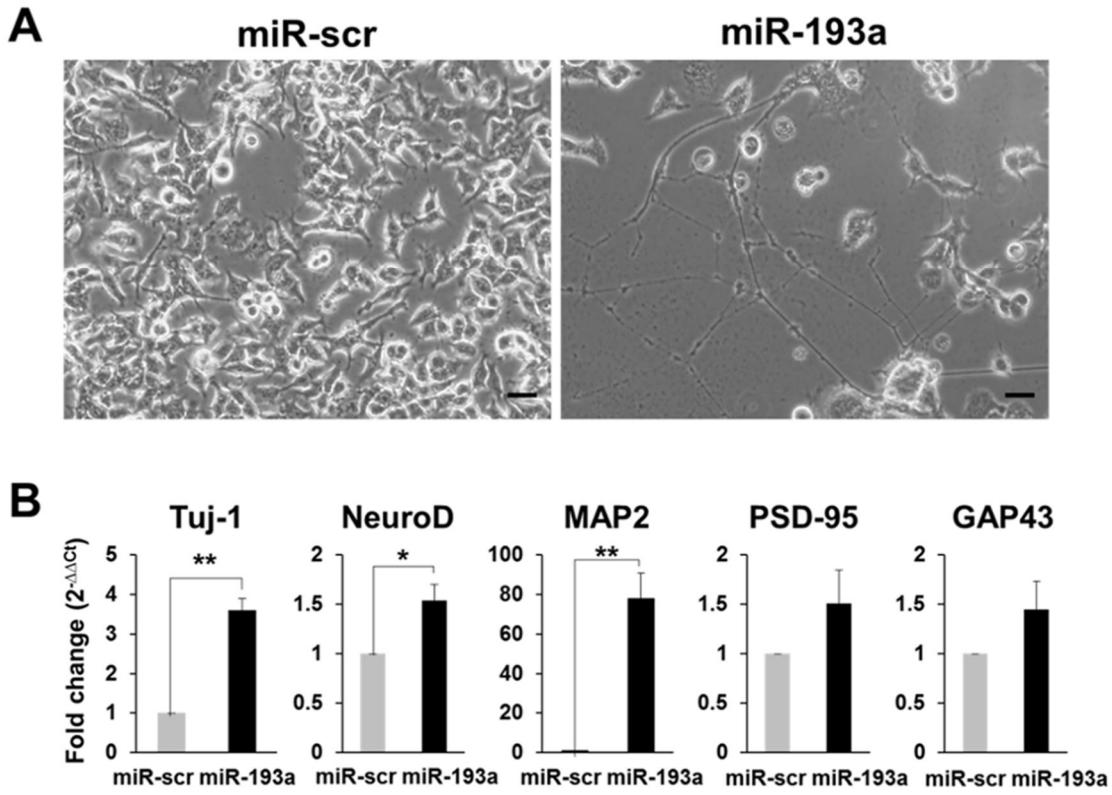

Figure 7. Novel neurogenic function of miR-193a.

(A) F11 cells were transfected with 50 nM miRNA-scr or miRNA-193a and then were incubated in DMEM containing 10% FBS for 3 days. Phase contrast images showing miRNA-193a-induced F11 cells had neuron-like morphological features with neurite outgrowth. Scale bar, 10 μm. (B) qRT-PCR was performed on total RNA extracted from F11 cells 3 days after treatment of miR-scr or miR-193a. In F11 cells overexpressed with miR-193a, the expression of several neuron-specific markers including MAP2 was higher than that in the F11 cells treated with miR-scr at 3 days. *$P<0.05$, *$P<0.005$.

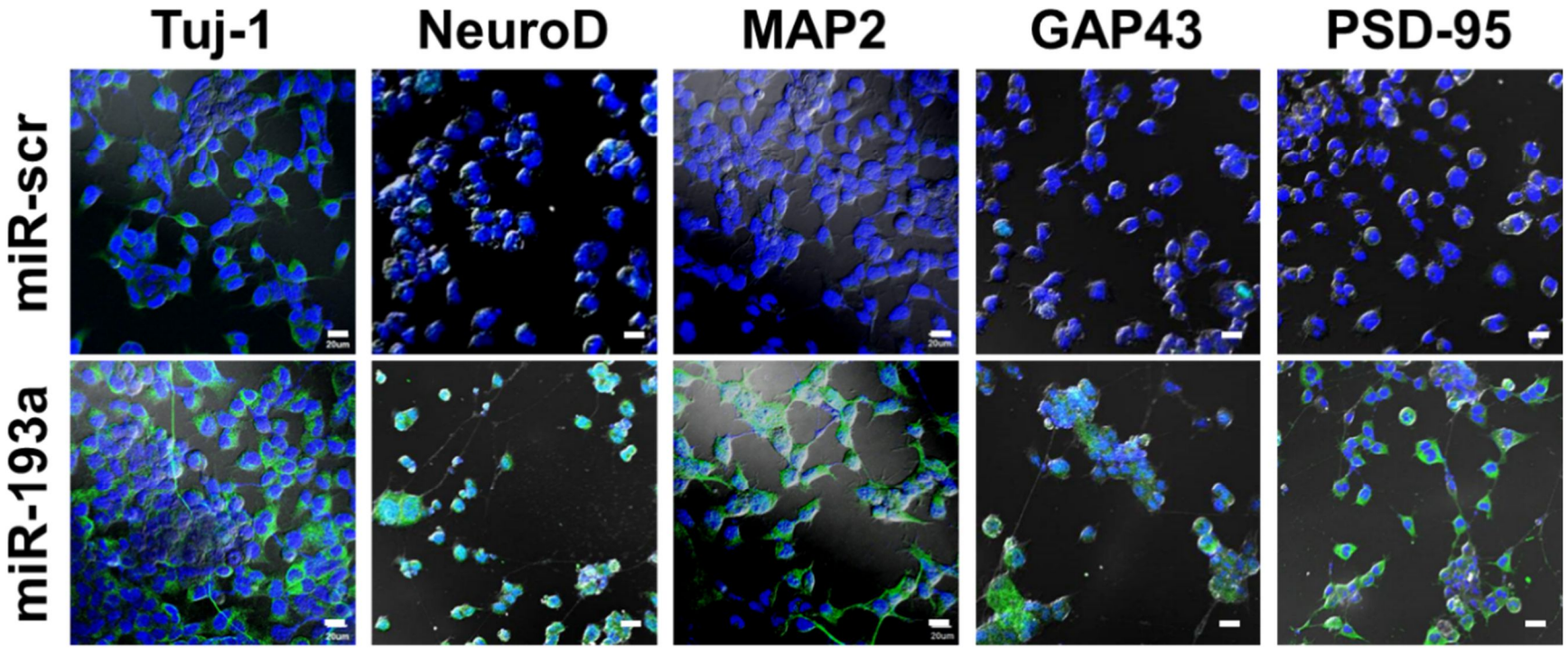

Figure 8. Immunofluorescence staining to examine miR-193a-induced neuronal differentiation in F11-miR-scr and F11-miR-193a cells.

Nuclei were counterstained with DAPI (blue). The increased expression of Tuj-1 (green), MAP2 (green), NeuroD (green), GAP43 (green) and PDS-95 (green) was shown in miR-193a-treated F11- cells, compared with miR-scr-treated F11 cells. Scale bar, 20 μm.

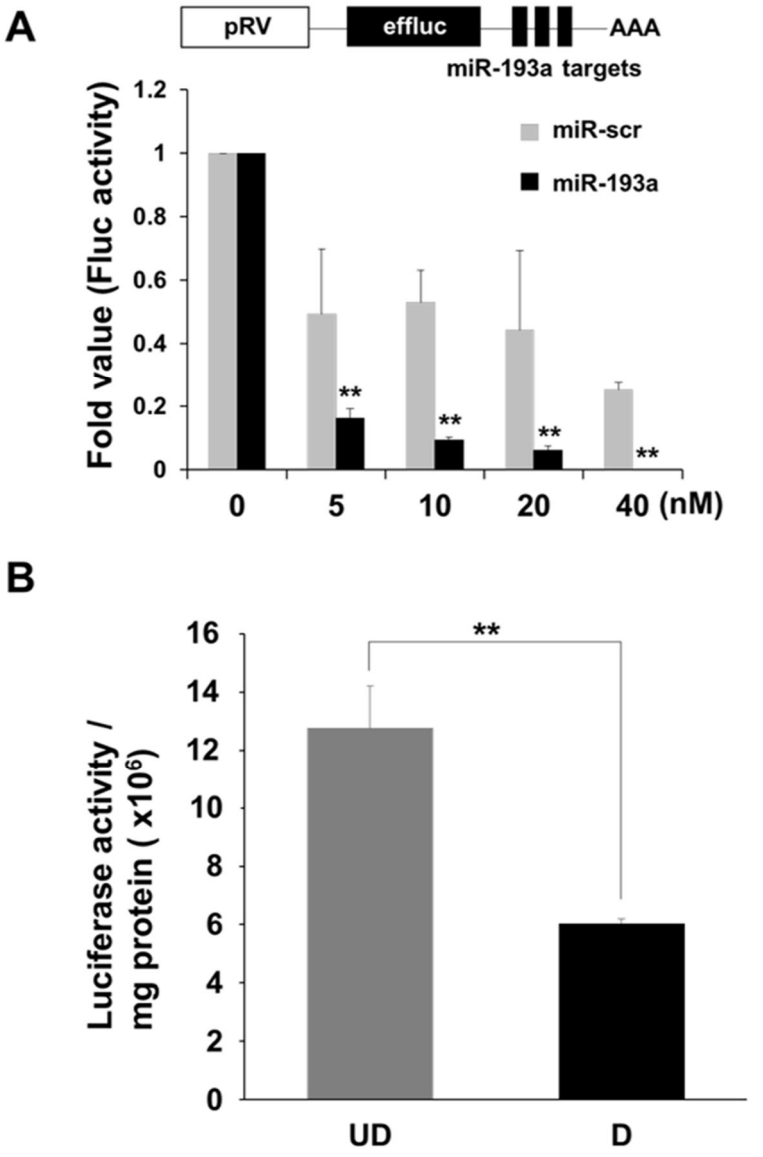

Figure 9. Luciferase assay for the expression of miR-193a.

(A) HeLa cells were transiently co-transfected with miR-scr or miR-193a and pRV/effLuc/3XPT_miR-193a to detect functional action of miR-193a. The luciferase signals were decreased with miRNA-193a treatment in a dose-dependent manner. The acquired values are represented as the average luciferase activity ratio ± sd. (B) Luciferase assay was examined to validate miR-193a expression as neuronal differentiation at 3 days after 1 mM db-cAMP treatment in F11 cells. Data are representative of three independent experiments each.

**$P<0.005$.

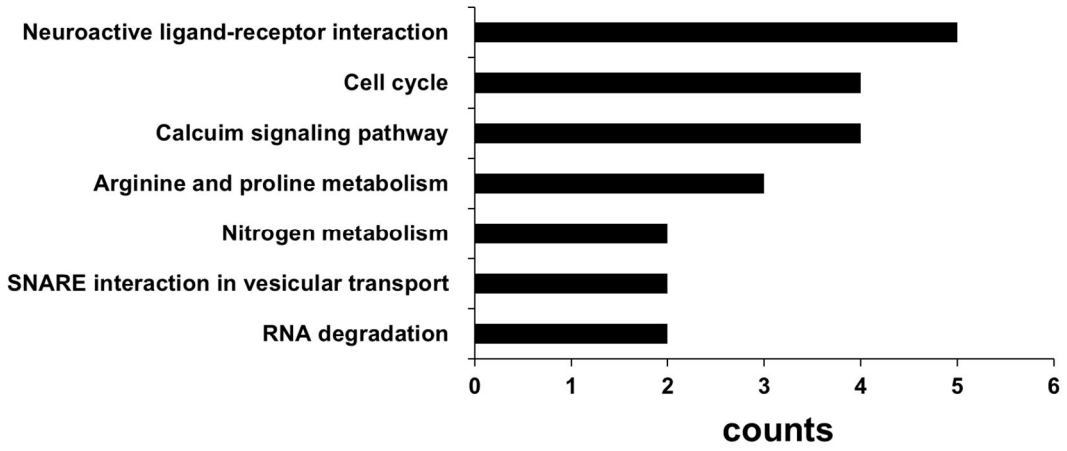

Figure 10. Signal pathway classification for target genes of miR-193a.

It was analyzed by KEGG_pathway in DAVID v6.7.

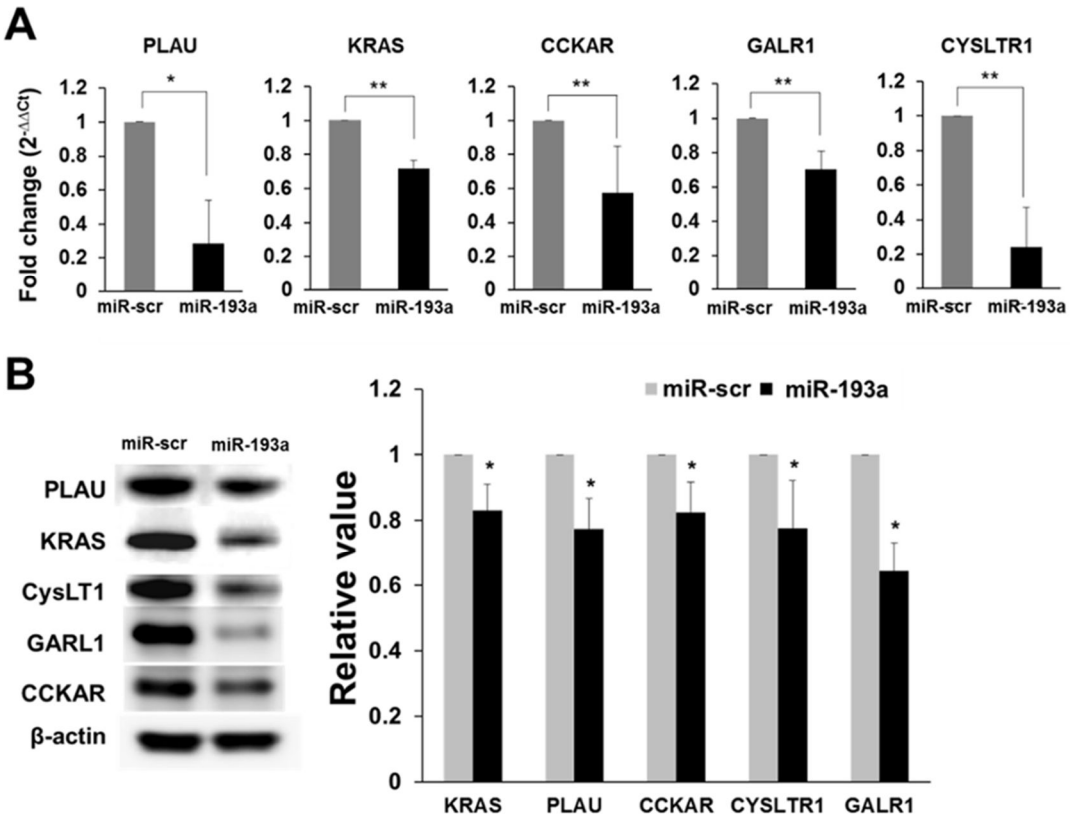

Figure 11. Validation for target genes of miR-193a.

(A) Three days after treatment of miR-scr or miR-193a, qRT-PCR was performed on total RNA extracted from F11 cells. Data are representative of three experiments each and are shown as mean ± s.d. ***P<0.005*. (B) Western blot analysis for expression for miR-193a targets, PLAU, KRAS, CCKAR, CYSLTR1 and GALR1. Representative data of three biologically independent experiments are shown. **P<0.05*.

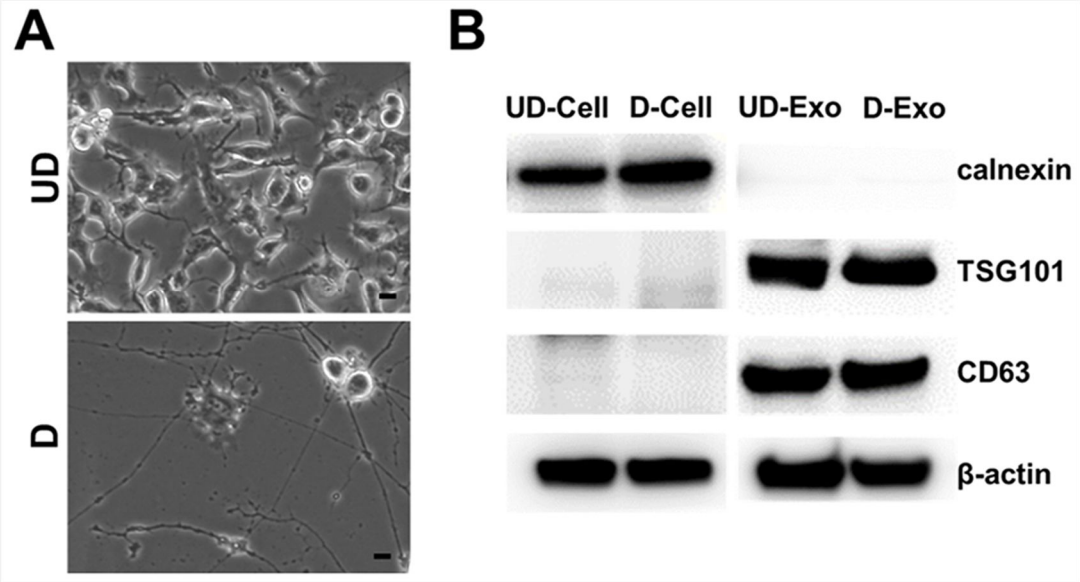

Figure 12. Enhanced levels of miR-193a in D-F11 cell-derived exosomes.

(A) Phase contrast images for morphology in UD- and D-F11 cells. Scale bar, 10 μm. (B) Western blot analysis for CDS63 and TSG101 exosomal marker proteins on UD- and D-Exo.

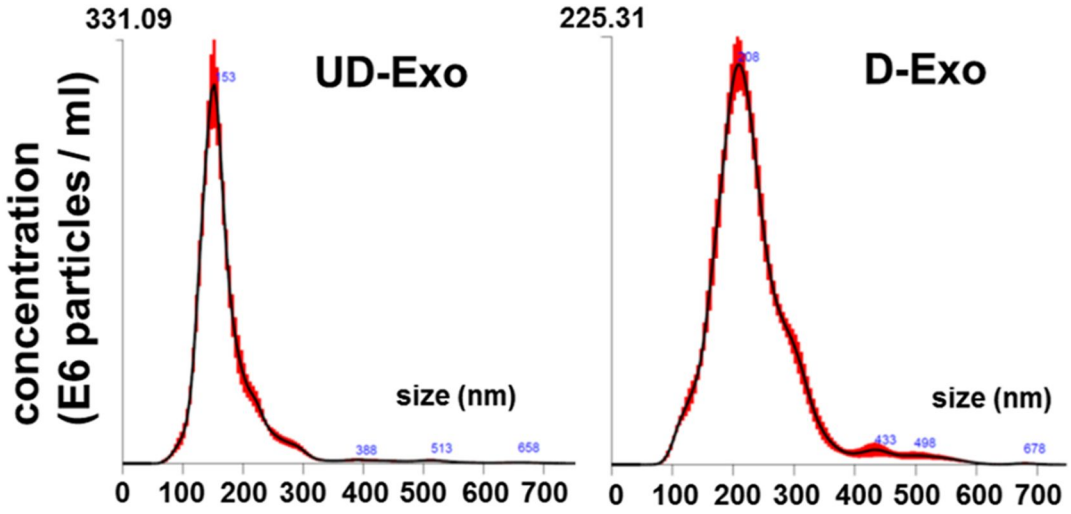

Figure 13. Size distribution of UD-Exo and D-Exo.

It was measured by nanoparticle tracking analysis using the Nanosight system.

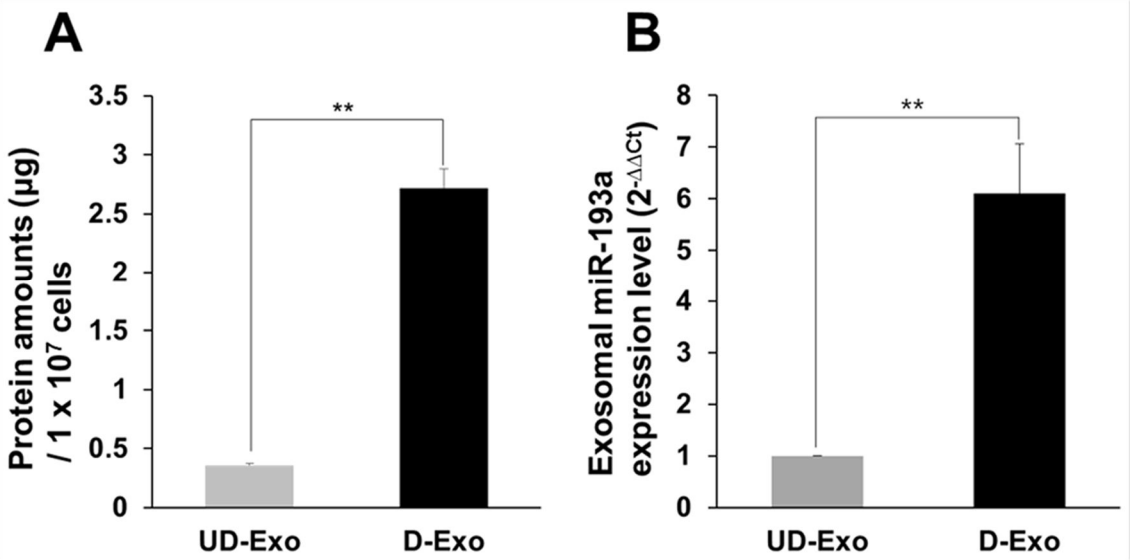

Figure 14. **Quantitative analysis for total number and exosomal miR-193a of UD- and D-Exo.**

(A) Total number of UD-Exo and D-Exo were measured as the total protein from 1 x 10^7 F11 cells, $^{**}P < 0.005$. (B) Quantitative RT-PCR (qRT–PCR) analysis for exosomal miR-193a of UD- and D-Exo. Data are representative of three experiments (mean ± s.d), $^{**}P < 0.005$. D-F11: differentiated F11, UD-F11: undifferentiated F11, D-Exo: exosomes from D-F11, UD-Exo: exosomes from UD-F11.

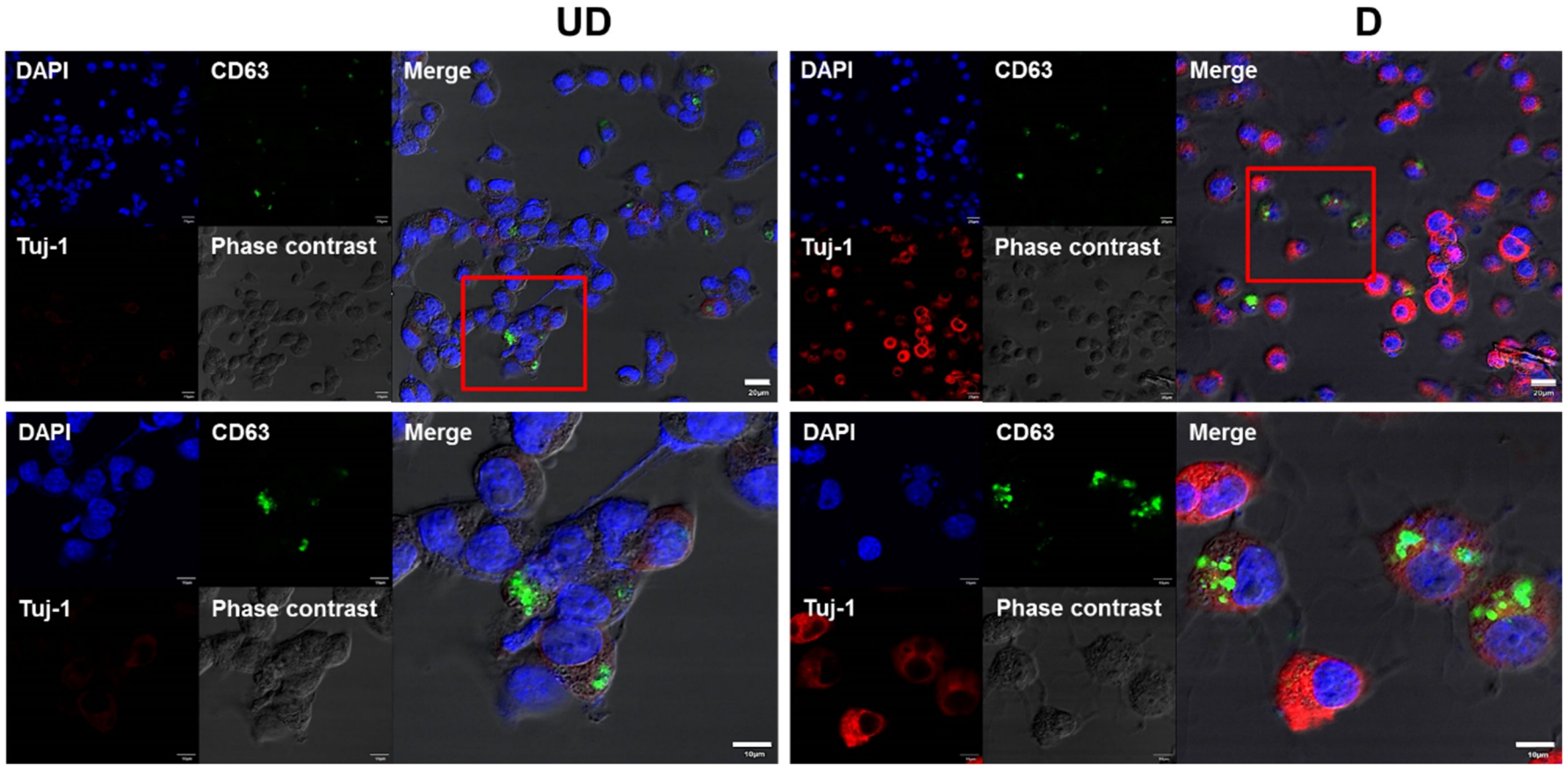

Figure 15. **Immunofluorescence staining for Tuj-1 of GFP-exosome UD-F11 and GFP-exosome D-F11 cells.**

Scale bar, 10, 20 μm.

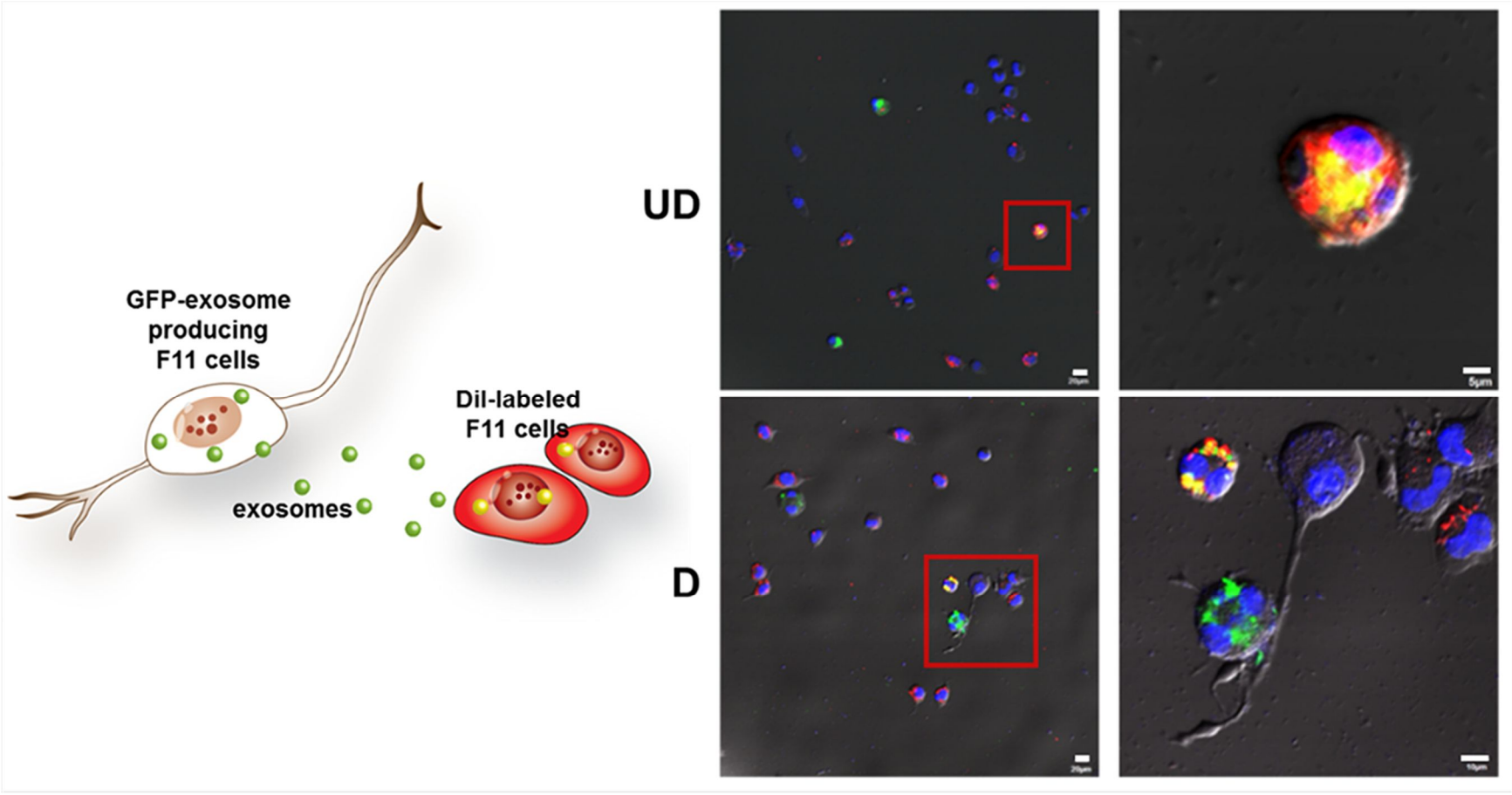

Figure 16. **GFP-exosome producing donor F11 cells co-cultured with DiI-labeled recipient F11 cells.**

Scale bar, 5, 10, and 20 μm.

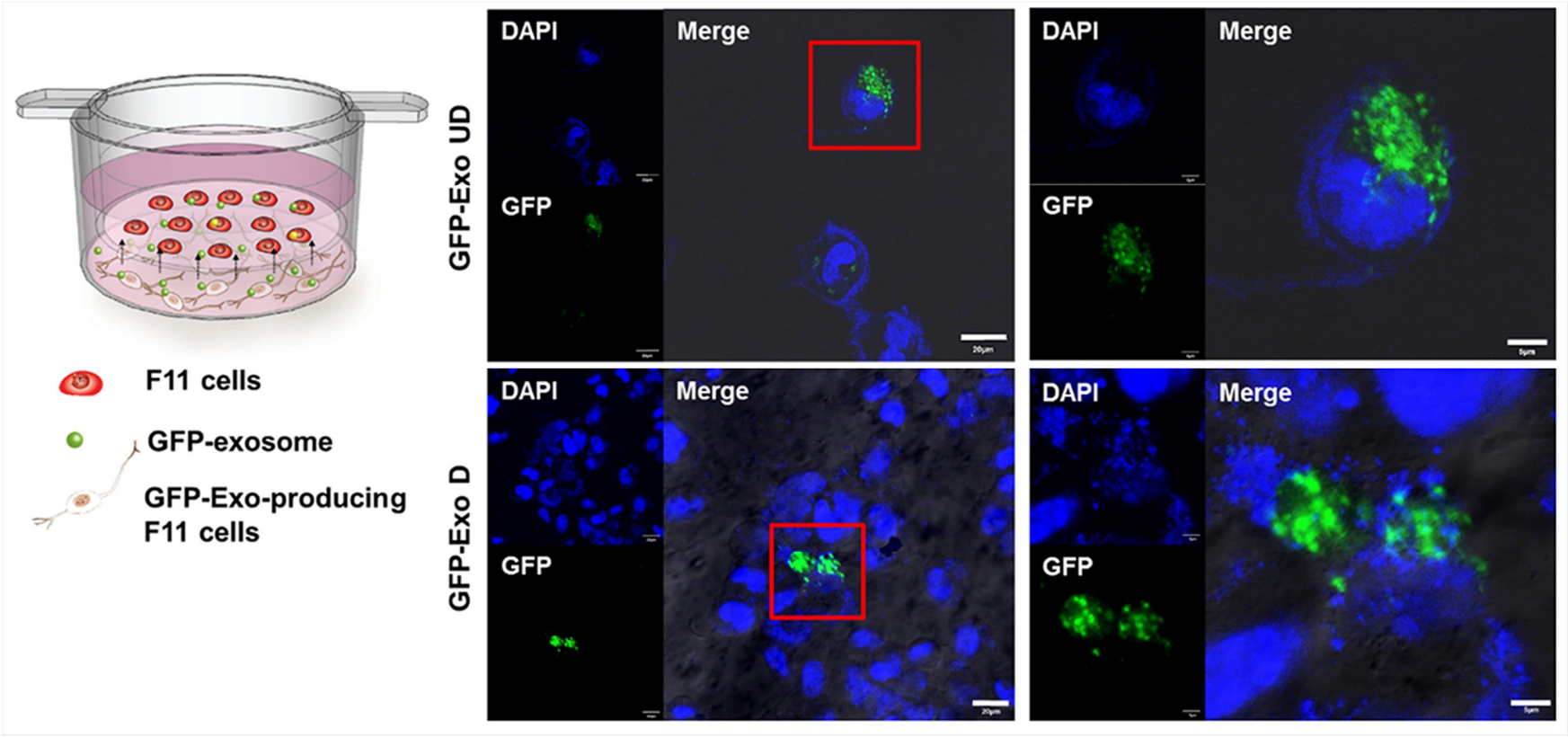

Figure 17. **Diagram of co-culture system of GFP-exosome producing donor F11 cells and recipient UD-F11 cells in the transwell system.**

Fluorescence images for recipient UD-F11 cells in insert chamber after co-culture. Scale bar, 5, 20 μm.

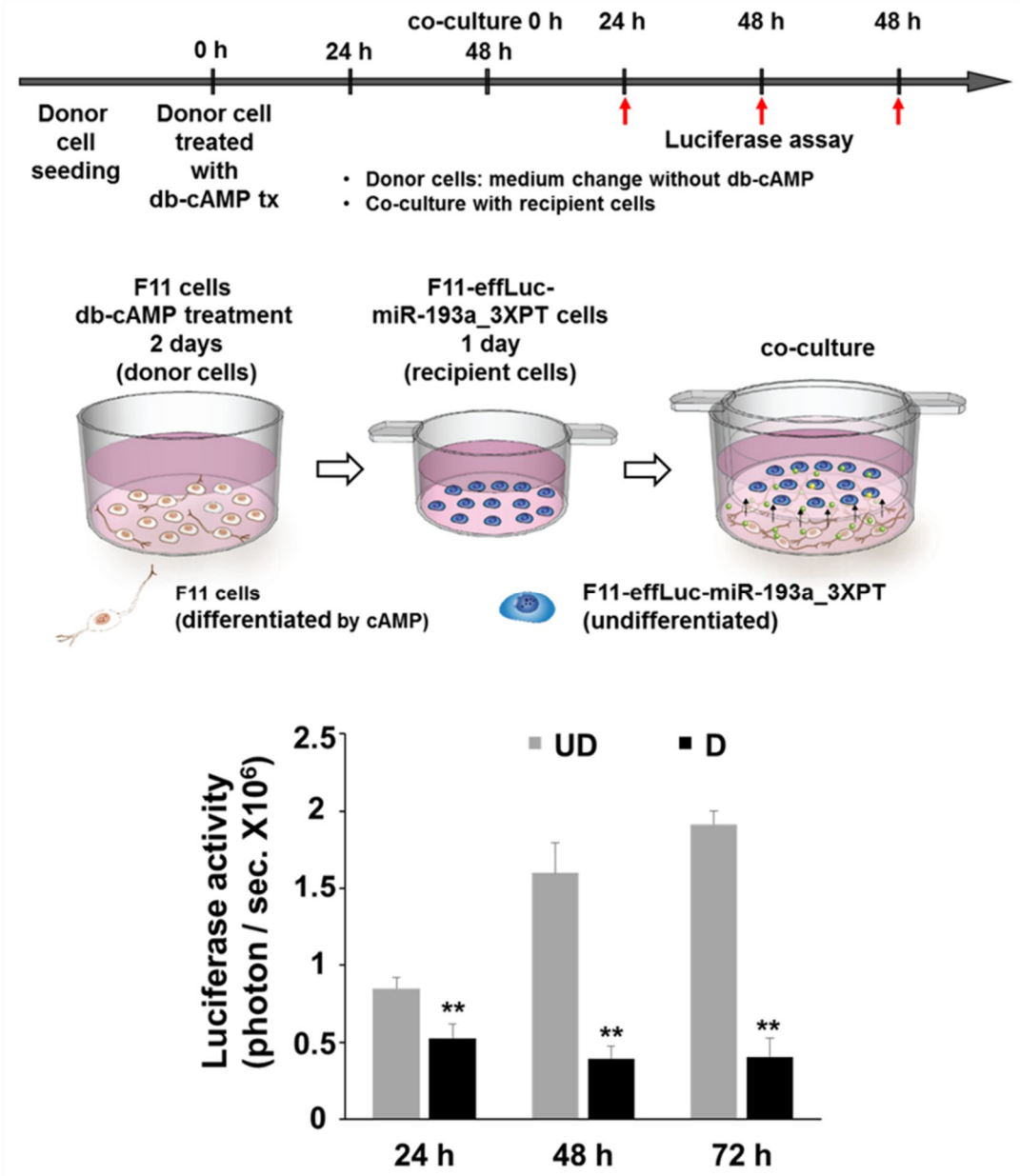

Figure 18. Schematic representation of the transwell co-culture system for donor D-F11 cells and recipient UD-F11/effLuc-miR-193a_3XPT cells.

The values are presented as the average luciferase activity ± s.d. $^{**}P < 0.005$.

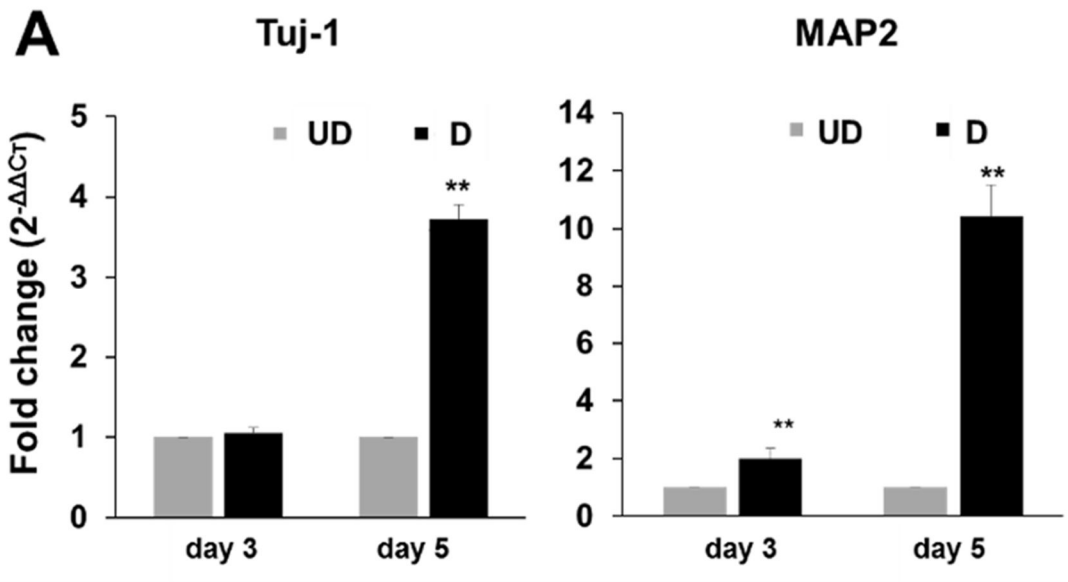
A
Tuj-1
MAP2
UD
D
Fold change (2-ΔΔCT)
day 3
day 5
**

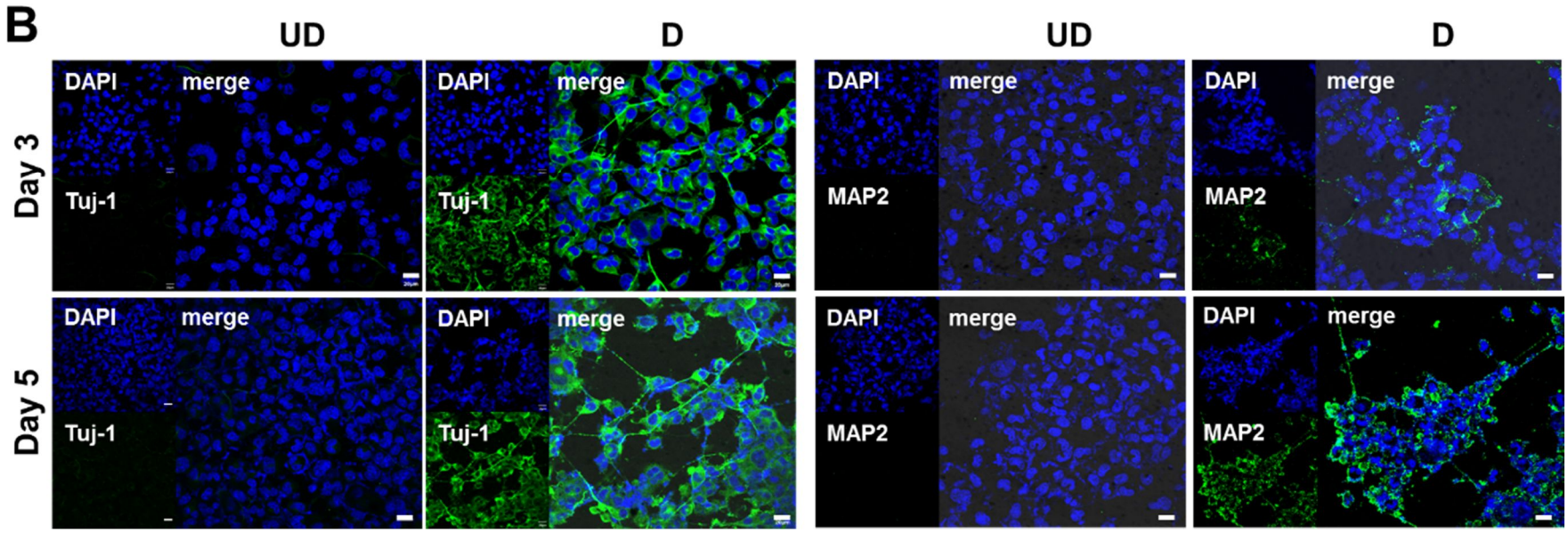

Figure 19. The induction of exosome-mediated neurogenesis in recipient cells cultured with D-donor cells.

(A) qRT-PCR analysis for the expression level of Tuj-1 and MAP2 in recipient cells. Data are representative of three experiments each (mean ± s.d.), $^{**}P < 0.005$. (B) Immunofluorescence staining of Tuj-1 and MAP2 in recipient cells. Scale bar, 20 μm.

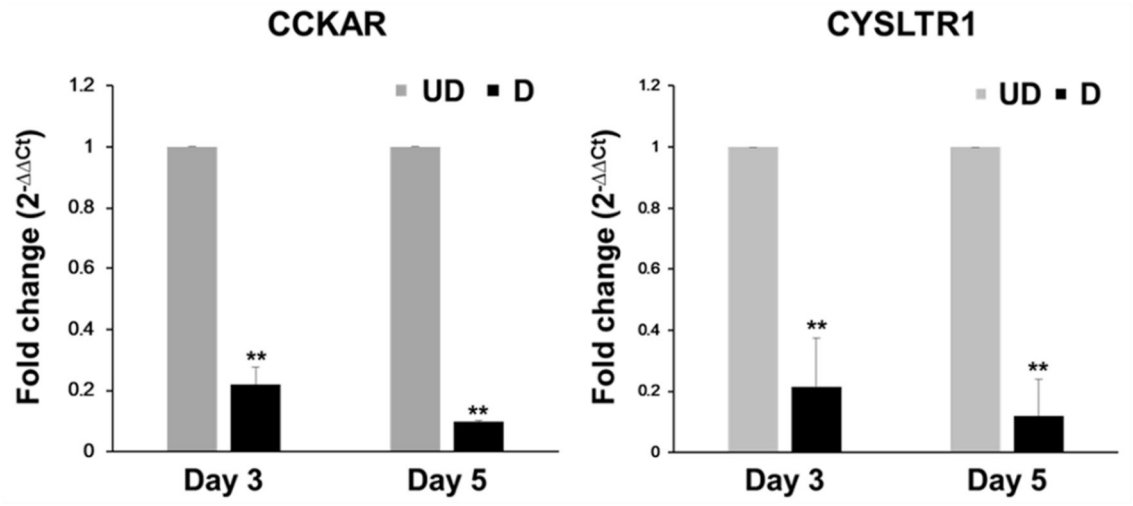

Figure 20. qRT-PCR analysis for target genes of miR-193a.

Data are representative of three experiments each (mean ± s.d.), $^{**}P < 0.005$.

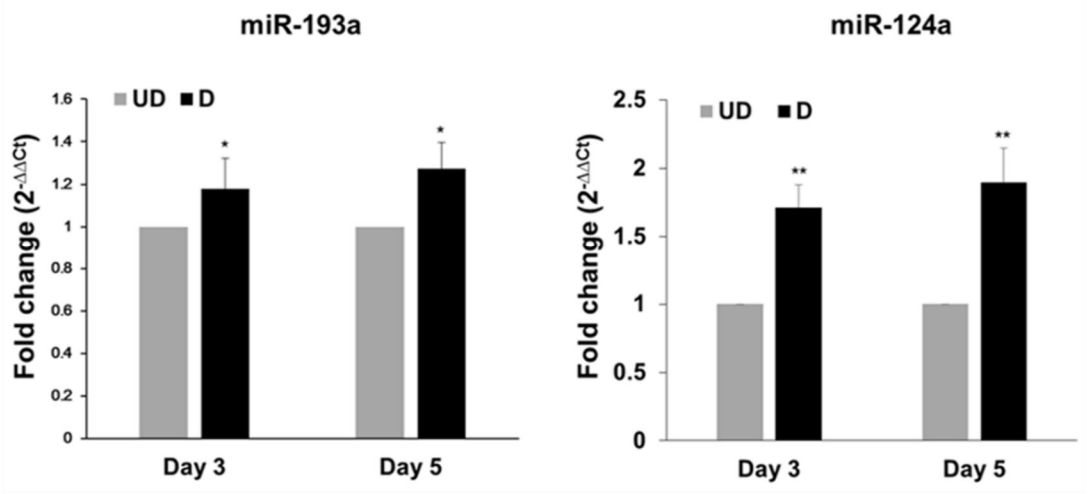

Figure 21. qRT-PCR results for miR-193a and miR-124a levels in recipient UD-F11 cells 3 and 5 days after co-culture with donor UD-F11 or D-F11 cells.

Data are representative of three experiments each (mean ± s.d.), $*P < 0.05$, $**P < 0.005$.

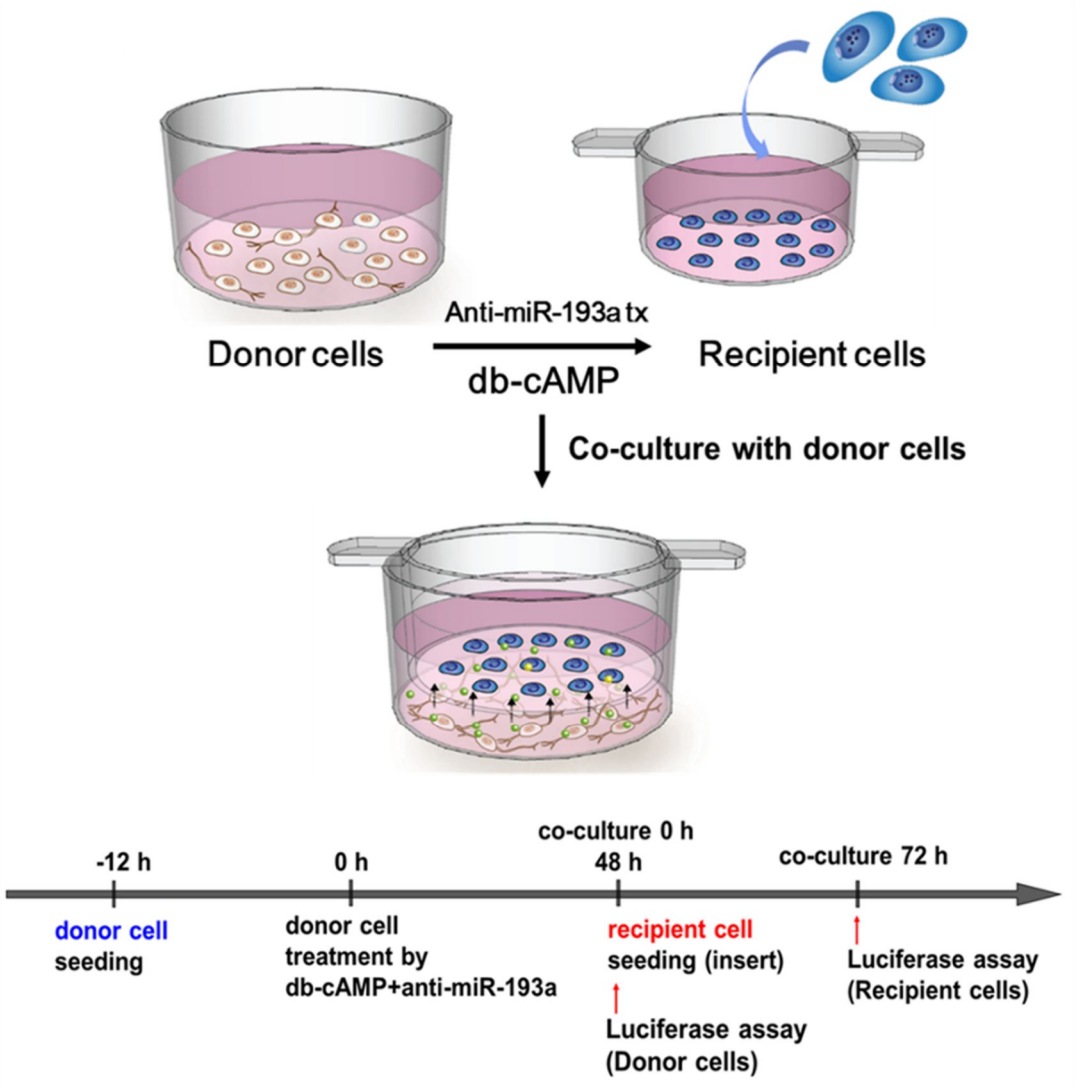
Anti-miR-193a tx
Donor cells
db-cAMP
Recipient cells
Co-culture with donor cells
-12 h
0 h
co-culture 0 h
48 h
co-culture 72 h
donor cell
seeding
donor cell
treatment by
db-cAMP+anti-miR-193a
recipient cell
seeding (insert)
Luciferase assay
(Donor cells)
Luciferase assay
(Recipient cells)

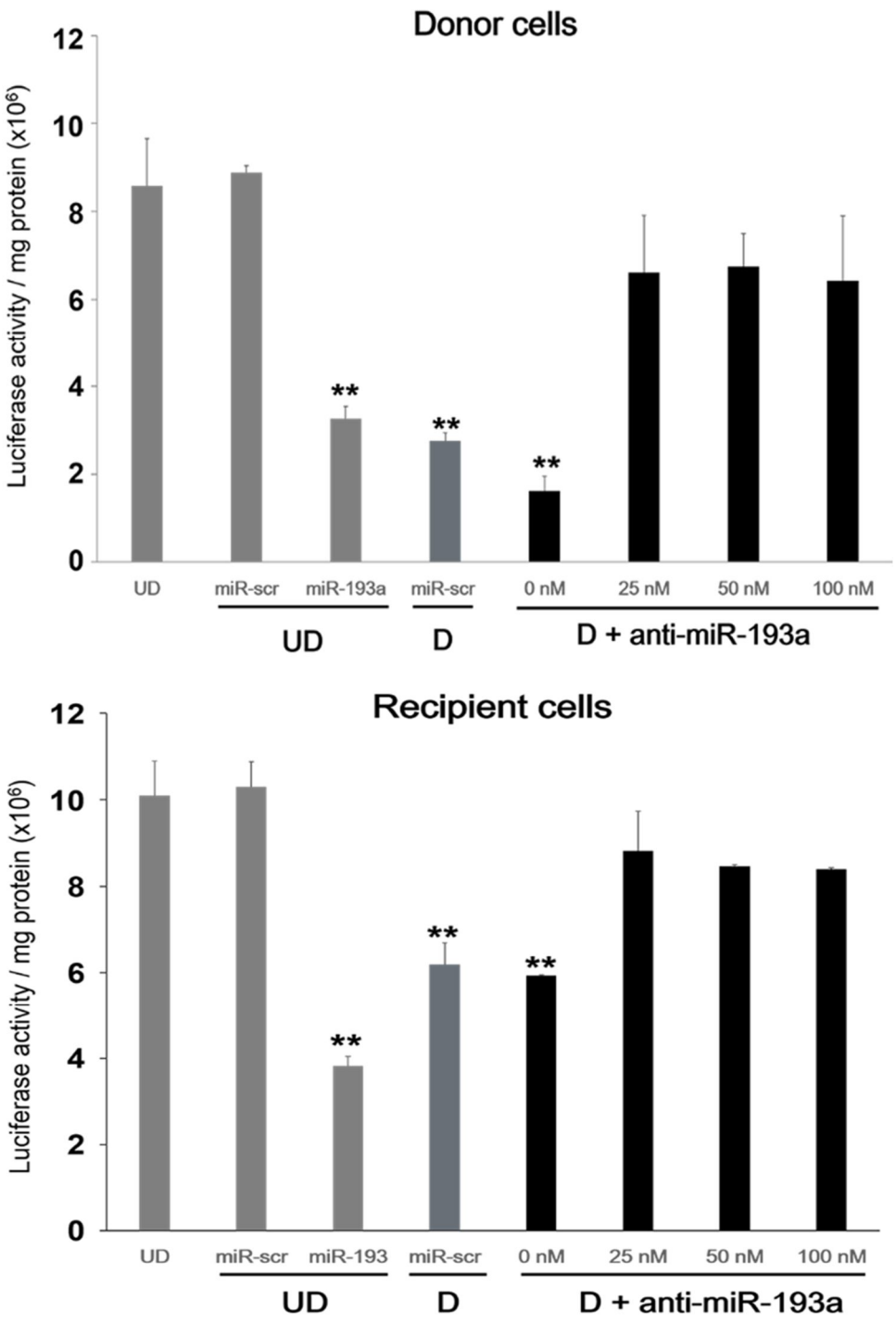

Figure 22. Luciferase assay for the expression of miR-193a in differentiating donor cells after anti-miR-193a treatment and in recipient cells 3 days after co-cultured with donor cells.

The acquired values are represented as the average luciferase activity ratio ± sd. $^{**}P < 0.005$.

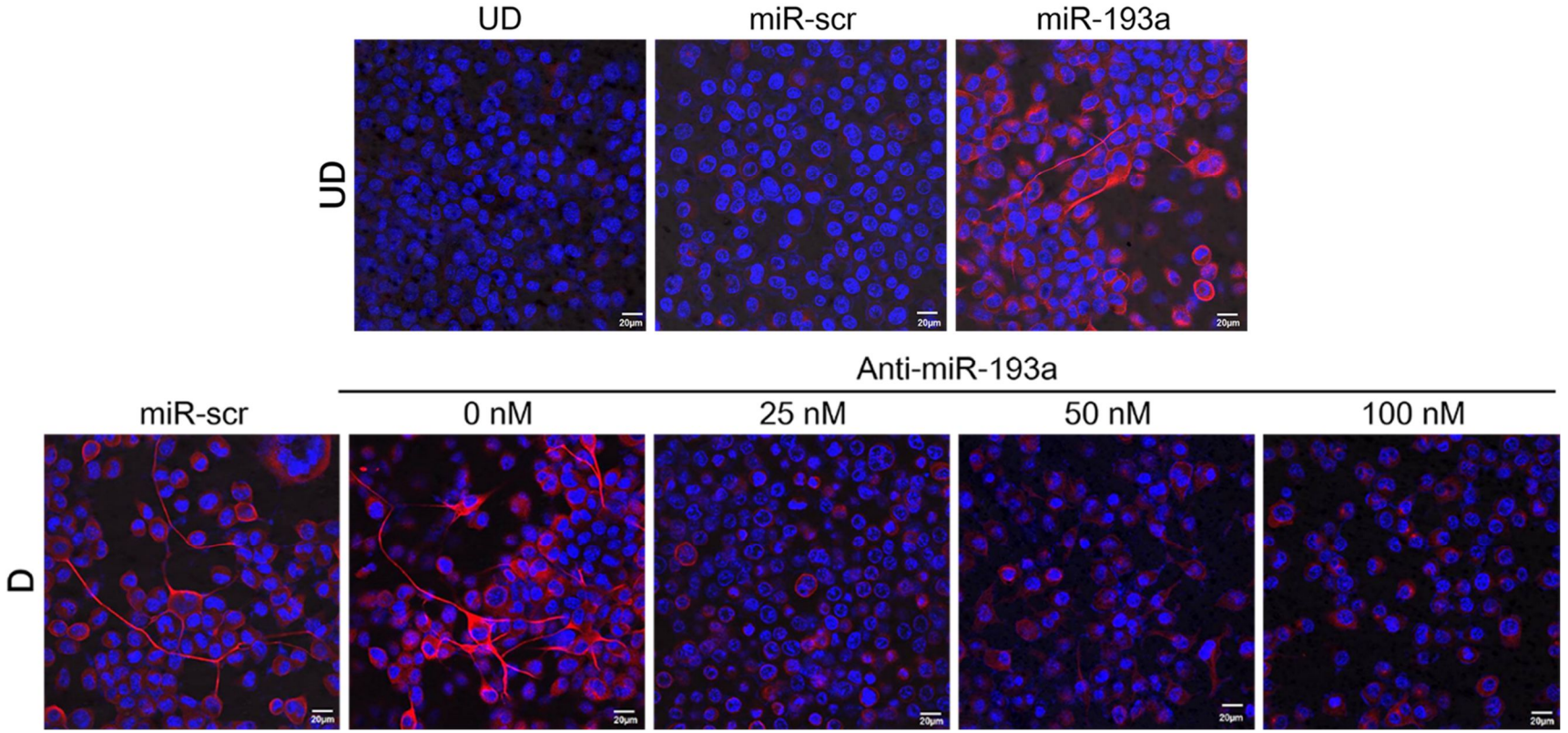

Figure 23. Immunofluorescence staining for neural marker, Tuj-1 in recipient cells 3 days after co-culture with undifferentiated or differentiated donor cells in the presence of anti-miR-193a.

Scale bar, 20 μm. UD: undifferentiated cells, D: differentiated cells.

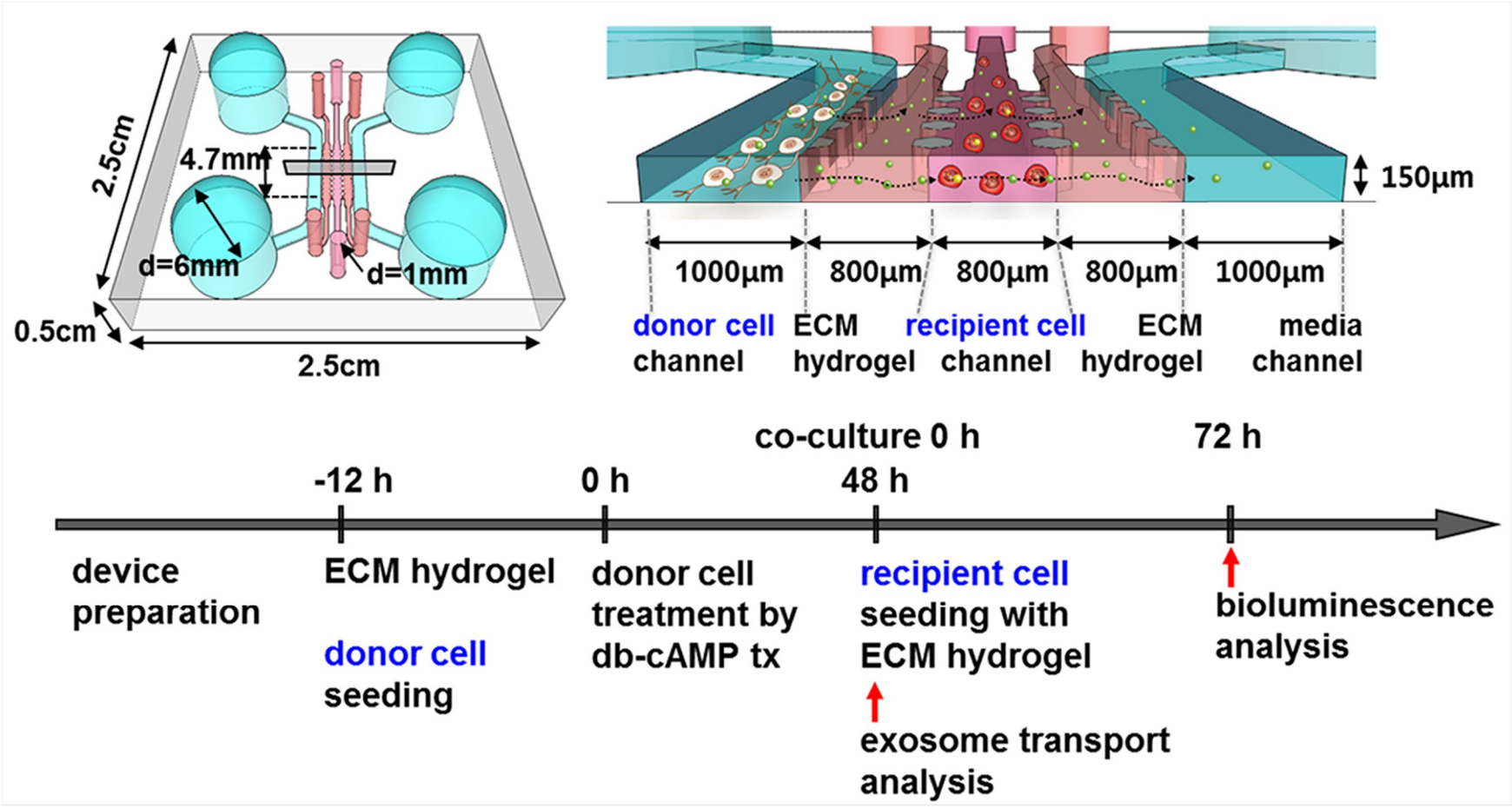

Figure 24. Schematic depiction of the microfluidic cell culture system.

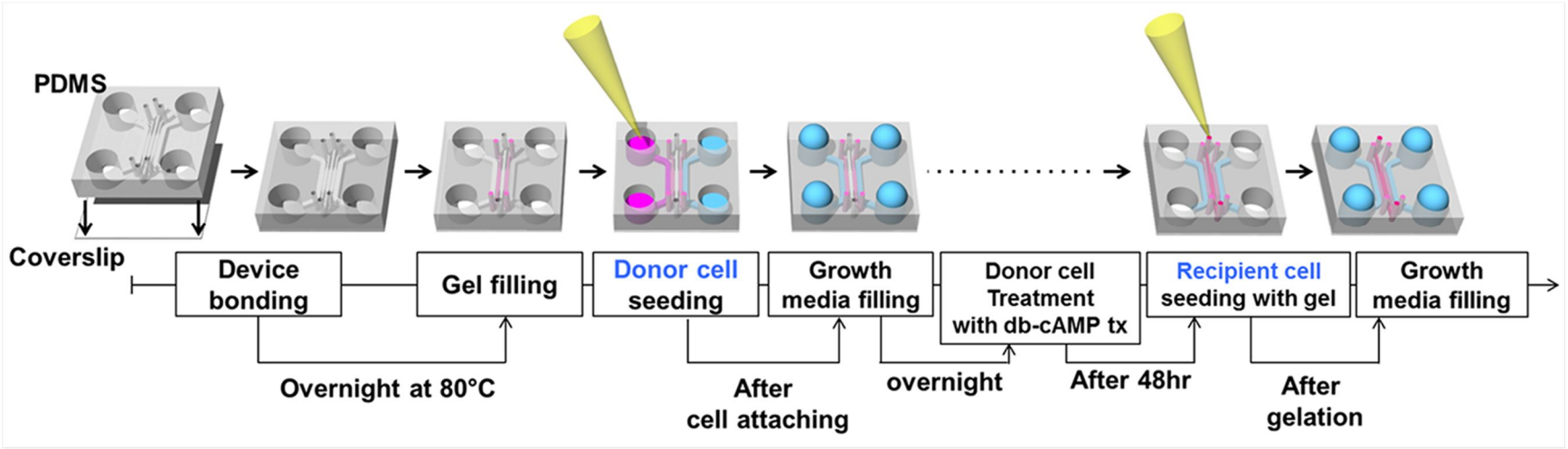

Figure 25. Procedure for preparation of hydrogel-incorporating microfluidic cell culture system.

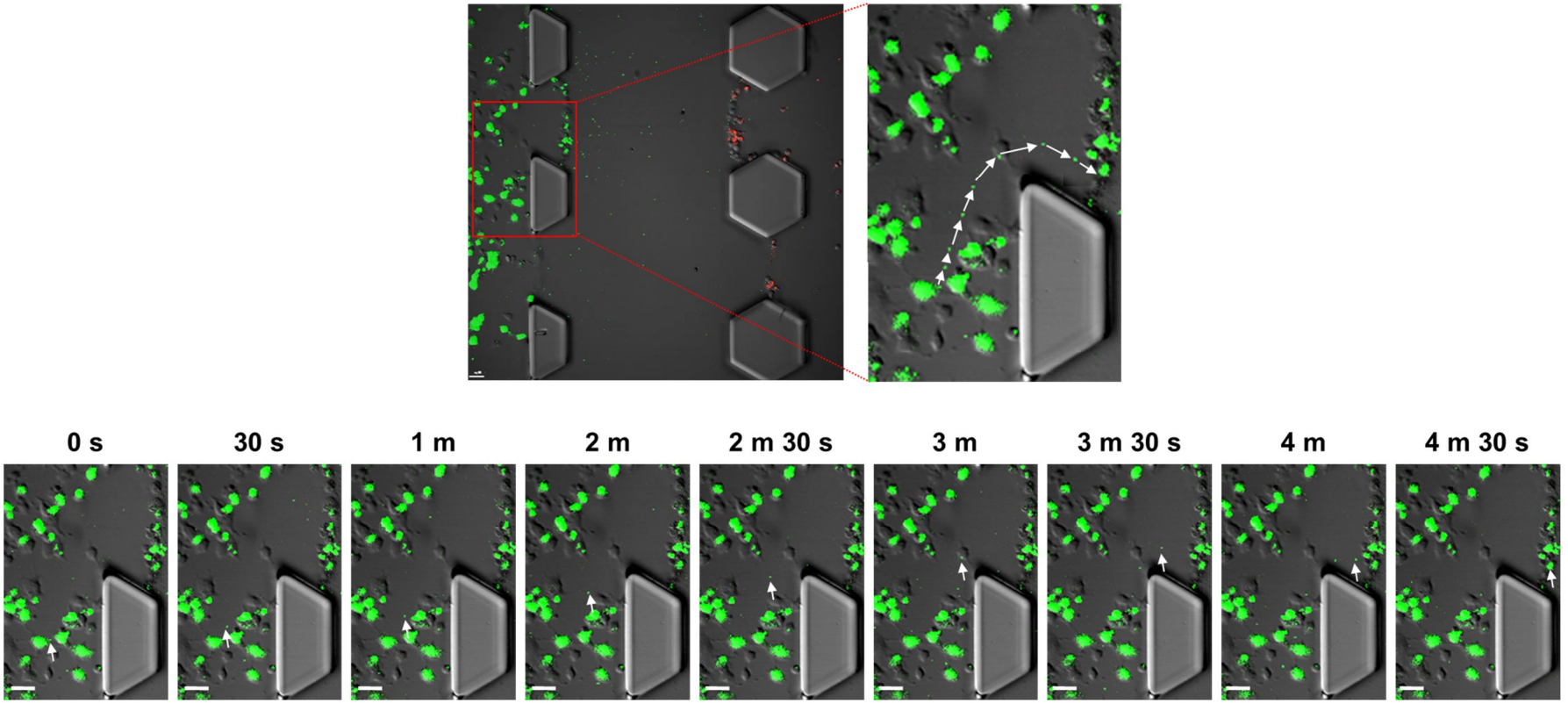

Figure 26. Live imaging to track for exosomes from GFP-exosome donor F11 cells cultured with recipient F11 cells.

Plates show confocal images for movements of exosome from donor cells by time. Scale bar, 50 μm.

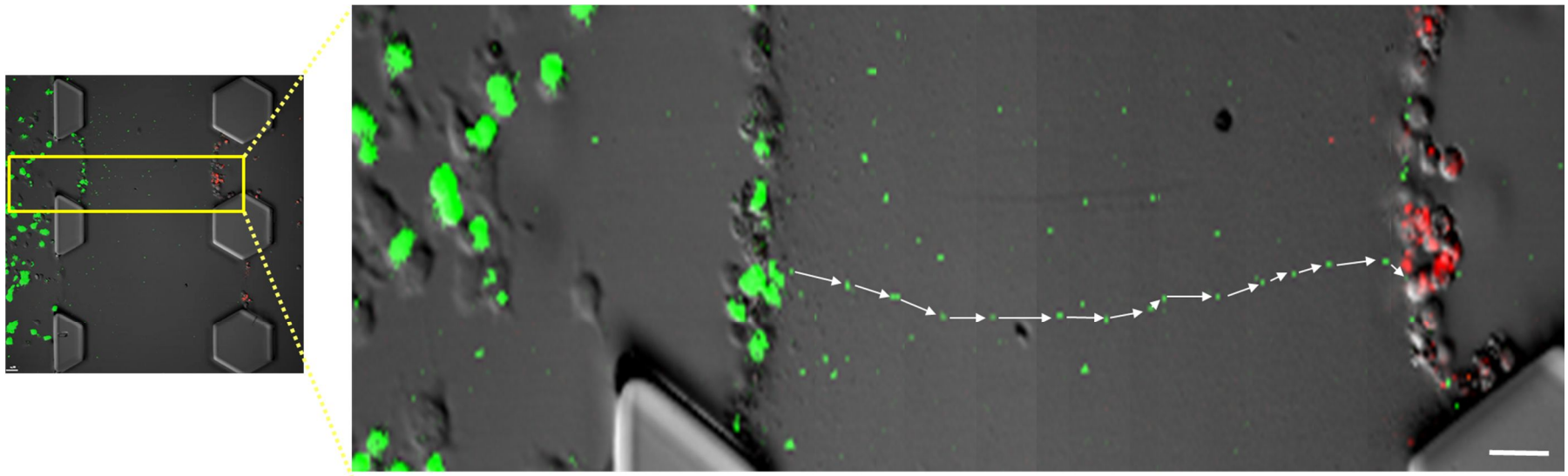

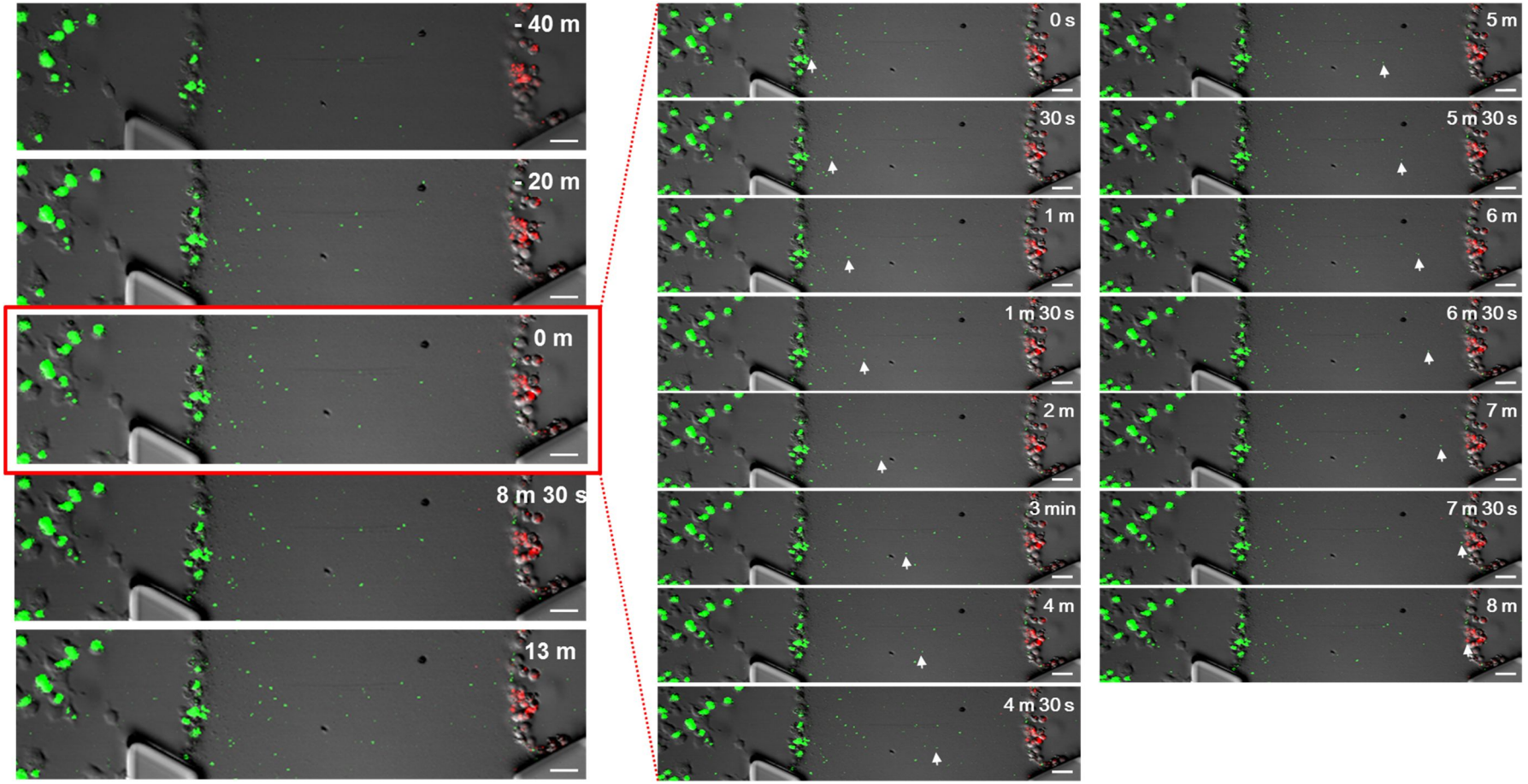

Figure 27. Representative fluorescence images show moving exosomes from donor cells to recipient cells in gel region.

Scale bar, 50 μm.

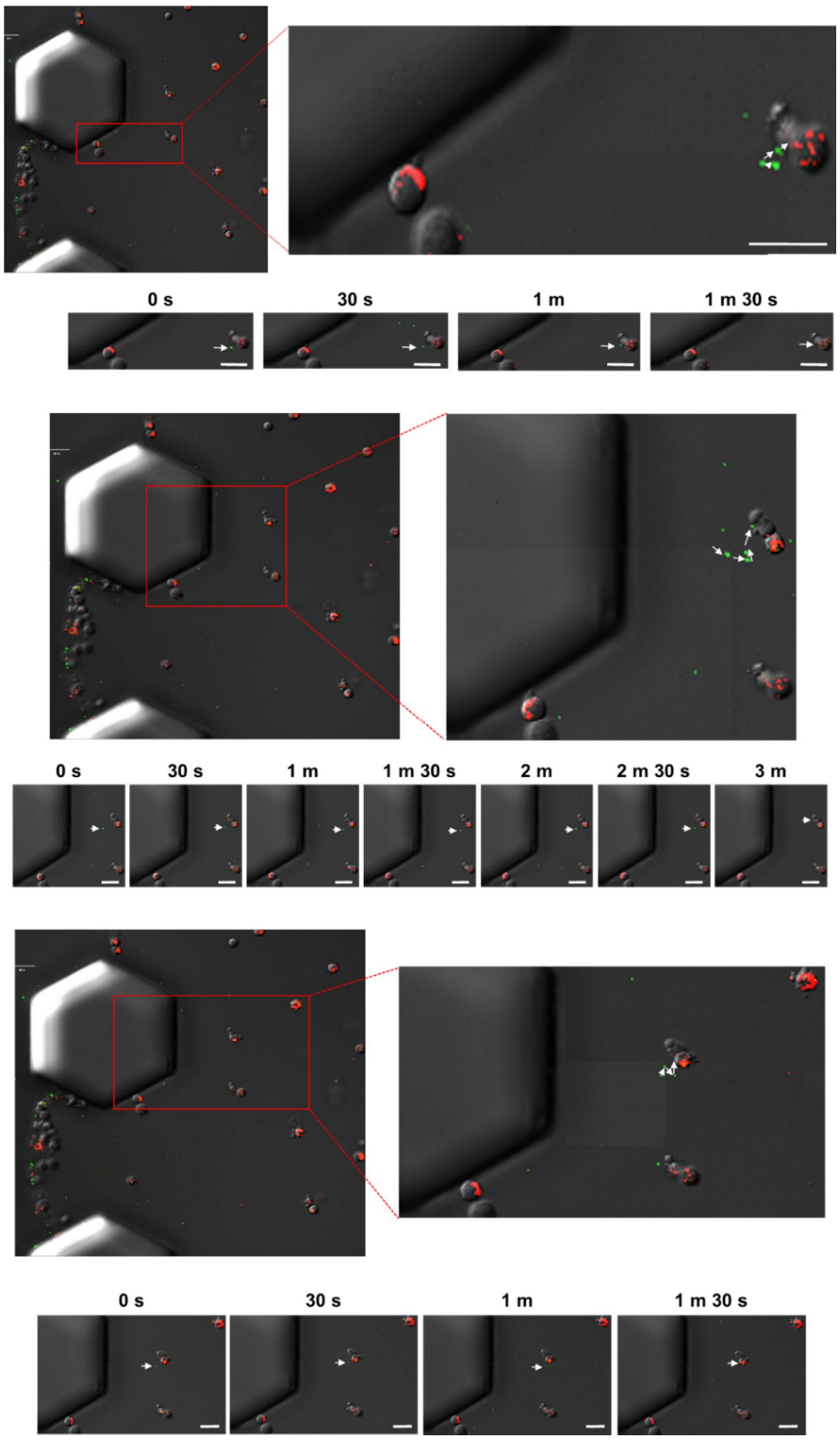

Figure 28. Time-lapse images for uptake of exosomes by recipient cells incorporated with hydrogel.

Scale bar, 50 μm.

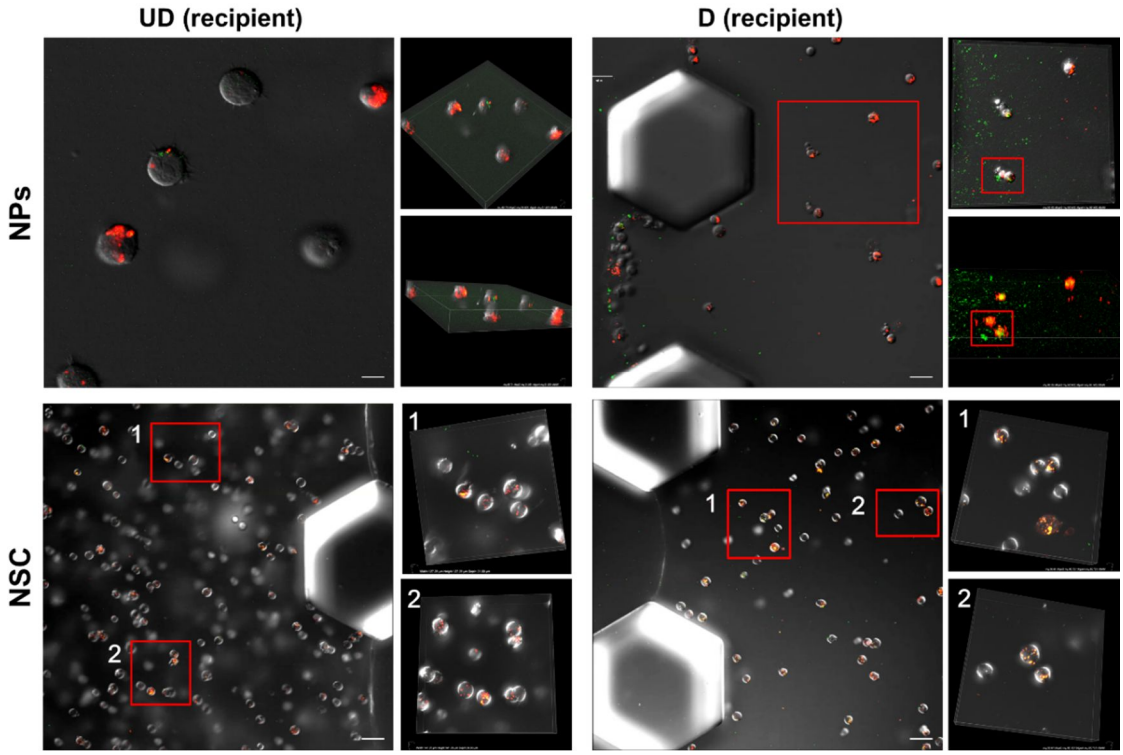

Figure 29. 3D fluorescence images for exosomes in recipient cells of neural stem and progenitor cells in the microfluidic assay.

Representative figures of fluorescence and 3D reconstruction of Z-stack images show uptake of exosomes by recipient cells of neural stem and progenitor cells co-cultured with donor UD- or D-cells. Red boxes indicate exosomes accumulated in recipient cells. Scale bar, 50 μm.

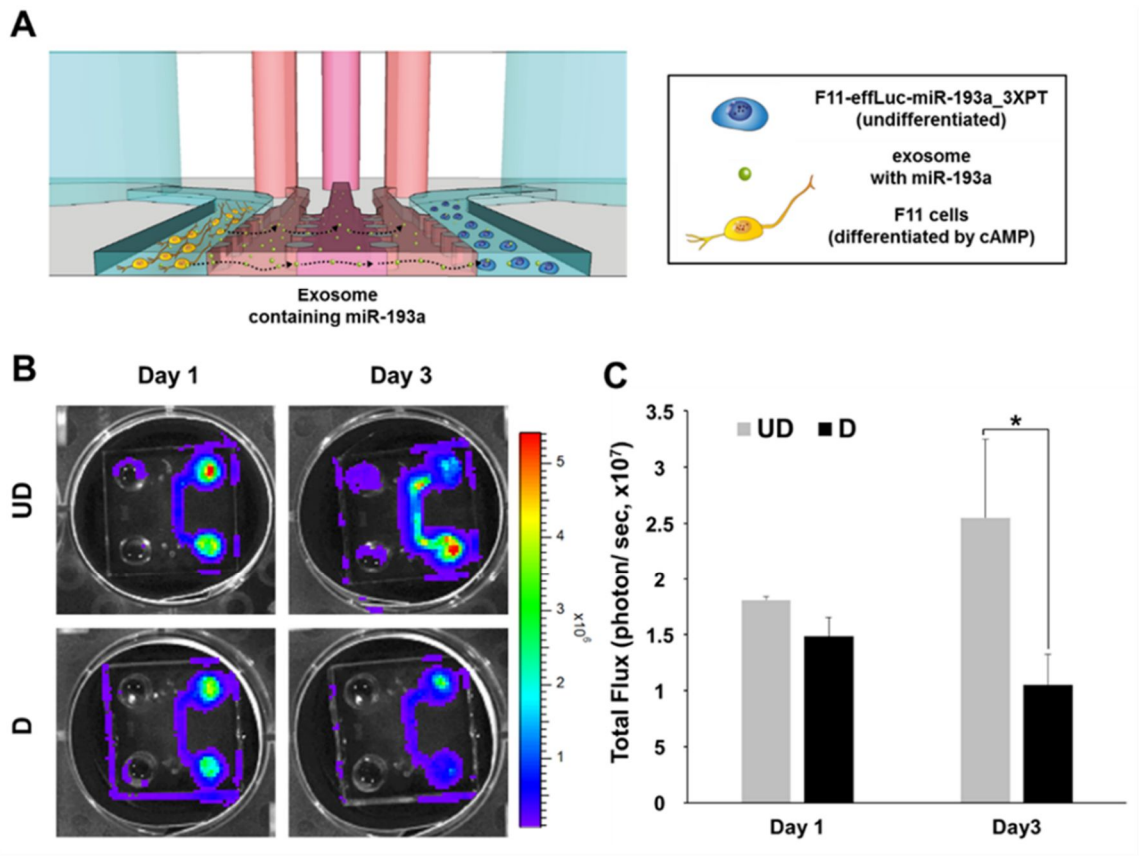

Figure 30. Microfluidic cell culture assay for exosome-mediated transfer of miR-193a.

(A) Schematic representation of the study for microfluidic co-culture system. (B) Bioluminescence images for exosome-mediated transfer of miR-193a in recipient F11/effLuc-miR-193a_3XPT cells. (C) Quantitative analysis for bioluminescence signals. Data are representative of three experiments each (mean ± s.d.), $*P < 0.05$.

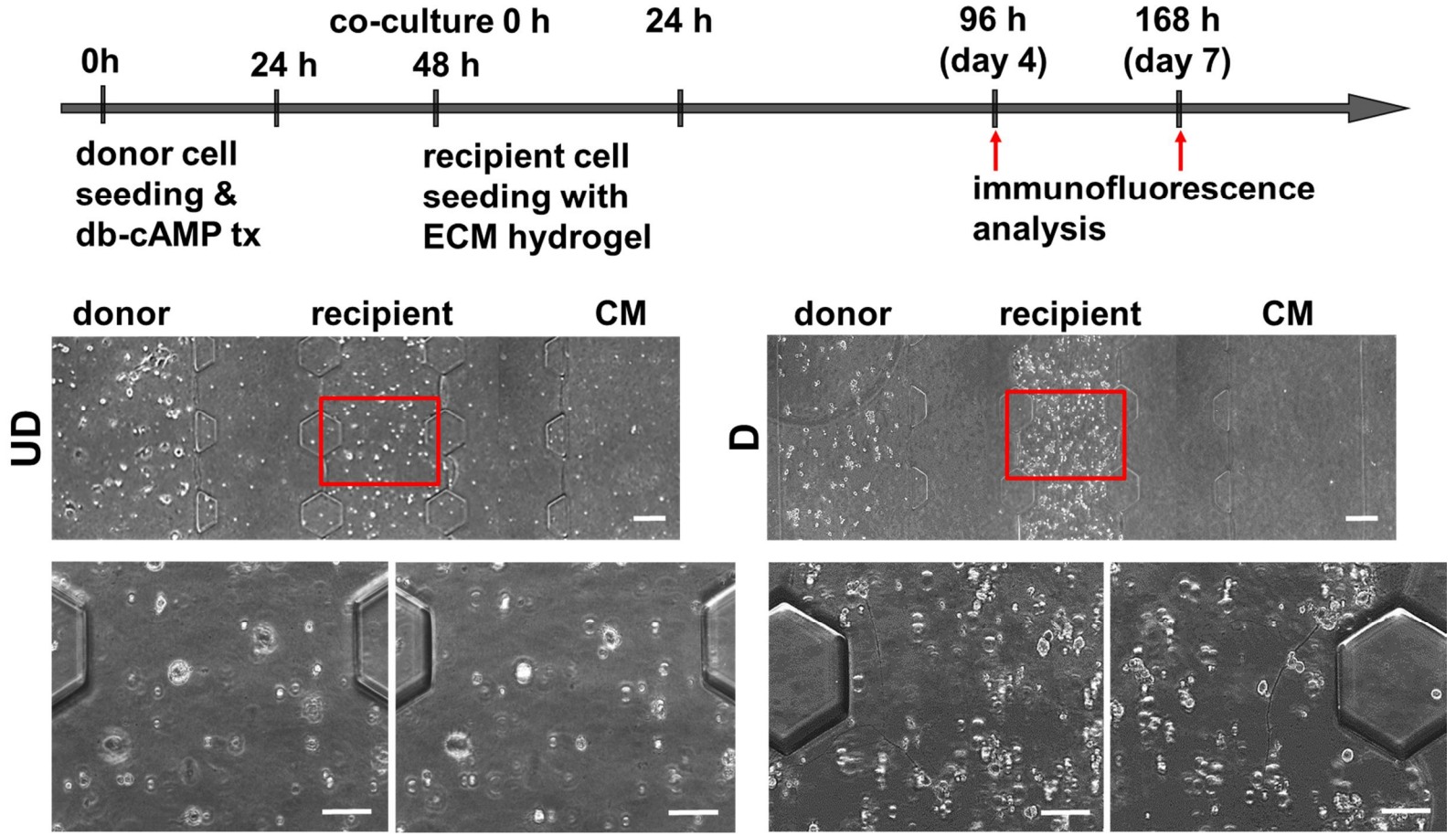

Figure 31. Phase contrast images for morphology of recipient cells incorporated with hydrogel 4 days after co-culture.

Scale bar, 100, 250 μm.

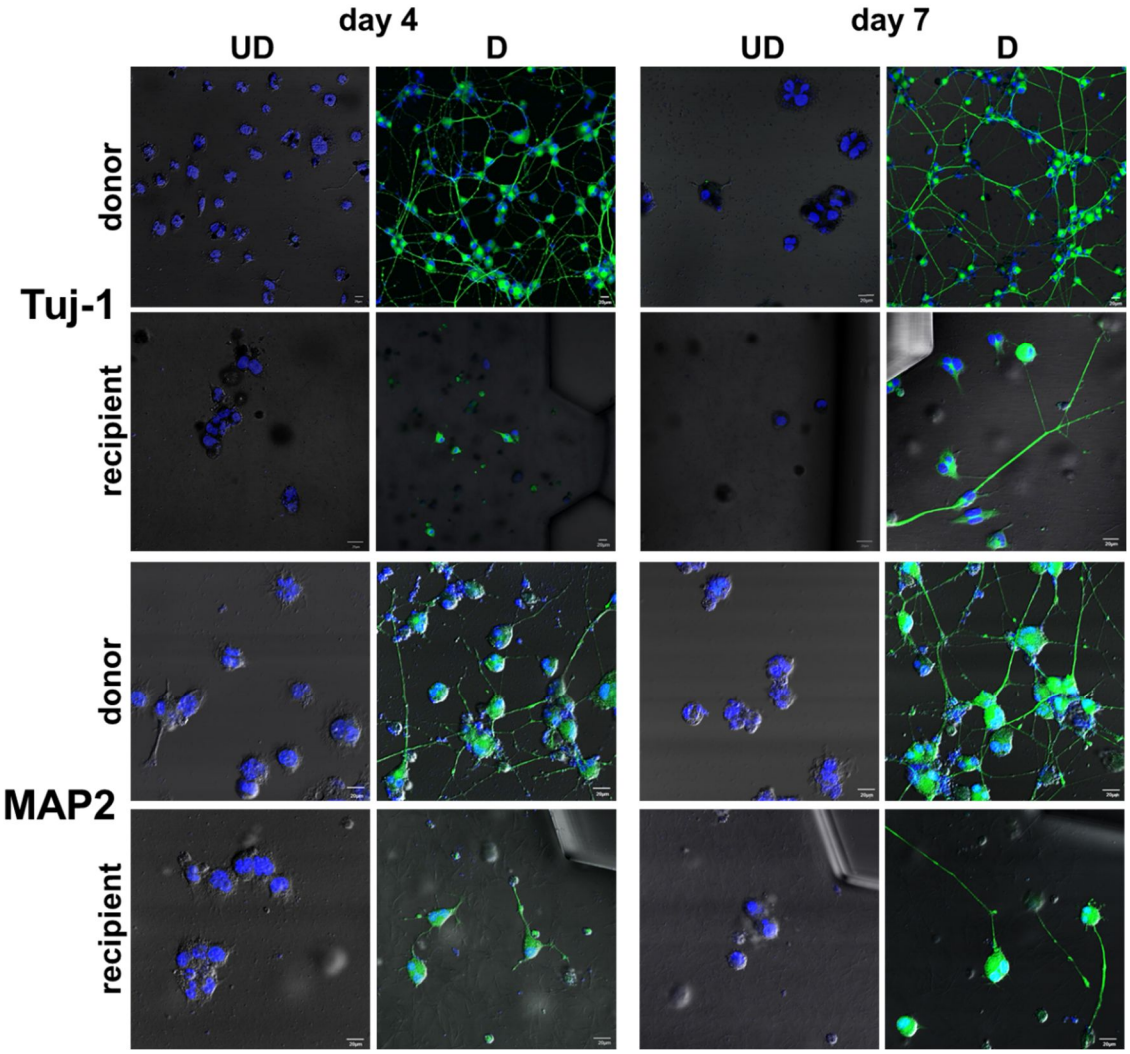

Figure 32. Immunofluorescence staining for the expression of Tuj-1 and MAP2 in donor and recipient cells 4 days and 7 days after co-culture.

Scale bar, 20 μm.

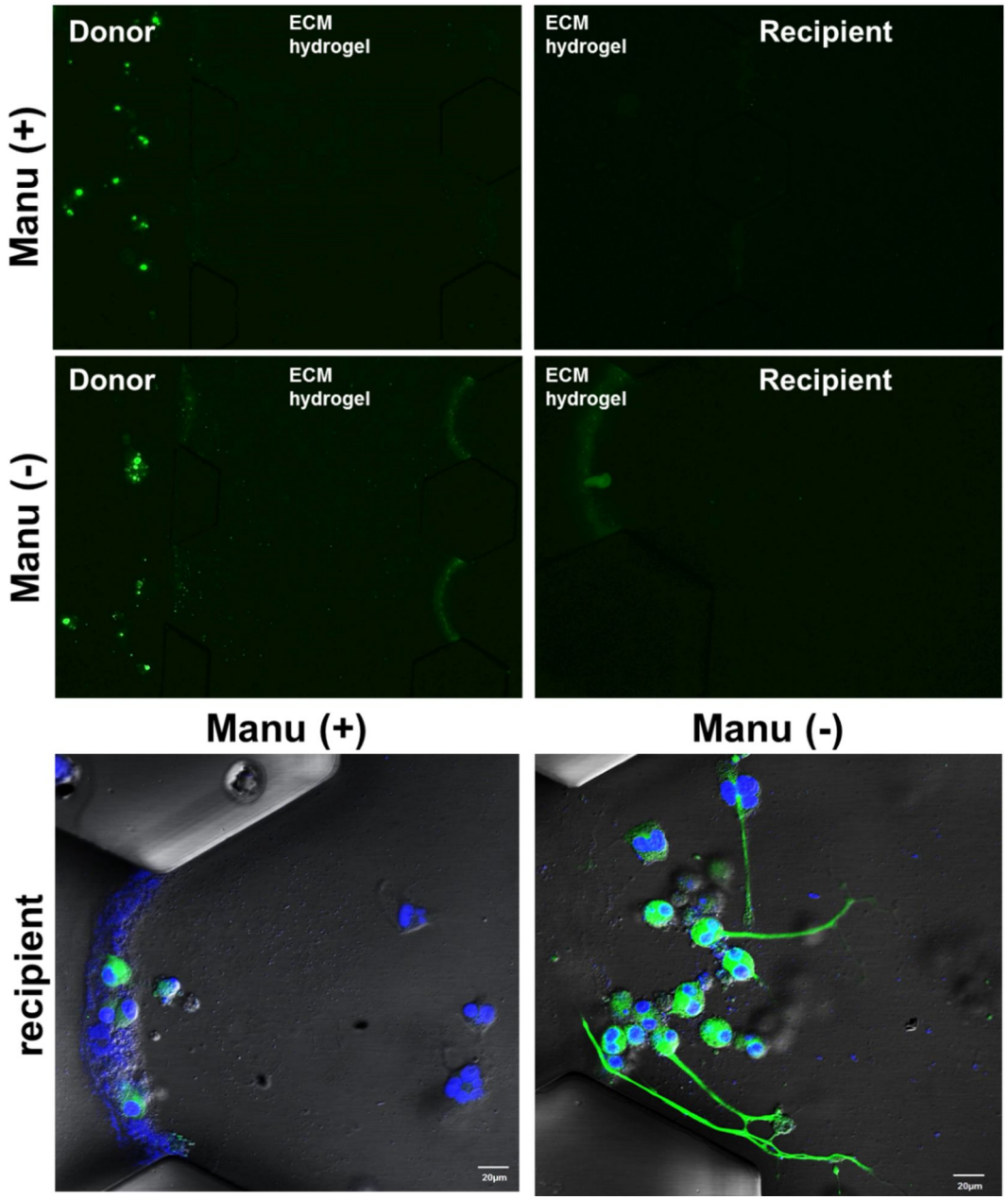

Figure 33. Inhibition of exosome biogenesis impairs transfer of exosome and the induction of neurogenesis in recipient F11 cells.

(top) Representative figures of fluorescence images show transfer of exosomes in ECM hydrogel and recipient cells 4 days after co-cultured with D-F11 cells in the presence of inhibitors of nSMase2 (manumycin-A, Manu); (bottom) Immunofluorescence staining for Tuj-1 in recipient cells at 4 days after co-cultured with donor cells in the presence of inhibitors of nSMase2 (manumycin-A, Manu). Scale bar, 20 μm.

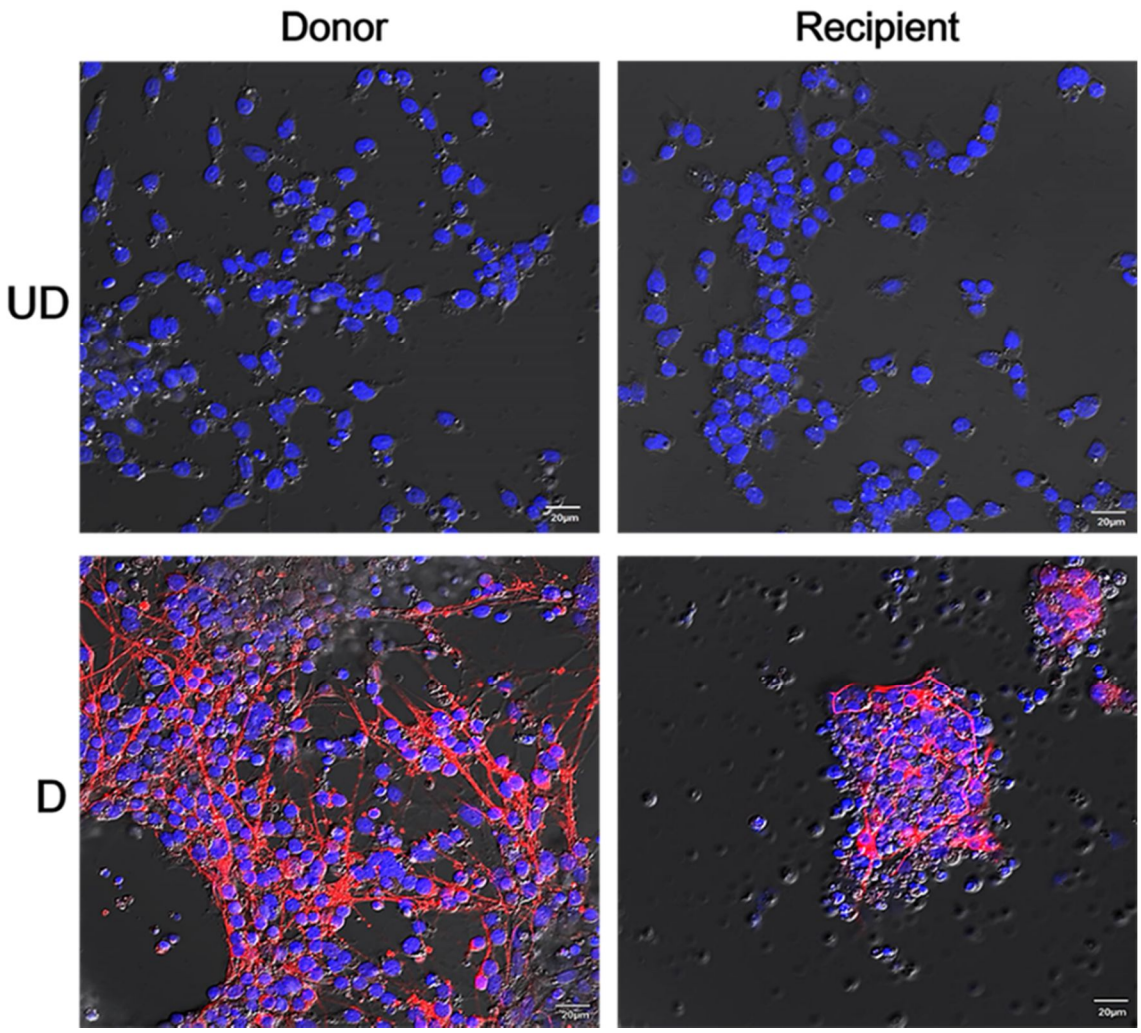

Figure 34. Exosome-mediated neurogenesis in neural stem cells.

Immunofluorescence staining to examine exosome-mediated neuronal differentiation in NE-4C, neural stem cells at 9 days after co-culture. Scale bar, 20 μm.

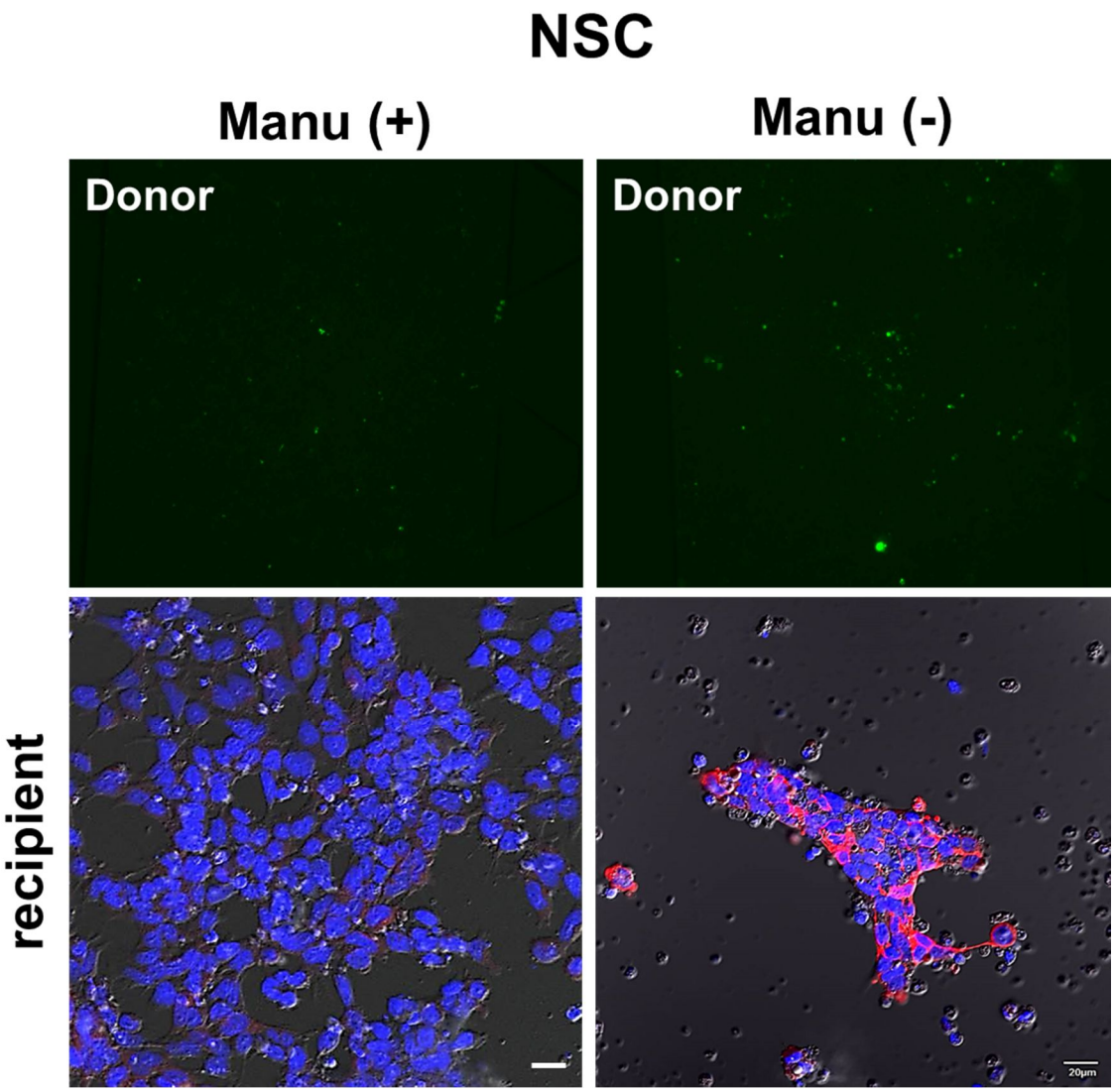

Figure 35. Inhibition exosome-mediated neurogenesis by blocking exosome secretion in neural stem cells.

(top) Representative fluorescence images represent secretion of exosomes in donor NSCs; (bottom) Immunofluorescence staining to examine exosome-mediated neurogenesis in NE-4C, neural stem cells after manumycin-A treatment. Scale bar, 20 μm.

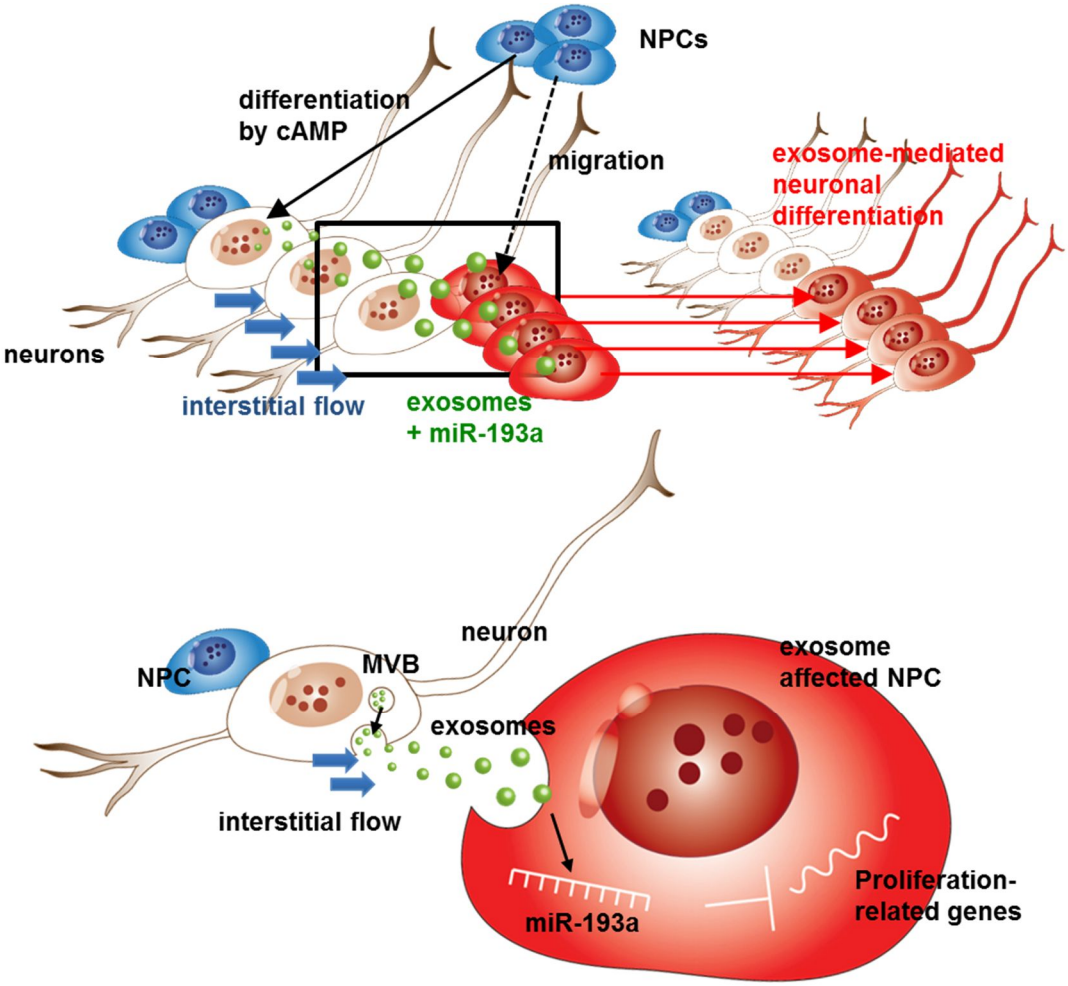

Figure 36. Representative scheme for elevated neuronal differentiation by exosome-mediated miR-193a transfer.

DISCUSSION

My findings can be summarized under three categories: (1) discovery of a miR-193a that is involved in regulating neuronal differentiation by suppressing proliferation-related target genes, (2) exosome-mediated communication from differentiated to undifferentiated cells through the transfer of miR-193a, and (3) the effect of neurogenic miRNA-loaded exosomes of differentiated neuronal cells on the neurogenesis of undifferentiated neural progenitor cells visualized by microfluidic technique.

EVs are important mediators of intercellular communication as evolutionarily conserved vehicles to deliver bioactive protein, lipids, and nucleic acids (Mittelbrunn et al., 2011). In previous reports, EVs have been described as mediators of paracrine mechanisms, associated with repair of injured regions and improvement in cell survival rates (Li et al., 2008; Liu et al., 2009). EVs released from stem cells are possible modulators of tissue repair by reprogramming injured cells (Camussi et al., 2013). Indeed, EVs released from human multipotent mesenchymal stem cells (MSCs) induce dedifferentiation of renal tubular epithelial cells to a stem-cell-like phenotype with subsequent activation of regenerative programs, leading to proliferation and resistance to apoptosis (Bruno et al., 2009). Endothelial progenitor cell (EPC)-derived EVs induced changes in the recipient endothelial cells by triggering transcription of critical components of the pro-angiogenic pathway by conveying miRNAs and altering gene expression of target cells (Cantaluppi et al., 2012). EVs derived from embryonic stem cells containing miRNA were transferred to mouse embryonic fibroblasts *in vitro* (Yuan et al., 2009). Specific miRNAs are efficiently transferred via EVs and, the involvement of mechanisms of miRNA compartmentalization and delivery has been suggested (Camussi et al., 2013).

In this study, I examined whether a specific unidentified miRNA acts as a gene modulator for neurogenesis by being transferred within exosomes released from differentiated cells of the adjacent undifferentiated cells. I established an *in vitro* microfluidic cell culture platform to observe the migration of miRNA-loaded exosomes released from differentiated neuronal cells to

undifferentiated cells.

First, using miRNA expression profiles on microarray after induction of neuronal differentiation by Ngn1 treatment, I identified the 240 up-regulated candidate neurogenic miRNAs, and chose miR-193a from among the top 17 miRNAs based on the its plausible involvement of target genes in cell cycle and neuronal activity. Between miR-193a and miR-193b, miR-193a was conserved in humans, mouse, and rat and up to this point there have been no reports on its function as a regulator of neuronal differentiation. MiR-193b was suggested as a tumor suppressor miRNA, as the overexpression of miR-193b induced activation of caspase 3/7 resulting in apoptotic cell death in ovarian cancer cells (Nakano et al., 2013). Here miR-193a expression increased during neuronal differentiation in F11 neural progenitor cells and overproduction of miR-193a facilitated neuronal differentiation of these cells with enhanced expression of Tuj1 and MAP2. F11 cells can differentiate to neurons by the addition of transcription factors (e.g, Ngn1; Oh et al., 2013a) or chemicals (e.g, db-cAMP; Cho et al., 2001; Kim et al., 2002). The predicted targets for miR-193a by gene ontology (GO) and pathway analysis were involved in pathways such as neuroactive ligand-receptor interaction, cell cycle, and others. Among these, I hypothesized neuroactive ligand-receptor interaction would be involved in induction of neuronal differentiation by miR-193a. Using computational algorithms, binding sites of miR-193a were found in the 3′-UTR such as the calcitonin receptor-like (CALCRL), cholecystokinin A receptor (CCKAR), cysteinyl leukotriene receptor 1 (CYSLTR1) and galanin receptor 1 (GALR1) genes and mRNAs and proteins were repressed by miR-193a overexpression on further quantitative assays. Based on these findings, I concluded that miR-193a has potential function as a neuron-inducing miRNA similar to other neurogenic miRNAs (miR-9, miR-124 and miR-132).

Exosome-mediated delivery of miR-193a and their effects on the recipient undifferentiated neural progenitor cells were examined using three platforms, i.e., 2D co-culture system, transwell system and microfluidic device. MiR-193a was delivered from differentiated cells to the recipient cells and miR-193a was effective on the target genes that produced morphological

and marker changes in the recipient cells. Among these, microfluidic device was an ideal miniaturized cell culture platform that permits imaging of biological processes at high resolution in real time which allowed easy modification and regulation of the sophisticated fluidic and 3D ECM microenvironments (Shin et al., 2012). The exosome-mediated miR-193a transfer was documented using a conventional transwell co-culture system and I could see that differentiated F11 cells communicated with undifferentiated cells to induce differentiation into neuronal lineage in the separated insert well chamber by transfer of miR-193a via exosomes. The delivery of neurogenic miRNAs of miR-193a modified the cell fate of the recipient cells. However, I could not see the exosome movements in transwell systems. Microfluidic device having a channel for recipient cell seeding composed of 3D structure allowed tracking the initial migration pattern of exosomes and individual exosomal movements could be traced through the ECM. As it took hours for the recipient cells to adhere to the bottom surface if 2D were used instead of 3D, and the initial release and movement of exosomes from donor cells would already occur during this preparation procedure, 2D constitution for the recipient cells were not appropriate.

The device also facilitated sequential seeding of donor and recipient cells and long-term observation for neurogenesis in the recipient cells, with improved viability of the 3D co-cultured cells by refreshing medium daily with minimized shear stress. Condition of supplied medium was also maintained different in donor (left) and recipient cell channel (right) (the FBS concentration of medium for donor was maintained lower than that of supplied medium for recipient cell channel (right)). Directional movement of exosomes secreted from differentiated cells was monitored to move under interstitial flow mimicking microenvironment toward undifferentiated cells, independent (opposite) from chemical concentration of FBS.

When GFP-exosome-producing donor cells were differentiated and co-cultured with undifferentiated recipient cells, transfer of exosomes from donor cells was detected soon after co-culturing with the recipient cells. In left cell channel having donor cells, exosomes from donor cells migrated toward hydrogel. Exosomes entered into the interfiber space of type 1

collagen hydrogel were hindered and interrupted by nanofibers. Fluorescence images for exosomes in type 1 collagen hydrogel are measured with a size of approximately 800-900 nm which is considered to be moving the two or three exosomes. After passing the hydrogel, exosomes entered into another interfiber space of type I collagen hydrogel with recipient cells. The exosomes reached the recipient cells and were taken into in 1 to 3 minutes (Figure 28). Color of the exosomes in the DiI-labelled recipient cells changed their color from green to yellow (Figure 29). Interestingly, the recipient undifferentiated F11 and NE-4C, neural stem cells spontaneously triggered their cell differentiation toward neuronal lineage after they received the exosomes (Figure 32 and 34). This was similar to the findings in coordinative morphogenetic developmental regulation (Prin et al., 2014; Wood et al., 2013), senescence propagation (Demaria et al., 2015), stress-response propagation among cells (Lu et al., 2014; Schinzel and Dillin, 2015; Taylor et al., 2014), spread of neurodegenerative changes (Hindle et al., 2013; Lu et al., 2014), spread of cancer metastasis signal/ suppression or drug resistance characteristics (Adi Harel et al., 2015; Chen et al., 2014a; Chen et al., 2014b; Papa et al., 2013; Tordonato et al., 2015), immune regulation or apoptosis (Perez-Garijo et al., 2013; Wing et al., 2011). External cAMP signal induced neuronal differentiation of a portion of progenitor cells, and exosomes acted as vehicles to convey the signal to the adjacent undifferentiated cells to join the differentiation, in which one of the signals happened to be miR-193a. This is the first clear proof that exosomes are involved in the cell-non-autonomous propagation of signals to join and express population behavior of differentiation. Though small or macro-molecules were long known to be solely in charge of this cell-non-autonomous population behavior in various physiologic process, exosome-mediated delivery of differentiation signal should now be considered to explain cell-non-autonomous differentiation of neural progenitors. Especially, if nucleic acids were to be involved in cell-non-autonomous synchronization of population cellular behavior, exosomes would have been the best choice. In this study, I definitely proved that exosomes carry a neurogenic miRNA and finally promote differentiation of recipient undifferentiated cells. Though I do not content that a miR-193a was the only mediator of this

information transfer from differentiated cell to undifferentiated cells, I could be sure that miR-193a was working in the recipient cells. Luciferase reporter transgene reported that mature miR-193a was active in suppressing both the target and luciferase genes (Hwang do and Lee, 2012; Ko et al., 2009). Once delivered to the recipient cells, nucleic acids especially microRNAs will immediately start to work on the target mRNAs. There is no need to wait for the nuclear transcriptional process of primary microRNAs to decay sense mRNA or inhibit its translation.

I visualized the movements of exosomes with slow flow through the ECM and entering the recipient cells on microfluidic device. Anyone can easily use this protocol and this combination of microfluidic assay and intermittent continuous confocal imaging will elucidate the individual exosomal behavior in cell-cell communication to yield various cell-non-autonomous physiologic behaviors. I propose this method be used to elucidate the individual exosomes and its behavior in cell-cell communication during cell-non-autonomous phenomenon. To name a few, the phenomena of developmental coordination (Prin et al., 2014; Wood et al., 2013), propagation of degenerative (Hindle et al., 2013; Lu et al., 2014) or senescence process (Demaria et al., 2015), cooperation or antagonism between cancer cells themselves (Papa et al., 2013; Tordonato et al., 2015) or between immune cells and cancer cells (Chen et al., 2014b), and epithelial/endothelial to mesenchymal or reverse transition during the initiation or spreading of metastasis are expected to be investigated using my system. The optimal construction of bioluminescence cellular imaging in the recipient cells would be necessary and in my study I used molecular action imaging of microRNAs, previously established and applied to both *in vitro* and *in vivo* studies (Hwang do and Lee, 2012; Ko et al., 2009; Oh et al., 2013b). Fluorescence-tagged of exosomes enabled visualization of live cells producing and releasing exosomes and also individual exosomes could be traced during migration. This will open the study of individual exosomes just like individual cell studies, which are under serious investigation by many scientists.

In this study, I found that other neurogenic miRNAs such as miR-124a also participated in promoting neurogenesis in recipient F11 cells (Figure 21) after co-culturing with differentiated

F11 cells. Likewise, even though the transfer of miR-193a and uptake of miR-193a into recipient cells were visualized using reporter system, other types of many neurogenic miRNAs such as let-7 or miR-9 in exosome have many chances to be also involved in promoting neurogenesis. Further studies regarding identification of characteristics of exosomal miRNA components in undifferentiated or differentiated F11 cells are mandatory to understand the exact mechanisms that induce neurogenesis in a cell population. Further works are warranted to apply this method to heterogeneous cell-cell communication and to the roles of other neurogenic miRNAs such as miR-124a.

In previous reports, MSCs transferred their therapeutic factors, especially miRNAs, to recipient cells and promoted therapeutic response by regulating gene expression (Xin et al., 2014). In addition, exosomes are recognized as main delivery vehicles, which spread the pathogenic materials such as prion, beta amyloid, and alpha-synuclein to promote neurodegenerative disorders (Emmanouilidou et al., 2010; Fevrier et al., 2004; Rajendran et al., 2006). Understanding the role of exosome-mediated transfer of miRNAs will be important in terms of determining the mechanisms of diseases and development of therapeutics. My finding and method are expected to eventually support the research regarding disease modeling and drug screening in well-defined microfluidic assay.

TABLE 1. Top 17 upregulated miRNAs in F11 cells following the expression of Ngn 1.

Mouse	***Rat***	***Fold change***
mmu-miR-805		14.07263851
mmu-miR-302b		12.89993328
mmu-miR-376a*		12.62111158
mmu-miR-1905		11.72654891
mmu-miR-1893		9.625092995
mmu-let-7c-1*	rno-let-7c-1*	9.491328504
mmu-miR-193	rno-miR-193	8.814449901
mmu-miR-1-2as		7.798290849
mmu-miR-10a-pre		7.472357042
mmu-miR-652-pre		7.35511971
mmu-miR-376a-pre		6.930148251
mmu-miR-183	rno-miR-183	6.905163844
mmu-miR-31*	rno-miR-31*	6.606051754
mmu-miR-718		6.537460886
mmu-miR-10b-pre		6.39345684
mmu-miR-509-3p		6.240349793
mmu-let-7g-pre		5.537988269

TABLE 2. List of qRT-PCR primers sequences for neuron-specific genes and target genes of miR-193a used in the study.

Gene	Forward	Reverse
Tuj-1	5′-aggtagccgtgtgtgaca-3′	5′-tcacttgggcccctggg-3′
NeuroD	5′-gccgctcagcatcaatgg-3′	5′-ctaatcgtgaaagatggcat-3′
MAP2	5′-cccaagaaccaagatgaa-3′	5′-aatcaaggcaagacatagcga-3′
CCKAR	5’-ggagcagtggttctgctg-3’	5’-gtggggcagaggtgctc-3’
GALR1	5’-gctatgccaaggtccttaa-3’	5’-gtgggtgcagttggtgg-3’
CYSLTR1	5’-catcatccctttgtcacca-3’	5’-ggcaaggaagctttcttcttg-3’

REFERENCES

Adi Harel, S., Bossel Ben-Moshe, N., Aylon, Y., Bublik, D.R., Moskovits, N., Toperoff, G., Azaiza, D., Biagoni, F., Fuchs, G., Wilder, S., et al. (2015). Reactivation of epigenetically silenced miR-512 and miR-373 sensitizes lung cancer cells to cisplatin and restricts tumor growth. Cell Death Differ 22, 1328-1340.

Akerblom, M., and Jakobsson, J. (2013). MicroRNAs as Neuronal Fate Determinants. The Neuroscientist : a review journal bringing neurobiology, neurology and psychiatry 20, 235-242.

Bartel, D.P. (2004). MicroRNAs: genomics, biogenesis, mechanism, and function. Cell 116, 281-297.

Blanchard, N., Lankar, D., Faure, F., Regnault, A., Dumont, C., Raposo, G., and Hivroz, C. (2002). TCR activation of human T cells induces the production of exosomes bearing the TCR/CD3/zeta complex. J Immunol 168, 3235-3241.

Brennecke, J., Hipfner, D.R., Stark, A., Russell, R.B., and Cohen, S.M. (2003). bantam encodes a developmentally regulated microRNA that controls cell proliferation and regulates the proapoptotic gene hid in Drosophila. Cell 113, 25-36.

Bruno, S., Grange, C., Deregibus, M.C., Calogero, R.A., Saviozzi, S., Collino, F., Morando, L., Busca, A., Falda, M., Bussolati, B., et al. (2009). Mesenchymal stem cell-derived microvesicles protect against acute tubular injury. Journal of the American Society of Nephrology : JASN 20, 1053-1067.

Bryder, D., Rossi, D.J., and Weissman, I.L. (2006). Hematopoietic stem cells: the paradigmatic tissue-specific stem cell. Am J Pathol 169, 338-346.

Camussi, G., Deregibus, M.C., Bruno, S., Cantaluppi, V., and Biancone, L. (2010). Exosomes/microvesicles as a mechanism of cell-to-cell communication. Kidney international 78, 838-848.

Camussi, G., Deregibus, M.C., and Cantaluppi, V. (2013). Role of stem-cell-derived microvesicles in the paracrine action of stem cells. Biochemical Society transactions 41, 283-287.

Cantaluppi, V., Gatti, S., Medica, D., Figliolini, F., Bruno, S., Deregibus, M.C., Sordi, A., Biancone, L., Tetta, C., and Camussi, G. (2012). Microvesicles derived from endothelial progenitor cells protect the kidney from ischemia-reperfusion injury by microRNA-dependent reprogramming of resident renal cells. Kidney international 82, 412-427.

Chen, F., Qi, X., Qian, M., Dai, Y., and Sun, Y. (2014a). Tackling the tumor microenvironment: what challenge does it pose to anticancer therapies? Protein Cell 5, 816-826.

Chen, L., Gibbons, D.L., Goswami, S., Cortez, M.A., Ahn, Y.H., Byers, L.A., Zhang, X., Yi, X., Dwyer, D., Lin, W., et al. (2014b). Metastasis is regulated via microRNA-200/ZEB1 axis control of tumour cell PD-L1 expression and intratumoral immunosuppression. Nature communications 5, 5241.

Cho, J.H., Kwon, I.S., Kim, S., Ghil, S.H., Tsai, M.J., Kim, Y.S., Lee, Y.D., and Suh-Kim, H. (2001). Overexpression of BETA2/NeuroD induces neurite outgrowth in F11 neuroblastoma cells. Journal of neurochemistry 77, 103-109.

Cocucci, E., Racchetti, G., and Meldolesi, J. (2009). Shedding microvesicles: artefacts no more. Trends in cell biology 19, 43-51.

Cossetti, C., Smith, J.A., Iraci, N., Leonardi, T., Alfaro-Cervello, C., and Pluchino, S. (2012). Extracellular membrane vesicles and immune regulation in the brain. Frontiers in physiology 3, 117.

Delaloy, C., Liu, L., Lee, J.A., Su, H., Shen, F., Yang, G.Y., Young, W.L., Ivey, K.N., and Gao, F.B. (2010). MicroRNA-9 coordinates proliferation and migration of human embryonic stem cell-derived neural progenitors. Cell stem cell 6, 323-335.

Demaria, M., Desprez, P.Y., Campisi, J., and Velarde, M.C. (2015). Cell Autonomous and Non-Autonomous Effects of Senescent Cells in the Skin. J Invest Dermatol 135, 1722-1726.

Deregibus, M.C., Cantaluppi, V., Calogero, R., Lo Iacono, M., Tetta, C., Biancone, L., Bruno, S., Bussolati, B., and Camussi, G. (2007). Endothelial progenitor cell derived microvesicles activate an angiogenic program in endothelial cells by a horizontal transfer of mRNA. Blood 110, 2440-2448.

Dostie, J., Mourelatos, Z., Yang, M., Sharma, A., and Dreyfuss, G. (2003). Numerous microRNPs in neuronal cells containing novel microRNAs. RNA 9, 180-186.

Emmanouilidou, E., Melachroinou, K., Roumeliotis, T., Garbis, S.D., Ntzouni, M., Margaritis, L.H., Stefanis, L., and Vekrellis, K. (2010). Cell-produced alpha-synuclein is secreted in a calcium-dependent manner by exosomes and impacts neuronal survival. The Journal of neuroscience : the official journal of the Society for Neuroscience 30, 6838-6851.

Eskildsen, T., Taipaleenmaki, H., Stenvang, J., Abdallah, B.M., Ditzel, N., Nossent, A.Y., Bak, M., Kauppinen, S., and Kassem, M. (2011). MicroRNA-138 regulates osteogenic differentiation of human stromal (mesenchymal) stem cells *in vivo*. Proceedings of the National Academy of Sciences of the United States of America 108, 6139-6144.

Fevrier, B., Vilette, D., Archer, F., Loew, D., Faigle, W., Vidal, M., Laude, H., and Raposo, G. (2004). Cells release prions in association with exosomes. Proceedings of the National Academy of Sciences of the United States of America 101, 9683-9688.

Forstemann, K., Tomari, Y., Du, T., Vagin, V.V., Denli, A.M., Bratu, D.P., Klattenhoff, C., Theurkauf, W.E., and Zamore, P.D. (2005). Normal microRNA maturation and germ-line stem cell maintenance requires Loquacious, a double-stranded RNA-binding domain protein. PLoS Biol 3, e236.

Fruhbeis, C., Frohlich, D., and Kramer-Albers, E.M. (2012). Emerging roles of exosomes in neuron-glia communication. Frontiers in physiology 3, 119.

Gagan, J., Dey, B.K., Layer, R., Yan, Z., and Dutta, A. (2011). MicroRNA-378 targets the myogenic repressor MyoR during myoblast differentiation. The Journal of biological chemistry 286, 19431-19438.

Gage, F.H. (2000). Mammalian neural stem cells. Science 287, 1433-1438.

George, J.N., Thoi, L.L., McManus, L.M., and Reimann, T.A. (1982). Isolation of human platelet membrane microparticles from plasma and serum. Blood 60, 834-840.

Harandi, O.F., and Ambros, V.R. (2015). Control of stem cell self-renewal and differentiation by the heterochronic genes and the cellular asymmetry machinery in Caenorhabditis elegans. Proceedings of the National Academy of Sciences of the United States of America 112, E287-296.

He, L., and Hannon, G.J. (2004). MicroRNAs: small RNAs with a big role in gene regulation. Nat Rev Genet 5, 522-531.

Heijnen, H.F., Schiel, A.E., Fijnheer, R., Geuze, H.J., and Sixma, J.J. (1999). Activated platelets release two types of membrane vesicles: microvesicles by surface shedding and exosomes derived from exocytosis of multivesicular bodies and alpha-granules. Blood 94, 3791-3799.

Hindle, S., Afsari, F., Stark, M., Middleton, C.A., Evans, G.J., Sweeney, S.T., and Elliott, C.J. (2013). Dopaminergic expression of the Parkinsonian gene LRRK2-G2019S leads to non-autonomous visual neurodegeneration, accelerated by increased neural demands for energy. Hum Mol Genet 22, 2129-2140.

Hwang do, W., and Lee, D.S. (2012). Optical imaging for stem cell differentiation to neuronal lineage. Nucl Med Mol Imaging 46, 1-9.

Janowska-Wieczorek, A., Majka, M., Kijowski, J., Baj-Krzyworzeka, M., Reca, R., Turner, A.R., Ratajczak, J., Emerson, S.G., Kowalska, M.A., and Ratajczak, M.Z. (2001). Platelet-derived microparticles bind to hematopoietic stem/progenitor cells and enhance their engraftment. Blood 98, 3143-3149.

Jing, L., Jia, Y., Lu, J., Han, R., Li, J., Wang, S., Peng, T., and Jia, Y. (2011). MicroRNA-9 promotes differentiation of mouse bone mesenchymal stem cells into neurons by Notch signaling. Neuroreport 22, 206-211.

Karbiener, M., Neuhold, C., Opriessnig, P., Prokesch, A., Bogner-Strauss, J.G., and Scheideler, M. (2011). MicroRNA-30c promotes human adipocyte differentiation and co-represses PAI-1 and ALK2. RNA biology 8, 850-860.

Kim, J., Krichevsky, A., Grad, Y., Hayes, G.D., Kosik, K.S., Church, G.M., and Ruvkun, G. (2004a). Identification of many microRNAs that copurify with polyribosomes in mammalian neurons. Proceedings of the National Academy of Sciences of the United States of America 101, 360-365.

Kim, S., Ghil, S.H., Kim, S.S., Myeong, H.H., Lee, Y.D., and Suh-Kim, H. (2002). Overexpression of neurogenin1 induces neurite outgrowth in F11 neuroblastoma cells. Experimental & molecular medicine 34, 469-475.

Kim, S., Yoon, Y.S., Kim, J.W., Jung, M., Kim, S.U., Lee, Y.D., and Suh-Kim, H. (2004b). Neurogenin1 is sufficient to induce neuronal differentiation of embryonal carcinoma P19 cells in the absence of retinoic acid. Cellular and molecular neurobiology 24, 343-356.

Ko, H.Y., Hwang do, W., Lee, D.S., and Kim, S. (2009a). A reporter gene imaging system for monitoring microRNA biogenesis. Nature protocols 4, 1663-1669.

Ko, H.Y., Lee, D.S., and Kim, S. (2009b). Noninvasive imaging of microRNA124a-mediated repression of the chromosome 14 ORF 24 gene during neurogenesis. FEBS J 276, 4854-4865.

Ko, M.H., Kim, S., Hwang do, W., Ko, H.Y., Kim, Y.H., and Lee, D.S. (2008). Bioimaging of the unbalanced expression of microRNA9 and microRNA9* during the neuronal differentiation of P19 cells. FEBS J 275, 2605-2616.

Kosik, K.S. (2006). The neuronal microRNA system. Nature reviews Neuroscience 7, 911-920.

Krichevsky, A.M., Sonntag, K.C., Isacson, O., and Kosik, K.S. (2006). Specific microRNAs modulate embryonic stem cell-derived neurogenesis. Stem Cells 24, 857-864.

Lee, J.Y., Kim, S., Hwang do, W., Jeong, J.M., Chung, J.K., Lee, M.C., and Lee, D.S. (2008). Development of a dual-luciferase reporter system for *in vivo* visualization of MicroRNA biogenesis and posttranscriptional regulation. J Nucl Med 49, 285-294.

Li, W., Sun, G., Yang, S., Qu, Q., Nakashima, K., and Shi, Y. (2008). Nuclear receptor TLX regulates cell cycle progression in neural stem cells of the developing brain. Molecular endocrinology 22, 56-64.

Li, X., and Jin, P. (2010). Roles of small regulatory RNAs in determining neuronal identity. Nature reviews Neuroscience 11, 329-338.

Liu, C.G., Calin, G.A., Volinia, S., and Croce, C.M. (2008). MicroRNA expression profiling using microarrays. Nature protocols 3, 563-578.

Liu, S.P., Fu, R.H., Yu, H.H., Li, K.W., Tsai, C.H., Shyu, W.C., and Lin, S.Z. (2009). MicroRNAs regulation modulated self-renewal and lineage differentiation of stem cells. Cell transplantation 18, 1039-1045.

Lo Cicero, A., Stahl, P.D., and Raposo, G. (2015). Extracellular vesicles shuffling intercellular messages: for good or for bad. Current opinion in cell biology 35, 69-77.

Lu, T., Aron, L., Zullo, J., Pan, Y., Kim, H., Chen, Y., Yang, T.H., Kim, H.M., Drake, D., Liu, X.S., et al. (2014). REST and stress resistance in ageing and Alzheimer's disease. Nature 507, 448-454.

Lund, E., Guttinger, S., Calado, A., Dahlberg, J.E., and Kutay, U. (2004). Nuclear export of microRNA precursors. Science 303, 95-98.

Majka, M., Janowska-Wieczorek, A., Ratajczak, J., Ehrenman, K., Pietrzkowski, Z., Kowalska, M.A., Gewirtz, A.M., Emerson, S.G., and Ratajczak, M.Z. (2001). Numerous growth factors, cytokines, and chemokines are secreted by human CD34(+) cells, myeloblasts, erythroblasts, and megakaryoblasts and regulate normal hematopoiesis in an autocrine/paracrine manner. Blood 97, 3075-3085.

Makeyev, E.V., Zhang, J., Carrasco, M.A., and Maniatis, T. (2007). The MicroRNA miR-124 promotes neuronal differentiation by triggering brain-specific alternative pre-mRNA splicing. Molecular cell 27, 435-448.

Markakis, E.A., Palmer, T.D., Randolph-Moore, L., Rakic, P., and Gage, F.H. (2004). Novel neuronal phenotypes from neural progenitor cells. The Journal of neuroscience : the official journal of the Society for Neuroscience 24, 2886-2897.

Mears, R., Craven, R.A., Hanrahan, S., Totty, N., Upton, C., Young, S.L., Patel, P., Selby, P.J., and Banks, R.E. (2004). Proteomic analysis of melanoma-derived exosomes by two-dimensional polyacrylamide gel electrophoresis and mass spectrometry. Proteomics 4, 4019-4031.

Meza-Sosa, K.F., Pedraza-Alva, G., and Perez-Martinez, L. (2014). microRNAs: key triggers of neuronal cell fate. Frontiers in cellular neuroscience 8, 175.

Mimeault, M., and Batra, S.K. (2006). Concise review: recent advances on the significance of stem cells in tissue regeneration and cancer therapies. Stem Cells 24, 2319-2345.

Mimeault, M., Hauke, R., and Batra, S.K. (2007). Stem cells: a revolution in therapeutics-recent advances in stem cell biology and their therapeutic applications in regenerative medicine and cancer therapies. Clin Pharmacol Ther 82, 252-264.

Ming, G.L., and Song, H. (2011). Adult neurogenesis in the mammalian brain: significant answers and significant questions. Neuron 70, 687-702.

Mittelbrunn, M., Gutierrez-Vazquez, C., Villarroya-Beltri, C., Gonzalez, S., Sanchez-Cabo, F., Gonzalez, M.A., Bernad, A., and Sanchez-Madrid, F. (2011). Unidirectional transfer of microRNA-loaded exosomes from T cells to antigen-presenting cells. Nature communications 2, 282.

Morel, O., Toti, F., Hugel, B., and Freyssinet, J.M. (2004). Cellular microparticles: a disseminated storage pool of bioactive vascular effectors. Curr Opin Hematol 11, 156-164.

Nakano, H., Yamada, Y., Miyazawa, T., and Yoshida, T. (2013). Gain-of-function microRNA screens identify miR-193a regulating proliferation and apoptosis in epithelial ovarian cancer cells. International journal of oncology 42, 1875-1882.

Oh, H.J., Hwang do, W., Youn, H., and Lee, D.S. (2013a). *In vivo* bioluminescence reporter gene imaging for the activation of neuronal differentiation induced by the neuronal activator neurogenin 1 (Ngn1) in neuronal precursor cells. European journal of nuclear medicine and molecular imaging 40, 1607-1617.

Oh, S.W., Hwang do, W., and Lee, D.S. (2013b). *In vivo* monitoring of microRNA biogenesis using reporter gene imaging. Theranostics 3, 1004-1011.

Pan, B.T., and Johnstone, R.M. (1983). Fate of the transferrin receptor during maturation of sheep reticulocytes *in vitro*: selective externalization of the receptor. Cell 33, 967-978.

Papa, A., Chen, M., and Pandolfi, P.P. (2013). Pills of PTEN? In and out for tumor suppression. Cell research 23, 1155-1156.

Pegtel, D.M., Cosmopoulos, K., Thorley-Lawson, D.A., van Eijndhoven, M.A., Hopmans, E.S., Lindenberg, J.L., de Gruijl, T.D., Wurdinger, T., and Middeldorp, J.M. (2010). Functional delivery of viral miRNAs via exosomes. Proceedings of the National Academy of Sciences of the United States of America 107, 6328-6333.

Perez-Garijo, A., Fuchs, Y., and Steller, H. (2013). Apoptotic cells can induce non-autonomous apoptosis through the TNF pathway. Elife 2, e01004.

Prin, F., Serpente, P., Itasaki, N., and Gould, A.P. (2014). Hox proteins drive cell segregation and non-autonomous apical remodelling during hindbrain segmentation. Development 141, 1492-1502.

Quesenberry, P.J., and Aliotta, J.M. (2008). The paradoxical dynamism of marrow stem cells: considerations of stem cells, niches, and microvesicles. Stem Cell Rev 4, 137-147.

Rajendran, L., Honsho, M., Zahn, T.R., Keller, P., Geiger, K.D., Verkade, P., and Simons, K. (2006). Alzheimer's disease beta-amyloid peptides are released in association with exosomes. Proceedings of the National Academy of Sciences of the United States of America 103, 11172-11177.

Raposo, G., Nijman, H.W., Stoorvogel, W., Liejendekker, R., Harding, C.V., Melief, C.J., and Geuze, H.J. (1996). B lymphocytes secrete antigen-presenting vesicles. J Exp Med 183, 1161-1172.

Ratajczak, J., Miekus, K., Kucia, M., Zhang, J., Reca, R., Dvorak, P., and Ratajczak, M.Z. (2006a). Embryonic stem cell-derived microvesicles reprogram hematopoietic progenitors: evidence for horizontal transfer of mRNA and protein delivery. Leukemia 20, 847-856.

Ratajczak, J., Wysoczynski, M., Hayek, F., Janowska-Wieczorek, A., and Ratajczak, M.Z. (2006b). Membrane-derived microvesicles: important and underappreciated mediators of cell-to-cell communication. Leukemia 20, 1487-1495.

Reinhart, B.J., Slack, F.J., Basson, M., Pasquinelli, A.E., Bettinger, J.C., Rougvie, A.E., Horvitz, H.R., and Ruvkun, G. (2000). The 21-nucleotide let-7 RNA regulates developmental timing in Caenorhabditis elegans. Nature 403, 901-906.

Roese-Koerner, B., Stappert, L., Koch, P., Brustle, O., and Borghese, L. (2013). Pluripotent stem cell-derived somatic stem cells as tool to study the role of microRNAs in early human neural development. Current molecular medicine 13, 707-722.

Rozmyslowicz, T., Majka, M., Kijowski, J., Murphy, S.L., Conover, D.O., Poncz, M., Ratajczak, J., Gaulton, G.N., and Ratajczak, M.Z. (2003). Platelet- and megakaryocyte-derived microparticles transfer CXCR4 receptor to CXCR4-null cells and make them susceptible to infection by X4-HIV. AIDS 17, 33-42.

Rustom, A., Saffrich, R., Markovic, I., Walther, P., and Gerdes, H.H. (2004). Nanotubular highways for intercellular organelle transport. Science 303, 1007-1010.

Saito, K., Ishizuka, A., Siomi, H., and Siomi, M.C. (2005). Processing of pre-microRNAs by the Dicer-1-Loquacious complex in Drosophila cells. PLoS Biol 3, e235.

Schinzel, R., and Dillin, A. (2015). Endocrine aspects of organelle stress-cell non-autonomous signaling of mitochondria and the ER. Current opinion in cell biology 33, 102-110.

Sempere, L.F., Freemantle, S., Pitha-Rowe, I., Moss, E., Dmitrovsky, E., and Ambros, V. (2004). Expression profiling of mammalian microRNAs uncovers a subset of brain-expressed microRNAs with possible roles in murine and human neuronal differentiation. Genome Biol 5, R13.

Sherer, N.M., and Mothes, W. (2008). Cytonemes and tunneling nanotubules in cell-cell communication and viral pathogenesis. Trends in cell biology 18, 414-420.

Shin, Y., Han, S., Jeon, J.S., Yamamoto, K., Zervantonakis, I.K., Sudo, R., Kamm, R.D., and Chung, S. (2012). Microfluidic assay for simultaneous culture of multiple cell types on surfaces or within hydrogels. Nature protocols 7, 1247-1259.

Siekevitz, P. (1972). Biological membranes: the dynamics of their organization. Annu Rev Physiol 34, 117-140.

Skog, J., Wurdinger, T., van Rijn, S., Meijer, D.H., Gainche, L., Sena-Esteves, M., Curry, W.T., Jr., Carter, B.S., Krichevsky, A.M., and Breakefield, X.O. (2008). Glioblastoma microvesicles transport RNA and proteins that promote tumour growth and provide diagnostic biomarkers. Nature cell biology 10, 1470-1476.

Taylor, R.C., Berendzen, K.M., and Dillin, A. (2014). Systemic stress signalling: understanding the cell non-autonomous control of proteostasis. Nat Rev Mol Cell Biol 15, 211-217.

Thery, C., Regnault, A., Garin, J., Wolfers, J., Zitvogel, L., Ricciardi-Castagnoli, P., Raposo, G., and Amigorena, S. (1999). Molecular characterization of dendritic cell-derived exosomes. Selective accumulation of the heat shock protein hsc73. The Journal of cell biology 147, 599-610.

Tordonato, C., Di Fiore, P.P., and Nicassio, F. (2015). The role of non-coding RNAs in the regulation of stem cells and progenitors in the normal mammary gland and in breast tumors. Frontiers in genetics 6, 72.

Trajkovic, K., Hsu, C., Chiantia, S., Rajendran, L., Wenzel, D., Wieland, F., Schwille, P., Brugger, B., and Simons, M. (2008). Ceramide triggers budding of exosome vesicles into multivesicular endosomes. Science 319, 1244-1247.

Valadi, H., Ekstrom, K., Bossios, A., Sjostrand, M., Lee, J.J., and Lotvall, J.O. (2007). Exosome-mediated transfer of mRNAs and microRNAs is a novel mechanism of genetic exchange between cells. Nature cell biology 9, 654-659.

Wing, K., Yamaguchi, T., and Sakaguchi, S. (2011). Cell-autonomous and -non-autonomous roles of CTLA-4 in immune regulation. Trends Immunol 32, 428-433.

Wood, W.M., Etemad, S., Yamamoto, M., and Goldhamer, D.J. (2013). MyoD-expressing progenitors are essential for skeletal myogenesis and satellite cell development. Developmental biology 384, 114-127.

Xin, H., Li, Y., and Chopp, M. (2014). Exosomes/miRNAs as mediating cell-based therapy of stroke. Frontiers in cellular neuroscience 8, 377.

Xu, P., Vernooy, S.Y., Guo, M., and Hay, B.A. (2003). The Drosophila microRNA Mir-14 suppresses cell death and is required for normal fat metabolism. Curr Biol 13, 790-795.

Yi, R., Qin, Y., Macara, I.G., and Cullen, B.R. (2003). Exportin-5 mediates the nuclear export of pre-microRNAs and short hairpin RNAs. Genes & development 17, 3011-3016.

Yu, X., Harris, S.L., and Levine, A.J. (2006). The regulation of exosome secretion: a novel function of the p53 protein. Cancer Res 66, 4795-4801.

Yuan, A., Farber, E.L., Rapoport, A.L., Tejada, D., Deniskin, R., Akhmedov, N.B., and Farber, D.B. (2009). Transfer of microRNAs by embryonic stem cell microvesicles. PloS one 4, e4722.

Zeng, Y., and Cullen, B.R. (2006). Recognition and cleavage of primary microRNA transcripts. Methods in molecular biology 342, 49-56.

Zeng, Y., Yi, R., and Cullen, B.R. (2005). Recognition and cleavage of primary microRNA precursors by the nuclear processing enzyme Drosha. EMBO J 24, 138-148.

Zernecke, A., Bidzhekov, K., Noels, H., Shagdarsuren, E., Gan, L., Denecke, B., Hristov, M., Koppel, T., Jahantigh, M.N., Lutgens, E., et al. (2009). Delivery of microRNA-126 by apoptotic bodies induces CXCL12-dependent vascular protection. Science signaling 2, ra81.

Zhang, L., and Wrana, J.L. (2014). The emerging role of exosomes in Wnt secretion and transport. Curr Opin Genet Dev 27, 14-19.

Zhao, C., Sun, G., Ye, P., Li, S., and Shi, Y. (2013). MicroRNA let-7d regulates the TLX/microRNA-9 cascade to control neural cell fate and neurogenesis. Sci Rep 3, 1329.

국 문 초 록

미세유체소자를 이용한 신경성 마이크로RNA의 엑소좀 매개 이동에 의한 신경분화 유도

오현정

서울대학교

융합과학기술대학원 분자의학 및 바이오제약학과

신경 세포들은 세포간의 상호 정보교환 역할을 하는 mRNA, 마이크로 RNA, 단백질을 운반하는 엑소좀과 같은 작은 소포들을 분비한다. 특히, 엑소좀이 운반하는 물질들 중 마이크로 RNA 들 중 마이크로 RNA124 혹은 마이크로 RNA9 와 같은 마이크로 RNA 는 신경세포 분화를 조절한다고 알려져 있다. 본 연구에서는 1) 신경세포 분화 후 발현이 증가하는 마이크로 RNA 중에 기존에 알려지지 않은 신경세포 분화 능이 있는 마이크로 RNA 를 새롭게 선별하였고, 2) 신경세포로 분화가 유도된 세포로부터 분화 전 세포로의 엑소좀의 분비, 이동 및 섭취의 되는 것을 미세유체 소자에서 타임 랩스 실시간 영상화 하는 방법을 확립하였고, 3) 신경세포 분화 후 발현이 증가되는 선별된 마이크로 RNA 가 엑소좀을 매개로 분화 전 세포로 이동되어 신경분화를 유도하는 새로운 현상에 대해 제안하였다. 신경세포 분화 능이 있는 마이크로 RNA 를 새롭게 선별하기 위해 신경 전구 세포인 F11 세포에서 신경세포 분화 후 발현이 증가되는 마이크로 RNA 에 대해 마이크로 어레이를 시행하였다. 신경세포 분화 유도를 위해 F11 세포에 db-cAMP 를 처리 하여 분화를 유도 하였다. 신경전구 세포인 F11 세포에 선별된 마이크로 RNA 가 결합 시 effLuc (enhanced firefly

luciferase) 의 발현이 저해되도록 재조합 된 플라스미드 벡터 (pRV-effLuc/3xPT_miR-193a) 를 계속적으로 발현 시켜 마이크로 RNA193a 의 발현을 모니터링 하였다. 신경 세포 분화 유도 전, 후의 F11 세포로부터 초 원심 분리기를 이용하여 엑소좀을 분리 한 뒤 western blot 을 이용하여 엑소좀 마커를 확인 하였다. 엑소좀을 형광 영상화 할 수 있는 리포터 유전자 (CD63-GFP) 를 이용하여 세포 내 발현하고 있는 엑소좀을 영상화 하였다. Transwell chamber 와 미세유체 소자를 이용하여 신경세포 분화 후 세포에서 분화 전 세포로의 엑소좀의 이동을 확인하였다. 엑소좀이 전달 된 세포의 신경세포 분화 유도를 확인하기 위해 신경세포 특이적인 마커의 발현을 정량 PCR 과 면역염색을 통해 검증하였다. 마이크로 어레이를 통해 선별된 마이크로 RNA193a 는 추가적인 타겟 유전자 분석을 통해 신경세포 분화 능이 있는 마이크로 RNA 로 최종 선별 되었다. 마이크로 RNA193a 가 처리된 신경전구 세포에서는 처리 후 3 일 내에 신경돌기가 뻣어 나오는 것을 관찰 할 수 있다. 또한, 면역 염색을 통해 마이크로 RNA193a 이 그룹에서 신경세포 특이적인 마커 Tuj-1, NeuroD 및 MAP2 의 발현이 유의하게 증가하는 것을 확인 함으로서 마이크로 RNA193a 의 신경 세포 분화 유도 기능에 대해 검증 하였다. F11 세포의 분화 전, 후로부터 분리한 엑소좀 내의 마이크로 RNA193a 의 발현을 확인 한 결과 분화 후 세포에서 분리한 엑소좀 내의 마이크로 RNA193a 의 발현이 유의하게 증가된 것을 확인 할 수 있다. 세포 간의 엑소좀의 이동을 확인하기 위해 엑소좀을 형광 표지할 수 있는 CD63-GFP 리포터 유전자가 처리된 세포를 donor 세포로 이용하여 2D co-culture 및 transwell chamber 에서 실험한 결과 co-culture 후 2 일 내에 recipient 세포에서 형광 표지 된 엑소좀을 세포질에서 관찰 하였다. 미세유체 소자를 이용하여 타임 랩스 실시간 confocal 이미징을 통해 분화 후 세포에서 분화 전 세포로 엑소좀이 이동 되는 것을 영상화 하였다. 마이크로 RNA193a 가 엑소좀을 매개로 분화 후 세포에서 분화 전 세포로 이동 되는 것을

확인하기 위한 리포터 유전자(pRV-effLuc/3xPT_miR-193a)를 계속 발현하고 있는 F11 세포를 recipient 세포로 사용하여 transwell chamber 와 미세유체 소자에서 신경세포 분화 전, 후 세포를 donor 세포로 하여 co-culture 를 진행한 결과 분화 후 donor 세포와 co-culture 한 그룹의 recipient 세포의 광학 시그널이 유의하게 감소된 것을 확인 할 수 있었다. 또한, transwell chamber 와 미세유체 소자에서 신경세포 분화 전, 후 donor 세포와 co-culture 를 진행한 recipient 세포를 면역 염색한 결과 분화 후 donor 세포와 co-culture 한 그룹에서만 신경세포 특이적인 마커의 발현이 유의하게 증가된 것을 확인 할 수 있었다. 이러한 현상은 신경 줄기 세포인 NE-4C 세포에서도 관찰 되었다. 신경세포로 분화 유도된 donor 세포에 Manumycin-A 에 의한 엑소좀 분비 억제와 안티 센스 마이크로 RNA193a 를 이용한 마이크로 RNA193a 의 발현 억제는 recipient 세포의 신경분화를 억제하는 것을 확인하였다. 본 연구는 신경세포 분화 후 발현이 증가하는 마이크로 RNA193a 의 신경세포 분화 유도에 대한 새로운 기능을 밝혔고, 신경세포 분화 기간 동안 분비가 증가하는 엑소좀이 분화 후 발현이 증가하는 마이크로 RNA193a 와 같이 분화 전 세포로 이동되어 신경세포 분화를 유도 한다는 현상을 새롭게 제안하였고 엑소좀의 이동 패턴을 미세 유체 소자에서 실시간으로 관찰 할 수 있는 시스템을 확립하였다. 따라서, 본 연구에서 제안된 현상 및 확립된 시스템은 세포간의 유전자 발현 조절, 엑소좀 매개 뇌 질환의 발병, 진행 및 치료의 메커니즘을 이해하고, 세포간의 물질 이동 양상을 실시간 모니터링 함으로써 생물학적인 현상을 더욱 정확히 이해하는 데 효과적으로 사용될 수 있을 것이라 기대한다.

주요어: 신경세포 분화, 세포 비 자율성, 단일 엑소좀 영상, 마이크로 RNA193a, 미세유체 소자

학번: 2013-30835